UNIVERSIDADE DA BEIRA INTERIOR
Engenharia

# Obstacle Detection and Collision Avoidance Method Based on Optical Systems

**(Versão final após defesa)**

**Ana Beatriz Botelho da Silva**

Dissertação para obtenção do Grau de Mestre em

**Engenharia Aeronáutica**

(ciclo de estudos integrado)

Orientador: Prof. Doutor Kouamana Bousson

**Covilhã, Novembro de 2017**

# Dedication

I dedicate this work to two special people who, although they are no longer present, continue to be the main foundations of my life, my biggest examples. My grandfather, Joaquim, who with his hard work and will to succeed in life taught me to pursue my dreams without ever losing sight of reality. And my grandmother, Hortensia, who showed me that patience and kindness are two virtues we should aspire to live by. Together, they guide me to be who I am. They showed me that there is no perfection in life just as there are no easy roads without obstacles. However, it is up to each of us to go beyond them.

# Acknowledgements

Although this dissertation was mainly developed in Portugal, it started in another European country, more specifically, in Poland. Between these two countries is, approximately, a trip of two thousand and five hundred kilometres by plane, which takes around three and a half hours. So, I would like to begin by thanking a Polish professor who not only helped me decide on the subject of my dissertation but was also by my side during the first steps, professor Paweł Rzucidło from Rzeszow University of Technology.

I would also like to thank all the professors of the department of Aerospace Sciences, who taught and guided me during these five years in Aeronautical Engineering. Especially professor Kouamana Bousson who agreed to be my supervisor and helped me overcome all the difficulties and new challenges.

To those friends, who I've known since childhood, thank you for the friendship that even with the distance was never lost. As for my classmates, thank you for all the moments that have become good memories.

To a special person from Terceira, who know me since I was born and was always available to help.

To my best friend and companion, thank you for your patience, company and help during this last journey.

In terms of family, I would start by thanking my sister and brother-in-law for always being by my side in this and all the journeys of my life, especially to my sister, who was there for me through good and bad moments since I was a small child who barely knew how to walk but dreamed of flying. To the most important people in my life, my parents, thank you for your patience, for listening to me, for teaching me and for encouraging me to fight for my dreams.

# Abstract

The development of a new collision avoidance method, which can detect and calculate the necessary changes to prevent imminent accident, is the focal interest of this work. In aviation, the risk of collision is a delicate and important subject, which merits the right approach. With the continuing growth of air traffic and the introduction of RPASs (Remotely Piloted Aircraft System), it is necessary to find better solutions and develop new systems to keep the control of the airspace. In this work, the main objective is to obtain a complete and functional computational algorithm, which could be included in an obstacle detection and avoidance system. Its unique feature of optical detection makes it mostly appropriated for RPASs.

The application of Optical Techniques is mostly used in aircrafts to detect objects under them [1] or even to prevent a collision with terrain [2]. Some technologies also use optic flow sensors to detect and prevent collisions [3, 4]. In this case, the optical system will be used to detect obstacles in front of the aircraft.

The detection of an obstacle will be performed by the two infrared cameras strategically positioned in the aircraft. The objectives to accomplish with this method are: capable of dealing with collision detection characteristics; in case of detecting a possible threat of collision, describing the safe zone as the area outside a conflict cone; assessing if the threat of collision previously detected is real; in case the danger is real, changing the aircraft's trajectory by altering one or more flight characteristics. To achieve the most efficient method possible some theoretical methods were explored, like the Convex Hull Method, which is a simple geometrical method, and a variation method based on differential equations.

With the aim of testing the algorithm in different situations, a total of six possible cases were generated. All the results showed coherence and efficiency, which confirms the success of this computational algorithm as a detection and collision avoidance method.

# Keywords

Aeronautic, Air Traffic, Collision Avoidance System, Optical Detection, Computational Algorithm

# Resumo

O desenvolvimento de um novo sistema de prevenção de colisões, que consiga detetar e calcular as mudanças necessárias para prevenir um acidente iminente, é o interesse focal deste trabalho. Na aviação, o risco de colisão é um assunto delicado e importante, o qual merece a correta abordagem. Com o crescimento continuo do trafego aéreo e a introdução dos RPASs (Remotely Piloted Aircraft System), é necessário procurar melhores soluções e desenvolver novos sistemas para manter o controlo do espaço aéreo. Neste trabalho, o principal objetivo é obter um algoritmo computacional completo e funcional, o qual poderá ser incluído num sistema de deteção e evasão de obstáculos. A sua característica única de deteção ótica torna-o principalmente apropriado para RPASs.

A aplicação de Técnicas Óticas é principalmente utilizada nas aeronaves para deteção de objetos debaixo destas [1] ou mesmo para prevenir uma colisão com o terreno [2]. Algumas tecnologias utilizam sensores de fluxo ótico para detetar e prevenir colisões [3, 4]. Neste caso, o sistema ótico será utilizado para detetar obstáculos à frente da aeronave.

Os objetivos a realizar com este sistema são: capaz de lidar com as características de deteção de colisão; em caso de detetar uma possível ameaça de colisão, descrever a zona segura como a área fora do cone de conflito; avaliar se a ameaça de colisão é real; no caso do perigo ser real, mudar a trajetória da aeronave alterando uma ou mais característica de voo. Para obter o sistema mais eficiente possível alguns métodos teóricos foram explorados, como o método do 'Convex Hull', o qual é um simples método geométrico, e um método de variação com base nas equações diferenciais.

Com o objetivo de testar o sistema em diferentes situações, um total de seis casos possíveis foram gerados. Todos os resultados mostraram coerência e eficácia, o que confirma o sucesso do algoritmo computacional como um sistema de deteção e evasão de colisões.

# Palavras-chave

Aeronáutica, Trafego Aéreo, Sistema de Prevenção de Colisões, Deteção Ótica, Algoritmo computacional

# Index

# List of Figures

# List of Tables

# List of acronyms

| | |
|---|---|
| TCAS | Traffic Collision Avoidance System |
| RPAS | Remotely Piloted Aircraft System |
| VD | Vertical Distance |
| LD | Lateral Distance |
| MVD | Minimum Vertical Distance |
| MLD | Minimum Lateral Distance |

# Chapter 1

# Introduction

The concept of globalization, which is related with two other important concepts: borderless countries and global village, is one of the reasons for a world in which all countries are increasingly connected. Globalization is a worldwide movement, which incorporates in many aspects all countries, all people and all cultures. Nowadays, these concepts influence everything around us, including us, so it has become more than a concept, it has become the new reality. Many economical and commercial sectors, like the Aeronautical and Aerospace sector, are important vehicles to globalization.

The Aviation sector had a huge impact from the beginning. It revolutionized the idea of traveling, people no longer needed cars and boats because they could cross oceans and continents by air. This new form of transport means you can travel in comfort, both short or long distances, in a much shorter period of time than ever before. The transportation of cargo and merchandise from all around the world is also easier and more efficient. Aviation, one of the most important globalization vehicles, is experiencing a growing demand.

The prospects for future decades are for a continuing growth of air traffic. More aircraft operating at the same time requires a higher level of control and of precision and efficiency. An aircraft is a complex machine and if there are risks while operating an aircraft in airspace with reasonable air traffic, in condensed air traffic those risks are much higher. However, one of many strands of this sector's development is 'Safety and Security'. Those two words are often connected but they are two different concepts with distinct meanings in aviation. Safety is associated with the defence and safeguarding against any accident or mistake/defect during all the most important phases of an aircraft (design, construction, maintenance and operation). On the other hand, security is all the existing procedures to avoid any type of malevolent actions, like terrorism, targeting the airplane and its occupants, crew and passengers. This strand goal is to minimise all risks associated with air transport. One specific risk is collision, between two or more aircraft or between an aircraft and an object. The minimum vertical distance between aircraft is three hundred meters [5]. In terms of the minimum lateral distance, it depends on the specific situation.

Collision is an important risk and a delicate subject, which merits the correct approach to find the most efficient solution. The investigation and development of new anti-collision systems is an ongoing process, actually there are several research activities in collision avoidance, each one with their own approach but all with the same main goal: finding the most efficient and innovative solution to this specific problem. One anti-collision system created, tested, improved and marketed is TCAS (Traffic Collision Avoidance System), which is currently installed in innumerable aircrafts. It is an anti-collision system based on monitoring the airspace around the aircraft looking for other aircrafts equipped with a transponder, and then informs the pilots of a possible threat [6]. This system only provides local separation. However, for areas with high density of air traffic this approach is considered by several people as not the most efficient. So, in opposition to the local separation there is the concept of global collision avoidance which considers global traffic in a specific area and not only pairs of aircrafts. Some research activities focus their attention on this last concept and combine the collision avoidance problem with the future possibility of free-flight [7]. Free-flight represents an increase in the autonomy of the aircraft, which means that each aircraft has the capacity to choose its own trajectory but at the same time must ensure its own security. It’s possible this idea will be implemented in the future if we think about the increasing air traffic, mentioned before, and all the complications involved, such as the high workload to Air Traffic Controllers. However, this concept involves an increase in the pilot’s responsibility and it is essential to support them with innovative systems and new interface designs [8].

The current problem is not only about the growing air traffic of conventional aircraft but also the introduction of new technologies like RPAS (Remotely Piloted Aircraft System) in the airspace, causing an even more complex situation in terms of air traffic. Different RPASs, with different autonomies, ranges and technologies, have become available on the market. Yet, unlike traditional aircraft, most RPASs are not equipped with any anti-collision system and with an increasing search for this equipment the number of incidents may grow. So, it is essential to find new solutions to maintain the smooth operation of air traffic. This matter is beginning to be addressed in several countries and by international associations, which means that appropriate regulations are being established and creative campaigns are beginning to be disclosed. However, there is still a lot of work ahead in order to develop and improve this area. One future possibility is to introduce an anti-collision system in each RPAS. However, it is important to understand that RPASs can serve different purposes, from a simple hobby to military uses, so, the anti-collision system must be in accordance with the needs and specifications of each RPAS. In terms of military uses, the privacy and autonomy of RPASs is a focal feature. Different studies related with obstacle avoidance systems in RPASs have been developed and show possible solutions to different problems. From exploring the possibility of using optical systems to maintain ground separation in order to prevent a collision with terrain [1], to studies with the idea of optimization by applying and comparing more than one optimisation algorithm [9]. There is also the idea of applying the Markov Decision Processes in terms of collision avoidance for RPASs [10].

In general terms, when developing a collision avoidance system, it is necessary to pay attention to all the details involved in the process and it is fundamental to assure that the new system meets not only the mission requirements but also the existing regulations regarding safety issues, for that the designing method should be consistent and efficient [11]. A complete anti-collision method should not only detect the danger of collision but, it should also be capable of preventing a possible collision. Still, we can divide an anti-collision system in two parts by logical order: the first one detects the danger and automatically determines the area that the aircraft must avoid; the second part assesses if the path of the aircraft is within the conflict area and, if it is, makes the necessary changes.

## 1.1 Objectives

This work focuses on the delicate subject of collision and the necessity of creating new approaches to preventing this specific risk. The main objective is to develop a collision avoidance method, based on optical detection, with the capacity to be used in real life situations.

To achieve a functional algorithm, several steps must be completed and any problems and difficulties that arise have to be overcome. Each step is an objective to accomplish.

The first step is to calculate the points' coordinates and the distance vectors between the aircraft and each point from the cameras' images, which will allow for determining the minimum value of vertical and lateral distances. Through these values, it is possible to assess whether there is a threat of collision or not.

In case the possibility of collision is affirmative the next step is to determine the detailed area in two dimensions that the aircraft must avoid in order to prevent an imminent collision. For this process, a method was chosen that is capable of determining based on the point coordinates an approximation to the real format of the obstacle to avoid. A simple geometrical method named as Convex Hull Method [12] was selected and will be explored in detail in the section 1.2.

A third objective is to assess the reality of each case and to conclude if the danger is in fact real or if the aircraft can continue its path.

If the threat of collision is real it is required to change the aircraft's trajectory, which is the last step. More specifically: modify one flight characteristic, in the ideal case, or more, if necessary, to prevent an imminent collision, keep the aircraft safe and to allow it to continue its mission.

## 1.2 Theoretical method: Convex Hull

This method is a geometrical method whose main goal is to incorporate a group of points in just one convex polygon. A complete and correct definition is: given a specific group of points in two or more dimensions the correspondent convex hull is a convex polygon with the smallest area/volume possible and it must include all the points of the group. Not all the points need to be or must be vertices of the polygon but those points must be inside the polygon.

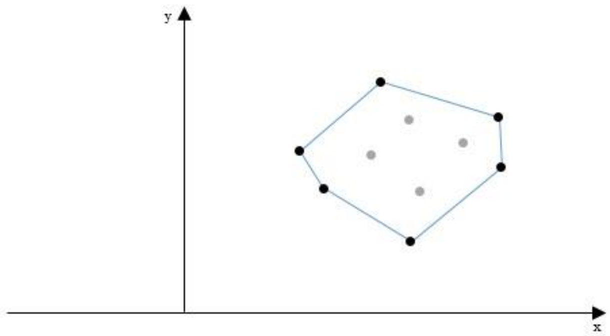


Figure 1.1- An illustration of one example of convex hull in a ‘xy’ plan.

There are many algorithms related to this method with different approaches. Three, which are considered the most accurate, were selected to be described next.

### 1.2.1 Jarvis March Algorithm

The Jarvis March Algorithm is a simple algorithm capable of defining the convex hull of a certain set of points [13].

To simplify we will assume that all points are in a general position and not in a special position. A special position could be for example three collinear points. Although we are making this assumption, it is important to note that we could actually include those special positions in the algorithm, it will only turn the algorithm more complex.

The complete implementation of Jarvis’ algorithm must include degenerative cases of Convex Hull with one or two vertices and take into consideration arithmetic precision problems.

To apply this algorithm correctly, it’s necessary to follow the next steps:

- First, we start with ‘i=0’ and one point ‘$p_0$’ that we know that belong to the convex hull, it is the leftmost point of the group.

- Then, we select the point ‘$p_{i+1}$’ making sure that all other points are on the right side of the line $p_ip_{i+1}$. This last point is chosen by polar angle comparison of all points relatively to ‘$p_i$’.

- This process is repeated consecutively, just like a cycle in computational programming.

Every time the process is repeated the parameter ‘i’ suffers an increase: ‘i=i+1’, which means that our initial point became the last point we found every time we repeat.

### 1.2.2 Graham Scan Algorithm

The Graham scan algorithm is a tool to determine the vertices of convex hull of a specific group of points [14].

To correctly understand this algorithm, it will be explained by steps:

- The first step is finding the point with smallest ‘y’ coordinate, if there is more than one point we must chose the point with smallest ‘x’ coordinate too. The chosen point should be named as point ‘P’.

- The second step is number in ascending order the rest of the points according to the angle that each point with point ‘P’ relatively to axis ‘x’ make. To successfully complete this step there is no need to calculate the angles, it is possible to use certain functions in an interval of [0,π].

- Considering the previous steps, it is now necessary to evaluate for each point if the dislocation to the next two points is a left or right turn. If it is a right turn the line from the second point to the last one (third point) does not belong to the convex hull. Nevertheless, we can conclude that the second point is on the inside.

- Then for the last point we must repeat this procedure. So on until a left turn happens. In that moment, the algorithm keeps the line from the second point to the last point and starts again with the last point. However, all the points already known as being inside the convex hull must not be taken into consideration when the process repeats after a left turn.

The correct application of all steps will result in obtaining the convex hull of the initial set of points.

This method does not require the calculation of the angles just simple arithmetic. To better understand, given three points (2D) it is necessary to calculate the ‘z’ coordinate of the vector product:

$$(x_2 - x_3)\times(y_3 - y_1) - (y_2 - y_1)\times(x_3 - x_1) \qquad (1.1)$$

where ‘$x_1$’, ‘$x_2$’ and ‘$x_3$’ are, respectively, the ‘x’ coordinate of point 1, point 2 and point 3 and ‘$y_1$’, ‘$y_2$’ and ‘$y_3$’ are, respectively, the ‘y’ coordinate of point 1, point 2 and point 3.

Then: if the product is equal to zero the points are collinear; if the result is positive it is a left turn; if the result is negative it is a right turn.

### 1.2.3 Chan's Algorithm

In computational geometry, Chan's algorithm has the capacity to determine the convex hull of a set of points in two dimensions (2D) [15]. This algorithm is mostly the combination of two other algorithms, which allows for optimization of time.

Considering a plane case, two possible algorithms are, for example, the Graham Scan and the Jarvis's March (two algorithms already exposed).

To better understand this algorithm, a more detailed explanation will be presented next. But first it is necessary to: establish a set of 'n' points, named 'P', and consider a two dimensions' case.

In a first phase, it is necessary to assume the value of parameter 'h' as known and considering that: m=h. Although this initial consideration is not realistic, it is required. Then:

- The set P must be divided in smaller subsets named 'Q'. The maximum number of subsets is:

$$\frac{n}{m}+1 \tag{1.2}$$

where 'n' is the number of points and 'm' is a constant with equal value to the parameter 'h'.

- Through the Graham Scan algorithm, or other algorithm with exactly O(nlogn) time, it is possible to compute the convex hulls of each subset.

The second phase is more complex and includes the application of the Jarvis' algorithm.

- In this phase the convex hulls of the subsets 'Q' are known and with them it is possible to determine the function $f(p_i,Q)$ in O(logm) time by using binary search. So in O((n/m) logm) time we have determine the function $f(p_i,Q)$ for all the subsets O(n/m) of 'Q'.

- Then it is possible to define the function $f(p_i,P)$ through the same technique used in the Jarvis' algorithm but considering only the points included on the function $f(p_i,Q)$.

Knowing that Jarvis March repeats these procedure O(h) times we can conclude that this second phase takes O(nlogm) time.

Executing correctly these two phases the result is the convex hull of a set of n points in O(nlogh) time.

Relatively to the parameter ‘m’, initially we must consider ‘m’ as a constant of lower value and then increase it until ‘m’ is bigger than ‘h’.

## 1.3 Theoretical method: Variation of a parameter

The study of the behaviour of the flight characteristics requires a method able of calculating the variation of a parameter. A simple and effective method based in differential equations [16] was chosen, which calculates how much the value of the parameter being studied changes in a specific interval of time.

In mathematical terms:

- Equation to calculate the rate of the variation in a specific interval of time:

$$\dot{x} = \tau \times (x_{ref} - x_i) \tag{1.3}$$

where ‘$\dot{x}$’ is the rate of variation of a specific feature; ‘$\tau$’ is the inverse of the time variable, ‘$x_{ref}$’ is the reference value for the feature and ‘$x_i$’ is the initial value that the feature assumes.

## 1.4 Brief Introduction of the Method to Develop

The method can be divided in two different phases: the Detection and the Prevention.

The process of obstacle detection is performed by two infrared cameras strategically placed in the aircraft (as described in the figure 1.2). Each camera will provide two angles for each point they detect.

Finalized the first phase, the second phase, named as prevention, begins, which means that the algorithm is initiated.

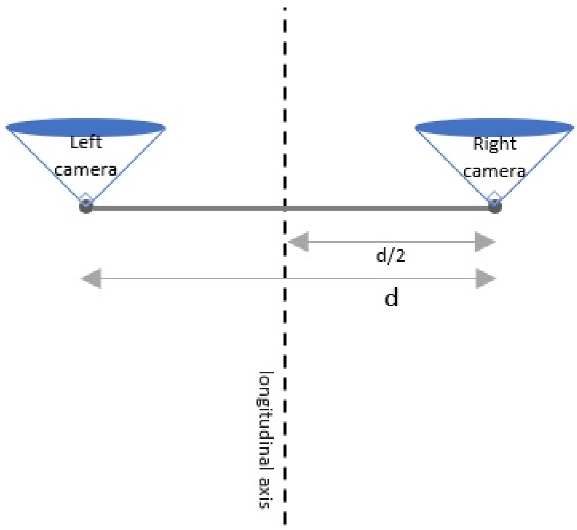


Figure 1.2- A scheme illustrating the position of the cameras in the aircraft.

## 1.5 Dissertation Plan

This first chapter consists in: an introduction of the main subject of this dissertation, a description of the objectives to accomplish and a detailed explanation of two theoretical methods.

In the second chapter, a detailed description will be presented of all the necessary steps to complete an anti-collision method based on optical detection. Along with the explanations there will also be illustrative schemes and fundamental equations.

The third chapter will contain all the necessary simulations to properly test the algorithm. For each unique situation, it will be possible to find the initial data, visualise the results (graphics and tables) and analyse a complete discussion of results.

In the fourth and last chapter, the final conclusions of this work will be drawn and explained.

# Chapter 2

# Development of a Collision Avoidance Method

In this second chapter, a detailed description is presented of all necessary steps to complete an anti-collision method based on optical detection. Along with the explanations will also be illustrative schemes and fundamental equations.

## 2.1 General Algorithm

Step 1: Conflict Assessment (section 2.2)

For each unique situation, determine based on the angles provided by the cameras if any threat of collision exists. This section is divided in two subsections, which will provide the necessary data to conclude this step.

- Components of the distance vector (subsection 2.2.1)

Calculate all the components of the distance vectors between the aircraft and each point captured by the cameras.

- Vertical and Lateral Distance (subsection 2.2.2)

With the information from the previous subsection, calculate the vertical and lateral distance between the aircraft and each point. An analysis of these distances will allow for the determination of the minimum value of the vertical and lateral distance between the aircraft and the obstacle.

The following steps will only be necessary in case of the existence of a possible threat of collision.

Step 2: Convex Hull Algorithm (section 2.3)

In this step, the Convex Hull method will be used to obtain the convex polygon of each situation. It will allow for visualization of an approximation to the real format of the obstacle.

- Implementation Algorithm (subsection 2.3.1)

Given that the computational tool selected is the Matlab, a specific matlab function will be applied.

Step 3: Conflict Zone (section 2.4)

Determine the area that the aircraft must avoid in order to prevent a possible collision. This section includes two subsections, each one is a specific phase of this step.

- Establish the Sphere (subsection 2.4.1)

The central point and the minimum radius of the sphere encompassing the obstacle will be calculated. Although it is always a three-dimensional situation, the projections in the ‘xz’ and ‘xy’ plan will be used.

- The Final Conflict Zone (subsection 2.4.2)

Having completed the sphere and its projections, it is necessary to find the remaining area to avoid. In three-dimensions, it will be resumed to a conflict cone. However, a different process will be applied, which will allow valuable information for future steps.

Step 4: Assessment of Reality (section 2.5)

The aircraft’s data will be compared with information regarding the conflict zone, previously determined, to analyse the reality of each situation and conclude if the threat of collision is real or not.

The following two steps will only be applied in the situations where the threat is confirmed to be real.

Step 5: Correction Method (section 2.6)

There are three possibilities to modify the aircraft’s path, changing the value of: the heading, the altitude or the velocity. The best option is to alter only one parameter, preferably the heading. However, sometimes it may be necessary to also change the altitude. Both will be analysed and, if needed, new values will be calculated.

- Heading Correction (subsection 2.6.1)

In this subsection, the new value for the aircraft’s heading will be calculated.

- Altitude Correction (subsection 2.6.2)

In this subsection, the new value for the aircraft’s altitude will be calculated.

Step 6: Variation of a Specific Parameter (section 2.7)

After changing one or both parameters a simple study based on differential equations will be performed to analyse their behaviour over time.

- Heading Variation over time (subsection 2.7.1)

In this subsection, the aircraft's heading will be studied.

- Altitude Variation over time (subsection 2.7.2)

In this subsection, the aircraft's heading will be studied.

Finishing all the steps, the algorithm starts over with new data provided by the cameras. Since the cameras detect points, it is a continuous cycle.

## 2.2 Step 1: Conflict Assessment

Knowing the exact distance between cameras, 'd', along with the data provided by them, it is possible to verify, for each situation, if any threat of collision exists.

First, it is necessary to calculate the distance vector between our aircraft and each point through the angles provided by the cameras (in the left camera – angles alpha and delta, in the right camera – angles beta and gamma, Figure 2.1). For each point the distance vector is:

$$\vec{D_i}(x_d, y_d, z_d) \tag{2.1}$$

where '$\vec{D_i}$' is the distance vector; 'i' is the indexing number to identify the point under study and '$x_d$', '$y_d$' and '$z_d$' are, respectively, the 'x', 'y' and 'z' components of the vector. These three components can also be interpreted as the points coordinates ('x', 'y' and 'z'), assuming that the axis origin is on the aircraft.

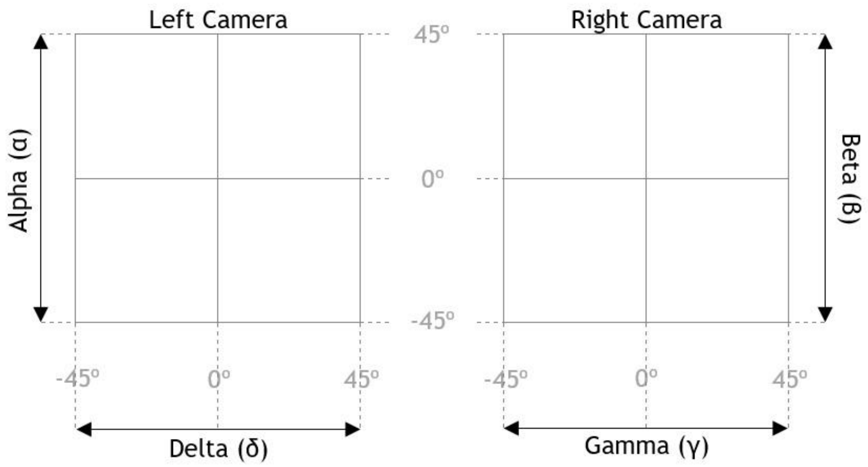


Figure 2.1- Illustration of an example of the left and right camera images with the respective angles.

After calculating all the distances, it is necessary to compare the results with the values of the minimum vertical distance (MVD) and the minimum lateral distance (MLD). If both vertical distance (VD) and lateral distance (LD) are greater than the minimum distance (VD>MVD and LD>MLD) or even if both distances are equal to the minimum distance (VD=MVD and LD=MLD) the danger of collision does not exist so, the aircraft can continue its path. If both distances are less than the minimum distance (VD<MVD and LD<MLD) the danger of collision is a possibility.

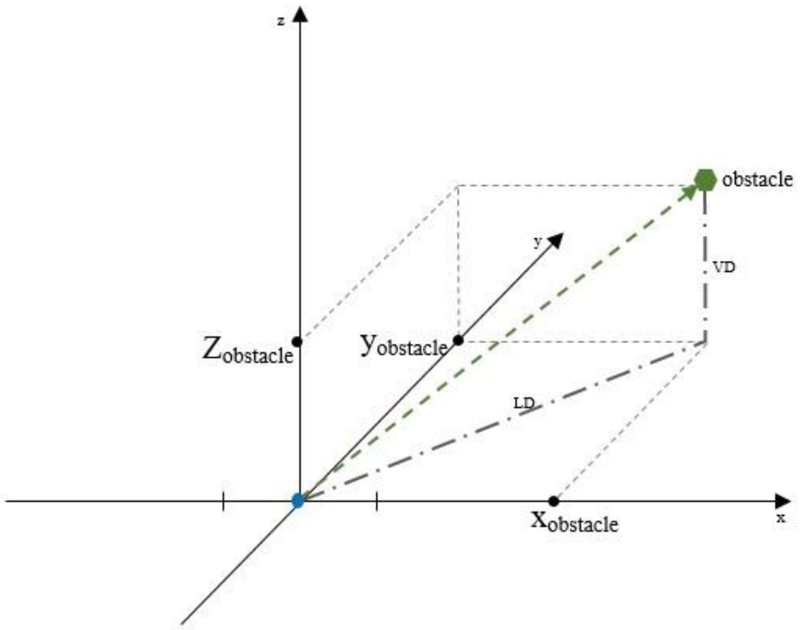


Figure 2.2- A three-dimension (x,y,z) scheme to demonstrate visually an example of the distances VD and LD. The blue circle represents the aircraft and the star is a representation of an obstacle.

### 2.2.1 Components of the distance vector

To correctly determinate all the points' coordinates there are two parameters essential to the process, the distance from the left camera to the obstacle in terms of the 'x' axis, 'DL', and the same but from the right camera, 'DR'.

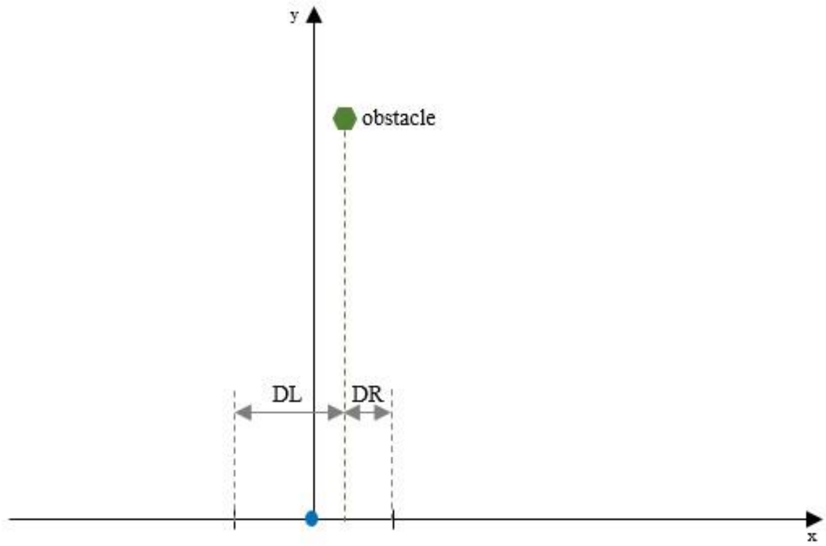


Figure 2.3- A two-dimension (x,y) scheme illustrating an example of the parameters 'DL' and 'DR'.

In the Figure 2.3, the blue circle represents the aircraft and the star is a representation of an object.

<u>Component 'y':</u> the equations to determine the value of this specific component can suffer small modifications depending on the zone where the obstacle is. There are a total of five possible zones.

- if the value of gamma is smaller than zero and delta is greater than zero (first zone, Figure 2.4), we have:

$$\xi_j = -\left|delta_j\right| \tag{2.2}$$

$$\varphi_j = -\left|gamma_j\right| \tag{2.3}$$

$$DR = \frac{\cot \xi_j \times d}{\cot \varphi_j + \cot \xi_j} \tag{2.4}$$

$$DL = d - DR \tag{2.5}$$

$$y = -\cot \varphi_j \times DR \tag{2.6}$$

where, '$\xi_j$' corresponds to the negative of the absolute value of '$delta_j$'; 'j' is the indexing number to identify the point under study; 'delta' is the angle provided by the left camera; '$\varphi_j$' corresponds to the negative of the absolute value of '$gamma_j$'; 'gamma' is the angle provided by the right camera; ‘DR’ is the distance in terms of axis ‘x’ between the object and the right camera (Figure 2.3); ‘d’ is the distance between the cameras; ‘DL’ is the distance in terms of axis ‘x’ between the object and the left camera (Figure 2.3) and ‘y’ is the component to be determined.

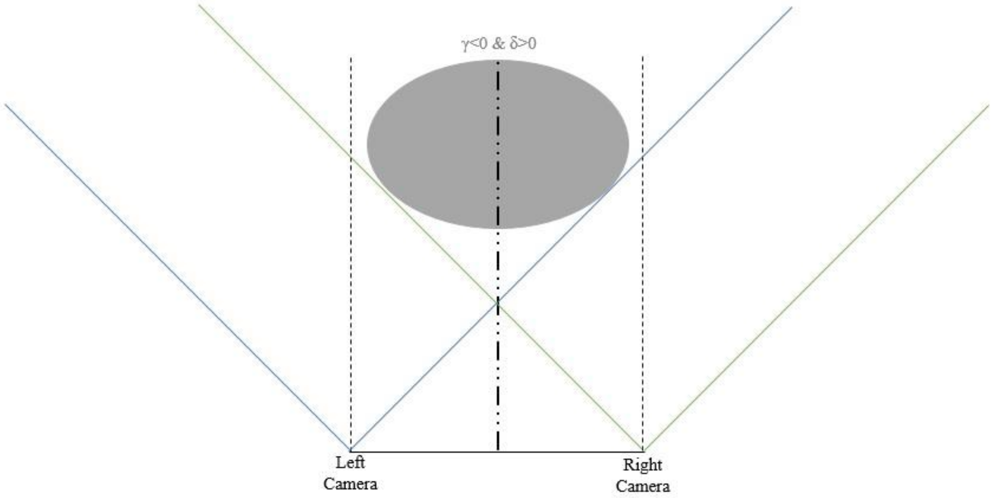


Figure 2.4- Scheme illustrating the first zone: the point detected is in the grey zone; which implies that the value of gamma is smaller than zero and delta is greater than zero.

- if the value of gamma is equal to zero and delta is greater than zero (second zone, Figure 2.5), we have:

$$\xi_j = -\left|delta_j\right| \quad (2.7)$$

$$DR = 0 \quad (2.8)$$

$$DL = d \quad (2.9)$$

$$y = -\cot \xi_j \times DL \quad (2.10)$$

where, ‘$\xi_j$’ corresponds to the negative of the absolute value of ‘$delta_j$’; ‘j’ is the indexing number to identify the point under study; ‘delta’ is the angle provided by the left camera; ‘DR’ is the distance in terms of axis ‘x’ between the object and the right camera (Figure 2.3); ‘d’ is the distance between the cameras; ‘DL’ is the distance in terms of axis ‘x’ between the object and the left camera (Figure 2.3) and ‘y’ is the component to be determined.

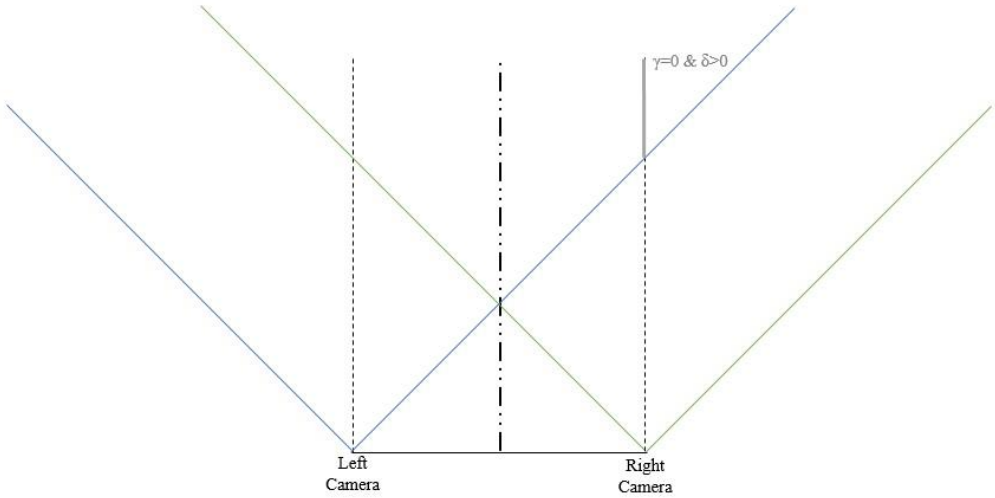


Figure 2.5- Scheme illustrating the second zone: the point detected is in the grey line; which implies that the value of gamma is equal to zero and delta is greater than zero.

- if the value of gamma is smaller than zero and delta is equal to zero (third zone, Figure 2.6), we have:

$$\varphi_j = -\left|gamma_j\right| \tag{2.11}$$

$$DR = d \tag{2.12}$$

$$DL = 0 \tag{2.13}$$

$$y = -\cot \varphi_j \times DR \tag{2.14}$$

where, '$\varphi_j$' corresponds to the negative of the absolute value of '$gamma_j$'; 'j' is the indexing number to identify the point under study; 'gamma' is the angle provided by the right camera; 'DR' is the distance in terms of axis 'x' between the object and the right camera (Figure 2.3); 'd' is the distance between the cameras; 'DL' is the distance in terms of axis 'x' between the object and the left camera (Figure 2.3) and 'y' is the component to be determined.

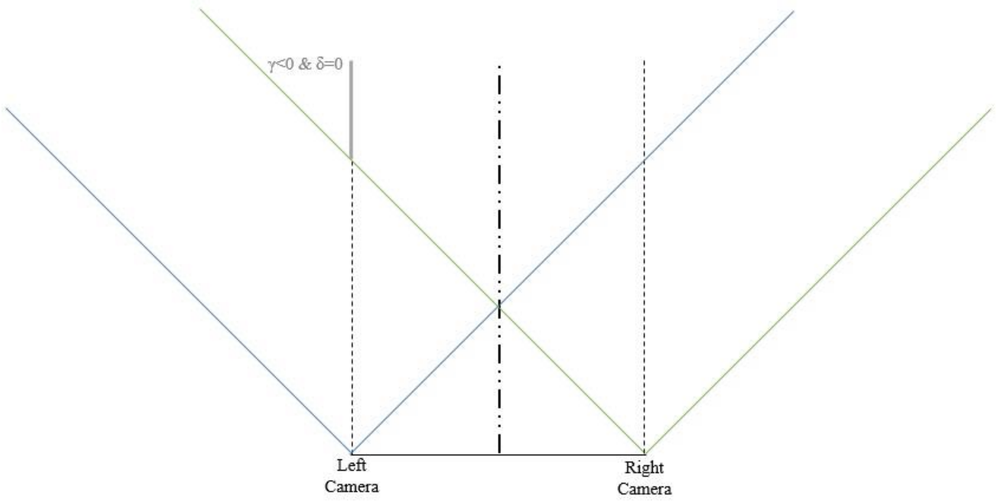


Figure 2.6- Scheme illustrating the third zone: the point detected is in the grey line; which implies that the value of gamma is smaller than zero and delta is equal to zero.

- if the values of gamma and delta are greater than zero (fourth zone, Figure 2.7), we have:

$$\xi_j = -\left|delta_j\right| \quad (2.15)$$

$$\varphi_j = -\left|gamma_j\right| \quad (2.16)$$

$$DR = \frac{\cot \xi_j \times d}{\cot \varphi_j - \cot \xi_j} \quad (2.17)$$

$$DL = d + DR \quad (2.18)$$

$$y = -\cot \varphi_j \times DR \quad (2.19)$$

where, '$\xi_j$' corresponds to the negative of the absolute value of '$delta_j$'; 'j' is the indexing number to identify the point under study; 'delta' is the angle provided by the left camera; '$\varphi_j$' corresponds to the negative of the absolute value of '$gamma_j$'; 'gamma' is the angle provided by the right camera; 'DR' is the distance in terms of axis 'x' between the object and the right camera (Figure 2.3); 'd' is the distance between the cameras; 'DL' is the distance in terms of axis 'x' between the object and the left camera (Figure 2.3) and 'y' is the component to be determined.

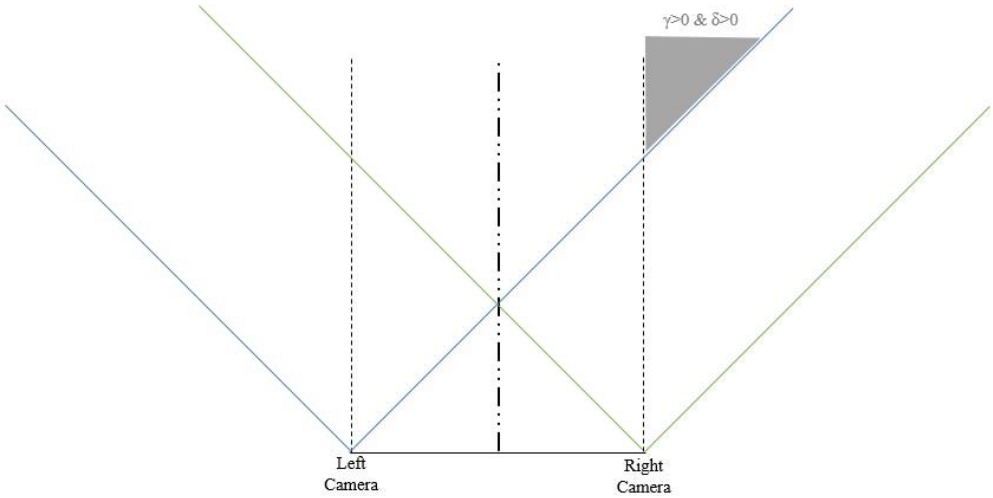


Figure 2.7- Scheme illustrating the fourth zone: the point detected is in the grey zone; which implies that the values of gamma and delta are greater than zero.

- if both values of gamma and delta are smaller than zero (fifth zone, Figure 2.8), we have:

$$\xi_j = -\left|delta_j\right| \tag{2.20}$$

$$\varphi_j = -\left|gamma_j\right| \tag{2.21}$$

$$DR = \frac{\cot \xi_j \times d}{\cot \xi_j - \cot \varphi_j} \tag{2.22}$$

$$DL = DR - d \tag{2.23}$$

$$y = -\cot \varphi_j \times DR \tag{2.24}$$

where, '$\xi_j$' corresponds to the negative of the absolute value of '$delta_j$'; 'j' is the indexing number to identify the point under study; 'delta' is the angle provided by the left camera; '$\varphi_j$' corresponds to the negative of the absolute value of '$gamma_j$'; 'gamma' is the angle provided by the right camera; 'DR' is the distance in terms of axis 'x' between the object and the right camera (Figure 2.3); 'd' is the distance between the cameras; 'DL' is the distance in terms of axis 'x' between the object and the left camera (Figure 2.3) and 'y' is the component to be determined.

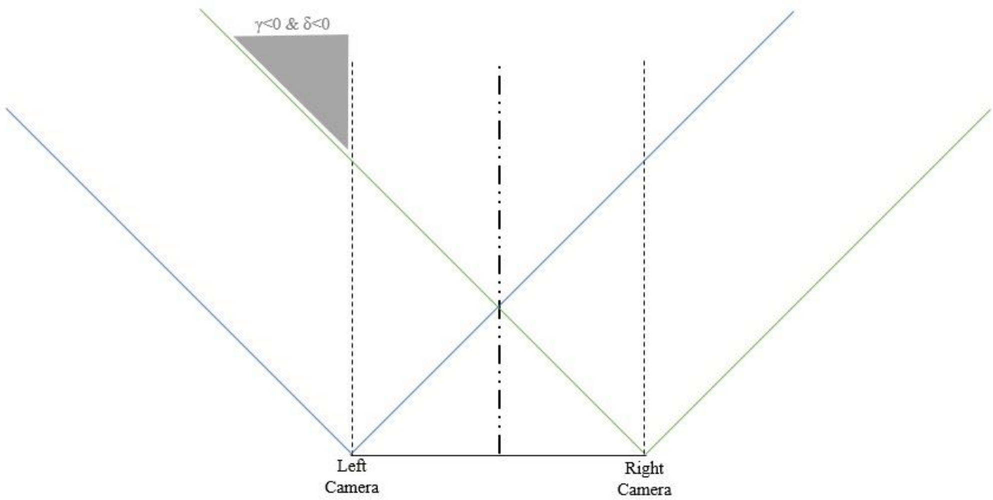


Figure 2.8- Scheme illustrating the fifth zone: the point detected is in the grey zone; which implies that the values of gamma and delta are smaller than zero.

Component ‘z’: the process to calculate this component may vary according to the values of the parameters ‘DL’ and ‘DR’ and it can be resumed in two possible cases, which are:

- if, independently of the value of ‘DL’, the value of ‘DR’ is greater than zero:

$$\text{hypotenuse} = \sqrt{(DR^2 + y^2)} \tag{2.25}$$

$$z = \tan(\text{beta}_j) \times \text{hypotenuse} \tag{2.26}$$

where ‘hypotenuse’ is the vector distance between our aircraft and the object when projecting in the ‘xy’ plane; ‘DR’ is the distance in terms of axis ‘x’ between the point and the right camera (Figure 2.3); ‘y’ is the component calculated before; ‘z’ is the component to be determined and ‘beta’ is an angle provided by the right camera.

- if the value of ‘DR’ is equal to zero and ‘DL’ is equal to ‘d’:

$$\text{hypotenuse} = \sqrt{(DL^2 + y^2)} \tag{2.27}$$

$$z = \tan(\text{alpha}_j) \times \text{hypotenuse} \tag{2.28}$$

where ‘hypotenuse’ is the vector distance between our aircraft and the object when projecting in the ‘xy’ plane; ‘DL’ is the distance in terms of axis ‘x’ between the point and the left camera (Figure 2.3); ‘y’ is the component calculated before; ‘z’ is the component to be determined and ‘alpha’ is an angle provided by the left camera.

Component ‘x’: for this last component three possible scenarios exist to determine:

- if DR>DL:

$$x = -(DR - \left(\frac{d}{2}\right)) \quad (2.29)$$

where ‘x’ is the component to be determined; ‘DR’ is the distance in terms of axis ‘x’ between the object and the right camera (Figure 2.3) and ‘d’ is the distance between the cameras.

- if DR<DL:

$$x = DL - \left(\frac{d}{2}\right) \quad (2.30)$$

where ‘x’ is the component to be determined; ‘DL’ is the distance in terms of axis ‘x’ between the object and the left camera (Figure 2.3) and ‘d’ is the distance between cameras.

- else:

$$x = 0 \quad (2.31)$$

where ‘x’ is the component to be determined.

## 2.2.2 Vertical and Lateral Distance

The VD between our aircraft and each point corresponds to the component ‘z’. However, in terms of the LD it is necessary to calculate based on the ‘x’ and ‘y’ coordinates. Vertical and lateral distance for each point ‘j’:

$$VD_j = z_j \quad (2.32)$$

$$LD_j = \sqrt{((x_j)^2 + \left(y_j\right)^2)} \quad (2.33)$$

where ‘$VD_j$’ is the vertical distance between our aircraft and the point ‘j’; ‘j’ is the indexing number to identify the point; ‘$z_j$’ is the component ‘z’ of the point ‘j’; ‘$LD_j$’ is the lateral distance between our aircraft and the point ‘j’; ‘$x_j$’ and ‘$y_j$ ’ are respectively the ‘x’ component and ‘y’ component of the point ‘j’.

## 2.3 Step 2: Convex Hull Algorithm

A definition of convex hull method and three of the most important algorithms were previously exposed. In this section, it will be applied in the process to determine the specific area that the aircraft must avoid. For each situation, we will determine the respective convex polygon. However, the convex polygon does not necessarily represent the real format of the obstacle being studied, it is just an approximation to the actual format.

### 2.3.1 Implementation Algorithm

Since the computational tool chosen for this work was Matlab the determination of the convex hull for each case will be through one specific Matlab function named 'convhull', which allows not only to find the specific points that are vertices but also to graphically demonstrate the convex hull.

Algorithm used for the convex hull method: assuming equal 'y' to all points (2D).

$$k = \text{convhull}(x,z) \tag{2.34}$$

where 'k' represents the convex hull function to determine; 'convhull(x,z)' is the matlab function; 'x' and 'z' are, respectively, the vector with all the 'x' and 'z' coordinates of the points.

## 2.4 Step 3: Conflict Zone

The determination of the convex hull is just the first step to accomplish a second objective, finding the specific area to avoid, there are two more necessary steps: first, establish the sphere involving the obstacle and, second, the cone, which represents the conflict zone.

### 2.4.1 Establish the Sphere

In the process to determine the convex hull the points are separated by two categories: inside the convex hull and vertices. Knowing the points belonging to the category 'vertices' it is possible to calculate a central point of the convex hull by the average of those points coordinates. If this same procedure is applied to all the points, instead of only the 'vertices', the result is the midpoint of the initial set, which will be the sphere centre.

The best method to correctly define the minimum radius possible is to calculate the distance between the centre and each other point, then the biggest distance calculated is the minimum radius. However, in terms of security and safety issues a safety margin must be added to the minimum radius calculated before.

In terms of algorithm:

Midpoint:

$$c_x = \frac{\sum x(j)}{n_j} \quad (2.35)$$

$$c_z = \frac{\sum z(j)}{n_j} \quad (2.36)$$

where '$c_x$' is the 'x' coordinate of the central point; 'x(j)' is the 'x' coordinate of the point 'j'; 'j' is the indexing number to identify the point; '$n_j$' is the total number of points; '$c_z$' is the 'z' coordinate of the central point and 'z(j)' is the 'z' coordinate of the point 'j'.

Distance between the midpoint and each point:

$$dis(j) = \sqrt{(x(j) - c_x)^2 + (z(j) - c_z)^2} \quad (2.37)$$

where 'dis(j)' is the distance between the central point and the point 'j'; 'j' is the indexing number to identify the point; 'x(j)' is the 'x' coordinate of the point 'j'; '$c_x$' is the 'x' coordinate of the central point; 'z(j)' is the 'z' coordinate of the point 'j' and '$c_z$' is the 'z' coordinate of the central point.

Minimum radius:

$$r = (1-\omega)\times dis_{max} \quad (2.38)$$

where 'r' is the radius of the circumference; '$\omega$' is the safety margin and '$dis_{max}$' is the maximum distance previously calculated.

This sphere can be projected in any plan and it will always have the same radius and centre coordinates.

### 2.4.2 The Final Conflict Zone

In a three-dimensional case, the result would be a cone and just two things are necessary, a base and a height, to define it. The cone base is a circumference, whose' characteristics were previously determined. And the cone height corresponds to the norm of the vector distance between the aircraft and the sphere centre (midpoint). This vector can be calculated since both aircraft's coordinates and the centre coordinates are known.

In terms of two-dimensions, the cone will be projected on the ‘xy’ plane and will correspond to a circumference and two specific lines, which must be tangent to the circumference and pass on the origin. To determine the equations of the lines it is essential to first find the only two points belonging both to one line and to the circumference. The equations to find the two necessary points are:

$$r = \sqrt{(p_x - c_x)^2 + (p_y - c_y)^2} \tag{2.39}$$

$$h_p = \sqrt{p_x^2 + p_y^2} \tag{2.40}$$

where ‘r’ is the circumference radius; ‘$p_x$’ is the ‘x’ coordinate of the tangent point; ‘$c_x$’ is the ‘x’ coordinate of the central point; ‘$p_y$’ is the ‘y’ coordinate of the tangent point; ‘$c_y$’ is the ‘y’ coordinate of the central point and ‘$h_p$’ is the distance vector between the aircraft and the new point. The result of this equation is two sets of ‘x’ and ‘y’ coordinates corresponding to two different points.

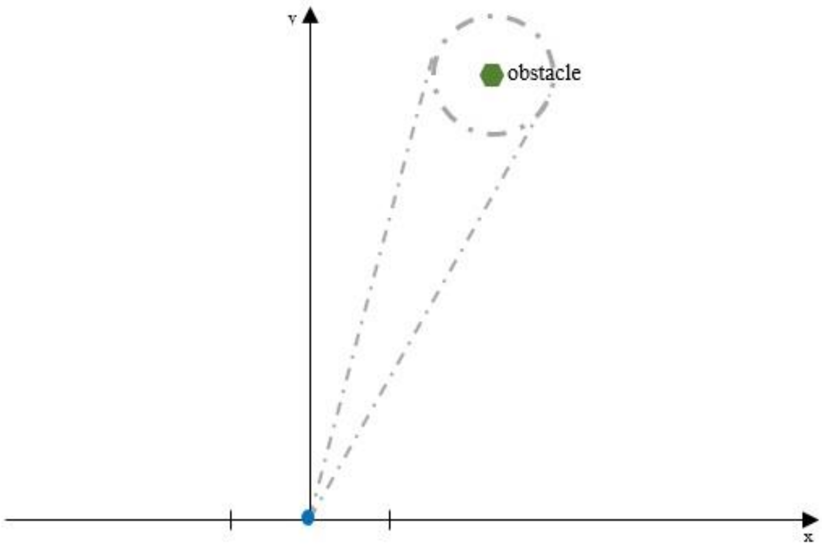


Figure 2.9- An example of a two-dimension (x,y) representation of the specific area to avoid. The blue circle represents the aircraft and the star is a representation of an obstacle.

## 2.5 Step 4: Assessment of Reality

After finding the specific area that the aircraft must avoid the following step is to compare it with the actual aircraft’s heading. Two results are possible: the aircraft’s heading is in the safe zone outside the cone or it is coincident with the conflict zone. The first result allows for concluding that the danger of collision is not real, which means that there is no need of changing anything in the aircraft’s path. On the other hand, the second result confirms the existence of danger of collision and the necessity of quickly change the aircraft’s path.

The angles named eta$_1$ ($\eta_1$) and eta$_2$ ($\eta_2$) are, respectively, the angles that the left border and the right border of the conflict zone makes with the 'x' axis (Figure 2.10). They will be needed in the process of assessment of reality, which will be performed by comparing angles.

In terms of algorithm:

- if heading is greater than eta$_2$ ($\eta_2$) and smaller than eta$_1$ ($\eta_1$): the danger of collision is real because the heading is exactly inside the cone (possibility 'c' in figure 2.10).
- if heading is equal to eta$_1$: although the aircraft's heading is on the left border it is still considered inside the cone, so the danger of collision is real (possibility 'd' in figure 2.10).
- if heading is equal to eta$_2$: this situation is similar to the previous case, the aircraft's heading is on the right border so, the danger of collision is real (possibility 'b' in figure 2.10).
- if the heading does not coincide with any of the previous options: the logical conclusion is that the aircraft's heading is in the safe zone (possibility 'a' and 'e' in figure 2.10).

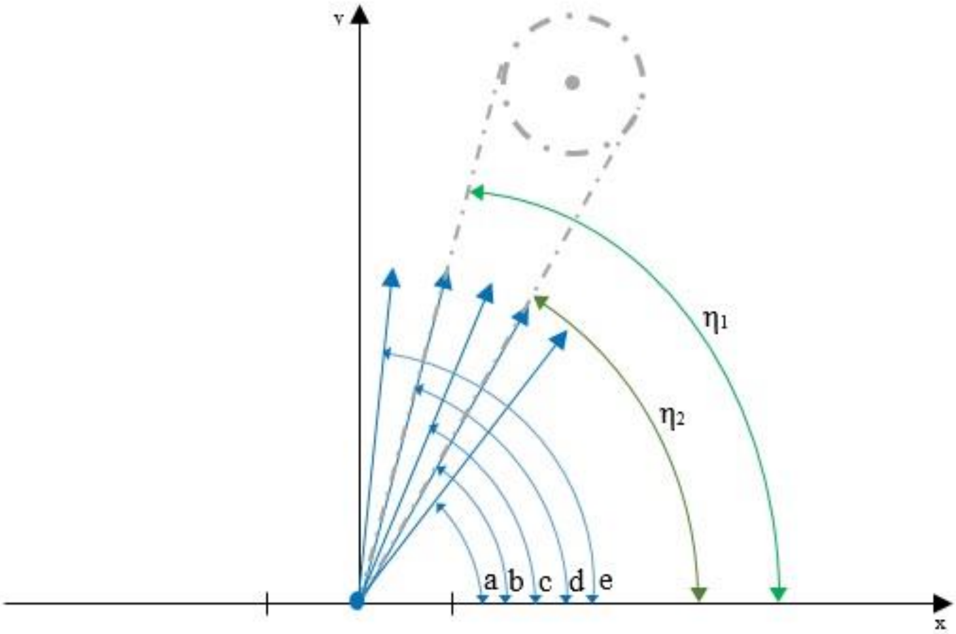


Figure 2.10- An illustration of the possibilities in the assessment of reality process.

The zone delimited by the grey lines is the conflict zone. The green curve lines describe the angles eta1 ($\eta_1$) and eta2 ($\eta_2$). The blue arrows, which each angle is represented by a letter ('a', 'b', 'c', 'd' and 'e'), represent five general possibilities to the aircraft's heading. The possibilities 'a' and 'e' are free from danger of collision. The other three, 'b', 'c' and 'd', represent situations where the danger of collision is real. The blue point in the origin represents our aircraft.

## 2.6 Step 5: Correction Method

The change in the aircraft's path must be quick and effective in order to prevent an imminent collision. So, it is necessary to find the best solution for each case. In fact, there are three possibilities to implement as a correction and each one involves a different flight characteristic, they are: the first is to change the value of the aircraft's heading, the second instead of heading the decision is to change the altitude and the last possibility is to modify the velocity. However, the third possibility is normally avoided, used only as a last resort. In fact, the ideal case is to change only the value of one flight characteristic, usually the heading, because the more features are changed the more complex it is to deal with the aircraft and its control. In some cases, when the heading is changed, the altitude must also be corrected, it will depend on if the value of the aircraft's altitude along with a safety margin corresponds inside the circumference.

Next, in this paper a detailed description will be presented for the heading correction and the altitude correction.

### 2.6.1 Heading Correction

The heading correction is a simple and assertive method well suited to any collision avoidance situation. First, it is necessary to comprehend if the value of the heading, which means the angle, should be increased or decreased. That decision must be made by comparisons: if the heading is closest or even equal to the left limit of the area to avoid the angle must increase, but if it is closest or even equal to the right limit the value of the angle must decrease and there is also the rare possibility of being exactly in the middle in this case the option will be to increase (Figure 2.11).

Previously, both $eta_1$ ($\eta_1$) and $eta_2$ ($\eta_2$) were introduced, now one more angle is necessary. The angle $eta_c$ ($\eta_c$) is the angle that the central line, which divides the conflict zone exactly in half (left and right side), makes with axis 'x'.

<u>New value of heading</u>

In this section, a description of the method to calculate the new value for the heading will be introduced. The first step is to assess if the value of heading is between the limits or equal to one limit. If it is equal to one limit the value can be automatically calculated but if it is inside limits it is necessary to proceed to one more process of comparisons. In this second comparison process we will evaluate if the heading is in the left part of the conflict zone or in the right part, for that the angle of heading will not only be compared to the angles that each limit makes with the axis 'x' but also compared with the angle $eta_c$ ($\eta_c$).

In terms of algorithm:

- if heading is equal to $eta_1$ (possibility 'e' in Figure 2.11) it is possible to immediately calculate the new value of heading, in this case it is necessary to increase the value of heading so it assumes a higher value than $eta_1$:

$$heading_{new} = (1+\lambda)\times heading \qquad (2.41)$$

where '$heading_{new}$' is the new value of heading to be calculated; 'λ' is a constant with the smallest value possible ($0 < \lambda \ll 1$) and 'heading' is the initial value.

- if heading is equal to $eta_2$ (possibility 'a' in Figure 2.11), just like in the previous possibility, the calculation of the new value is immediate, in this case it is necessary to decrease the value of heading so it assume a smaller value than $eta_2$:

$$heading_{new} = (1-\lambda)\times heading \qquad (2.42)$$

where '$heading_{new}$' is the new value of heading to be calculated; 'λ' is a constant with the smallest value possible ($0 < \lambda \ll 1$) and 'heading' is the initial value.

- if we have heading greater than $eta_2$ and smaller than $eta_1$ it means that heading is inside the limits so, we proceed to the second process of comparison where three possible cases exist:

- if heading is greater than $eta_2$ and smaller than $eta_c$ (possibility 'b' in Figure 2.11) it is in the right side of the conflict zone so, in this case it is necessary to decrease the value of heading in order to assume a smaller value than $eta_2$:

$$heading_{new} = heading - (1+\lambda)\times(heading-eta_2) \qquad (2.43)$$

where '$heading_{new}$' is the new value of heading to be calculated; 'heading' is the initial value; 'λ' is a constant with the smallest value possible ($0 < \lambda \ll 1$) and $eta_2$ is an angle.

- if heading is greater than $eta_c$ and smaller than $eta_1$ (possibility 'd' in Figure 2.11) it is in the right side of the conflict zone so, in this case it is necessary to increase the value of heading in order to assume a higher value than $eta_1$:

$$heading_{new} = heading + (1+\lambda)\times(eta_1-heading) \qquad (2.44)$$

where '$heading_{new}$' is the new value of heading to be calculated; 'heading' is the initial value; 'λ' is a constant with the smallest value possible ($0 < \lambda \ll 1$) and $eta_1$ is an angle.

- if heading is equal to $eta_c$ (possibility 'c' in Figure 2.11), it is exactly in the middle of the conflict zone, although rare it is a possible situation, so, in this case the decision is to decrease the value of heading in order to assume a smaller value than $eta_2$:

$$heading_{new} = heading - (1+\lambda)\times(heading-eta_2) \qquad (2.45)$$

where ‘$heading_{new}$’ is the new value of heading to be calculated; ‘heading’ is the initial value; ‘λ’ is a constant with the smallest value possible ($0 < \lambda \ll 1$) and $eta_2$ is an angle.

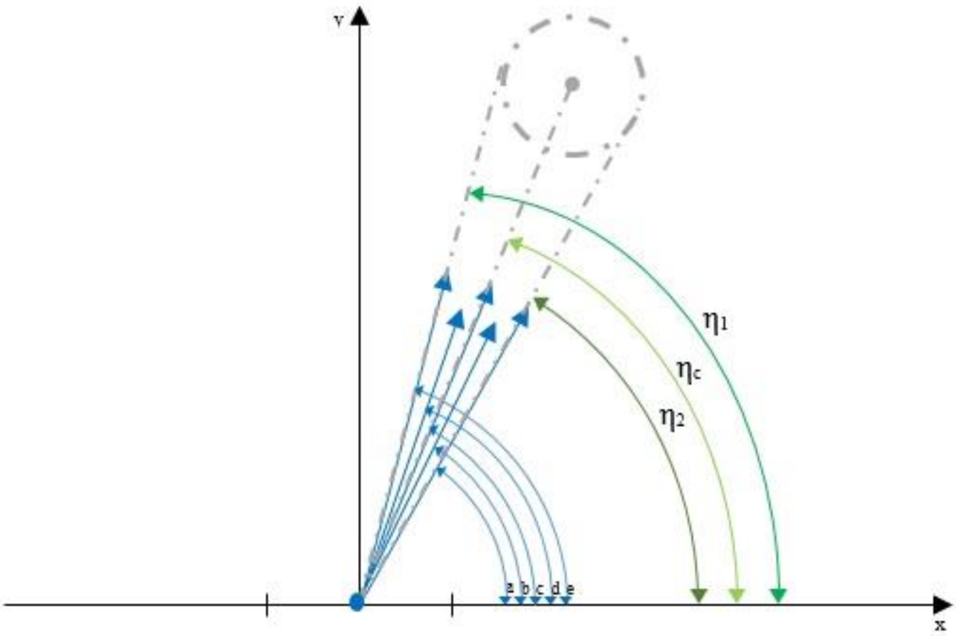


Figure 2.11- This figure is an illustration of the existing possibilities in the process of calculating the new value for the aircraft’s heading.

The zone demarked by the grey lines is the conflict zone. The green and curve lines describe the angles $eta_1$ ($\eta_1$), $eta_c$ ($\eta_c$) and $eta_2$ ($\eta_2$). The blue arrows, which each angle is represented by a letter (‘a’, ‘b’, ‘c’, ‘d’ and ‘e’), represent the five possibilities to the aircraft’s heading when the danger of collision is real. The blue point in the origin represents our aircraft.

## 2.6.2 Altitude Correction

This correction method will be applied only if the aircraft’s altitude coincides inside the area to avoid in terms of ‘xz’ plane, so before calculating the new altitude it will be necessary to analyse the situation. Just like in the heading correction, it is fundamental to understand if the value of altitude must increase or decrease to calculate the most appropriate new value for each case.

New value of altitude

To calculate the new value for the altitude it is essential to know if the obstacle captured by the cameras is, relatively to our aircraft, higher, lower or at the same altitude. Since all point’s coordinates and distance vectors were calculated on the basis of our aircraft’s position, this task is complete by analysing the value of the ‘z’ coordinate of the central point of the circumference.

If the value is smaller than zero (negative) it means the obstacle has a lower altitude than the aircraft. In this case, it is essential to calculate the maximum altitude of the area to avoid and then, compare it with the aircraft's altitude plus a safety margin.

In case the value of the 'z' coordinate is greater than zero (positive), the situation is the opposite, the obstacle has a higher altitude. In terms of the procedure to follow, it is basically the same as the previous case, the only difference is that it is necessary to calculate the minimum value and not the maximum value.

If the 'z' coordinate of the midpoint assumes the value zero, the obvious conclusion is that both the aircraft and the obstacle are precisely at the same altitude.

In terms of algorithm:

- if the 'z' coordinate of the central point is greater than zero (Figure 2.12, scenario 'a'), the process to follow is:

$$altitude_{conflict\ zone_{min}} = (altitude + c_z) - r \qquad (2.46)$$

$$altitude_{conflict\ zone_{min}} > (1+\lambda)\ altitude \qquad (2.47)$$

where '$altitude_{conflict\ zone_{min}}$' is the minimum value in terms of the 'z' coordinate of the area to avoid in the 'xz' plane; 'altitude' is the initial value; '$c_z$' is the 'z' coordinate of the circumference central point; 'r' is the previously calculated value for the radius of the circumference and 'λ' is a constant with the smallest value possible ($0 < \lambda \ll 1$).

- if the equation (2.47) is false (Figure 2.13 possibility 'a'), the best decision is to decrease the value of the aircraft's altitude because the distance to descend is smaller than the distance to climb, so:

$$altitude_{new} = altitude - (1+\lambda) \times (|r - c_z|) \qquad (2.48)$$

where '$altitude_{new}$' is the new value of altitude to be calculated; 'altitude' is the initial value; 'λ' is a constant with the smallest value possible ($0 < \lambda \ll 1$); 'r' is the previously calculated value for the radius of the circumference and '$c_z$' is the 'z' coordinate of the circumference central point.

- if the equation (2.47) is true (Figure 2.13 possibility 'b') the value of the altitude does not suffer any modification:

$$alitude_{new} = altitude \qquad (2.49)$$

where ‘$altitude_{new}$’ is the new value of altitude to be calculated and ‘altitude’ is the initial value.

- if the ‘z’ coordinate of the central point is smaller than zero (Figure 2.12, scenario ‘c’), the process to follow is:

$$altitude_{conflict\ zone_{max}} = (altitude + c_z) + r \tag{2.50}$$

$$altitude_{conflict\ zone_{max}} < (1-\lambda) \times altitude \tag{2.51}$$

where ‘$altitude_{conflict\ zone_{max}}$’ is the maximum value in terms of the ‘z’ coordinate of the area to avoid in the ‘xz’ plane; ‘altitude’ is the initial value; ‘$c_z$’ is the ‘z’ coordinate of the circumference central point; ‘r’ is the previously calculated value for the radius of the circumference and ‘λ’ is a constant with the smallest value possible ($0 < \lambda \ll 1$).

- if the equation (2.51) is false (Figure 2.14 possibility ‘a’), the value of the aircraft’s altitude must increase because the distance to climb is smaller than the distance to descend, so:

$$alitude_{new} = altitude + (1+\lambda) \times (|r + c_z|) \tag{2.52}$$

where ‘$altitude_{new}$’ is the new value of altitude to be calculated; ‘altitude’ is the initial value; ‘λ’ is a constant with the smallest value possible ($0 < \lambda \ll 1$); ‘r’ is the previously calculated value for the radius of the circumference and ‘$c_z$’ is the ‘z’ coordinate of the circumference central point.

- if the equation (2.51) is true (Figure 2.14 possibility ‘b’) the value of the altitude does not suffer any modification:

$$alitude_{new} = altitude \tag{2.53}$$

where ‘$altitude_{new}$’ is the new value of altitude to be calculated and ‘altitude’ is the initial value.

- if the ‘z’ coordinate of the central point is equal to zero (Figure 2.12, scenario ‘b’), for safety reasons the best option is to increase the altitude:

$$altitude_{new} = altitude + (1+\lambda) \times (r) \tag{2.54}$$

where ‘$altitude_{new}$’ is the new value of altitude to be calculated; ‘altitude’ is the initial value; ‘λ’ is a constant with the smallest value possible ($0 < \lambda \ll 1$) and ‘r’ is the previously calculated value for the radius of the circumference.

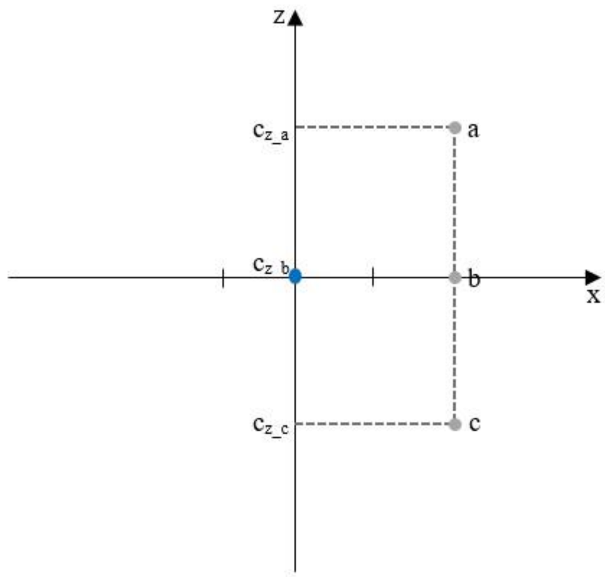


Figure 2.12- This figure is an illustration of the three possible scenarios in the process of calculating the new value for the aircraft's altitude.

The grey points named 'a', 'b' and 'c' represent the three possible scenarios. For each situation, the 'z' coordinate of the point is represented in the 'z' axis by: '$c_{z\_a}$', '$c_{z\_b}$' and '$c_{z\_c}$'. The blue point in the origin represents our aircraft.

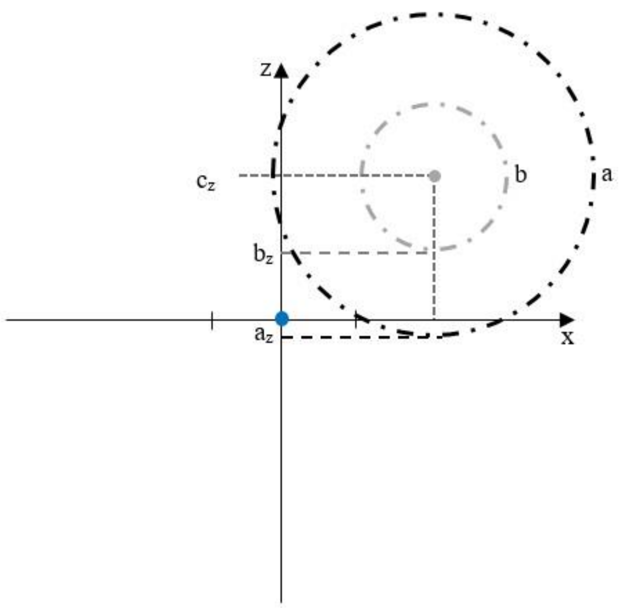


Figure 2.13- An illustration of the two possibilities in the process of calculating the new value for the altitude when the 'z' coordinates of the central point is greater than zero.

In Figure 2.13, each letter 'a' and 'b' represent a possible area to avoid in the 'xz' plan. The 'z' coordinate of the central point is represented in the 'z' axis by '$c_z$'. The '$a_z$' and '$b_z$' are, respectively, the minimum value in terms of the ‘z’ coordinate of the area to avoid in the ‘xz’ plane for the situation ‘a’ and ‘b’. The blue point in the origin represents our aircraft.

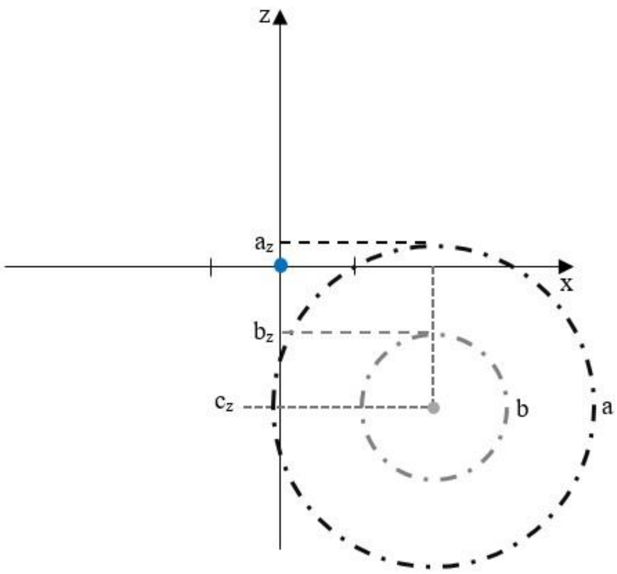


Figure 2.14- An illustration of the two possibilities in the process of calculating the new value for the altitude when the ‘z’ coordinates of the central point is smaller than zero.

In Figure 2.14, each letter ‘a’ and ‘b’ represent a possible area to avoid in the ‘xz’ plan. The ‘z’ coordinate of the central point is represented in the ‘z’ axis by ‘$c_z$’. The ‘$a_z$’ and ‘$b_z$’ are, respectively, the maximum value in terms of the ‘z’ coordinate of the area to avoid in the ‘xz’ plane for the situation ‘a’ and ‘b’. The blue point in the origin represents our aircraft.

## 2.7 Step 6: Variation of a specific parameter

In terms of navigation, it is essential to comprehend the behaviour of the aircraft and its own flight characteristics. In the specific cases in which the value of the heading changes, two studies will be implemented. They will be a tool to analyse how the value of the heading and the altitude change over time.

### 2.7.1 Heading Variation over time

In terms of algorithm:

$$\dot{\text{heading}}_{\text{study}_k} = (\text{heading}_{\text{new}} - \text{heading}_k)/t \qquad (2.55)$$

where '$\dot{heading}_{study_k}$' is the value of heading to be calculated every instant; 'k' is the indexing number to identify the instant under study; 't' is the time variable; '$heading_{new}$' is the reference value and '$heading_k$' is the initial value from each instant.

## 2.7.2 Altitude Variation over time

In terms of algorithm:

$$\dot{altitude}_{study_k} = (altitude_{new} - altitude_k)/t \quad (2.56)$$

where '$\dot{altitude}_{study_k}$' is the value of altitude to be calculated every instant; 'k' is the indexing number to identify the instant under study; 't' is the time variable; '$altitude_{new}$' is the reference value and '$altitude_k$' is the initial value from each instant.

# Chapter 3

# Simulation and Results

With the aim of testing the final product of the computational algorithm, six situations were created, each one implies exclusive initial data and unique results. The diversity of situations will allow for more coherent conclusions about the success of the computational algorithm. It is also necessary to note that the number of points must be equal or greater than five in each case, because a lower number of points will not guarantee efficient and consistent results.

The initial information for each situation is a set of angles provided by the two cameras and the distance between them. Each situation will have their own unique set of angles. In order to generate different scenarios for each situation, it was necessary to establish more than one set of values for the aircraft's heading and altitude. A total of four sets were created (Table 3.1 to Table 3.4) and the procedure will be to apply all the sets only in the situations where the threat of collision is a possibility.

To proceed with the simulations, it is fundamental to clarify some initial considerations, which were established having in mind that the method was applied to a RPAS with constant altitude. So, in all simulations:

- the distance between cameras, 'd', is equal to one meter ('1m');
- both the MVD and the MLD considered are equal to three hundred meters ('300m');
- the safety margin, '$\omega$', will assume the value of zero point five ('0.5');
- the constant 'λ', to be in accordance with the previous established condition of: '$0 < \lambda \ll 1$', will assume the value of zero point one ('0.1');
- in terms of studying the parameters (heading and altitude) behaviour, both studies will start at instant zero and varies with a step of zero point one (0.1).

Table 3.1 - First set of heading and altitude.

| | | |
|---|---|---|
| Heading | (degrees) | (radians) |
| | 73.1000 | 1.2758 |
| Altitude | (meters, m) | (feet, ft) |
| | 150 | 492.1260 |

Table 3.2 - Second set of heading and altitude.

| | | |
|---|---|---|
| Heading | (degrees) | (radians) |
| | 82.5500 | 1.4408 |
| Altitude | (meters, m) | (feet, ft) |
| | 150 | 492.1260 |

Table 3.3 - Third set of heading and altitude.

| | | |
|---|---|---|
| Heading | (degrees) | (radians) |
| | 90 | 1.5708 |
| Altitude | (meters, m) | (feet, ft) |
| | 150 | 492.1260 |

Table 3.4 - Fourth set of heading and altitude.

| | | |
|---|---|---|
| Heading | (degrees) | (radians) |
| | 96.5500 | 1.6851 |
| Altitude | (meters, m) | (feet, ft) |
| | 150 | 492.1260 |

Regarding the results, it is better to divide them in three groups:

- the first group is the results that allows to conclude if a possible threat of collision exists or not;
- the second group includes the results from the process to determine the area that the aircraft must avoid;
- the last one has the results from assessing the reality and, for each scenario, the results will be different, because they depend specifically on the value of the heading.

Both first and second group of results are independent of the values of the heading and altitude so, they do not differ from one scenario to another when applied in the same situation.

## 3.1 Situation I

In this subsection, the initial data, the results and the discussion of results are related to the first situation.

### 3.1.1 Data

Table 3.5 - Initial data for the first simulation.

| Points | Angles | | | | | | | |
|---|---|---|---|---|---|---|---|---|
| | Beta | | Alpha | | Gama | | Delta | |
| | (degrees) | (radians) | (degrees) | (radians) | (degrees) | (radians) | (degrees) | (radians) |
| 1 | -4.9157 | -0.0858 | -4.9088 | -0.0857 | 16.0051 | 0.2793 | 16.2834 | 0.2842 |
| 2 | -4.9053 | -0.0856 | -4.8983 | -0.0855 | 16.4222 | 0.2866 | 16.6992 | 0.2915 |
| 3 | -4.5490 | -0.0794 | -4.5426 | -0.0793 | 16.3172 | 0.2848 | 16.5902 | 0.2896 |
| 4 | -4.7813 | -0.0834 | -4.7744 | -0.0833 | 16.6436 | 0.2905 | 16.9215 | 0.2953 |
| 5 | -4.9494 | -0.0864 | -4.9422 | -0.0863 | 16.7272 | 0.2919 | 17.0063 | 0.2968 |
| 6 | -5.0696 | -0.0885 | -5.0623 | -0.0884 | 16.6436 | 0.2905 | 16.9215 | 0.2953 |
| 7 | -4.8876 | -0.0853 | -4.8804 | -0.0852 | 17.1133 | 0.2987 | 17.3884 | 0.3035 |

### 3.1.2 Results

Table 3.6 - Points coordinates from first situation.

| Points | Coordinates | | |
|---|---|---|---|
| | x | y | z |
| 1 | 54.9886 | 189.9598 | -16.9966 |
| 2 | 56.5118 | 190.0390 | -17.0035 |
| 3 | 57.0111 | 193.0370 | -16.0030 |
| 4 | 56.9956 | 188.9847 | -16.4986 |
| 5 | 57.0017 | 188.0050 | -17.0004 |
| 6 | 56.9956 | 188.9847 | -17.4985 |
| 7 | 58.9864 | 189.9555 | -16.9960 |

Table 3.7 - Vertical and Lateral distances from first situation.

| Points | Separation | | | |
|---|---|---|---|---|
| | Vertical | | Lateral | |
| | (meters, m) | (feet, ft) | (meters, m) | (feet, ft) |
| 1 | -16.9966 | -55.7630 | 197.7586 | 648.8144 |
| 2 | -17.0035 | -55.7856 | 198.2634 | 650.4706 |
| 3 | **-16.0030** | **-52.5034** | 201.2798 | 660.3667 |
| 4 | -16.4986 | -54.1292 | 197.3923 | 647.6126 |
| 5 | -17.0004 | -55.7755 | **196.4563** | **644.5417** |
| 6 | -17.4985 | -57.4097 | 197.3923 | 647.6126 |
| 7 | -16.9960 | -55.7612 | 198.9032 | 652.5697 |

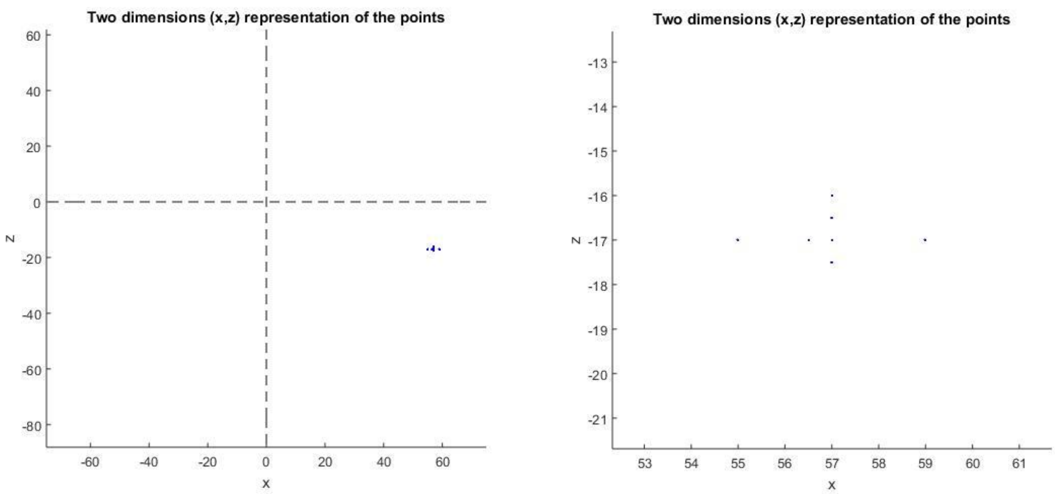


Figure 3.1 - Two dimensions (x,z) representation of the points in the space from first situation.

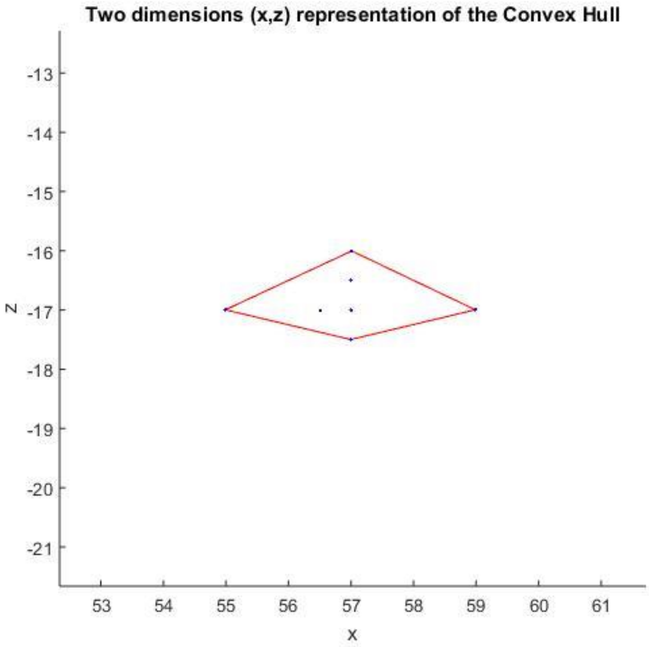


Figure 3.2 - Two dimensions (x,z) representation of the convex hull, more specifically the convex polygon from first situation.

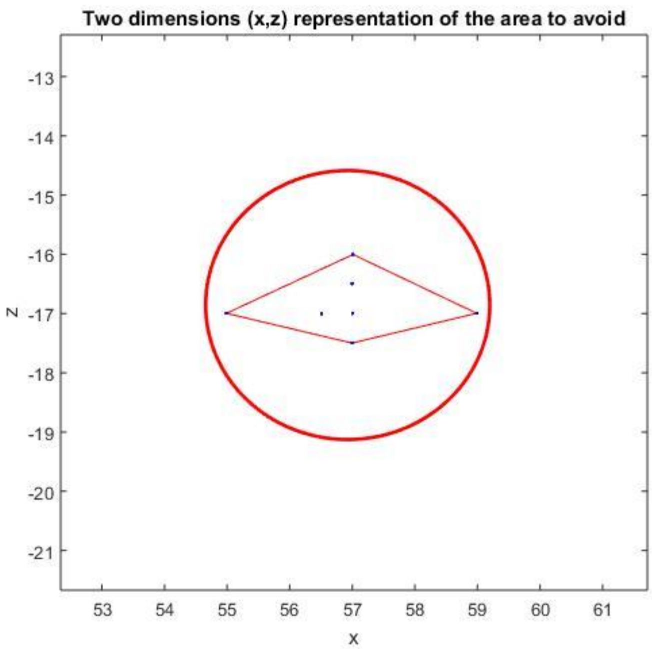


Figure 3.3 - Two dimensions (x,z) representation of the area that the aircraft must avoid in the first situation.

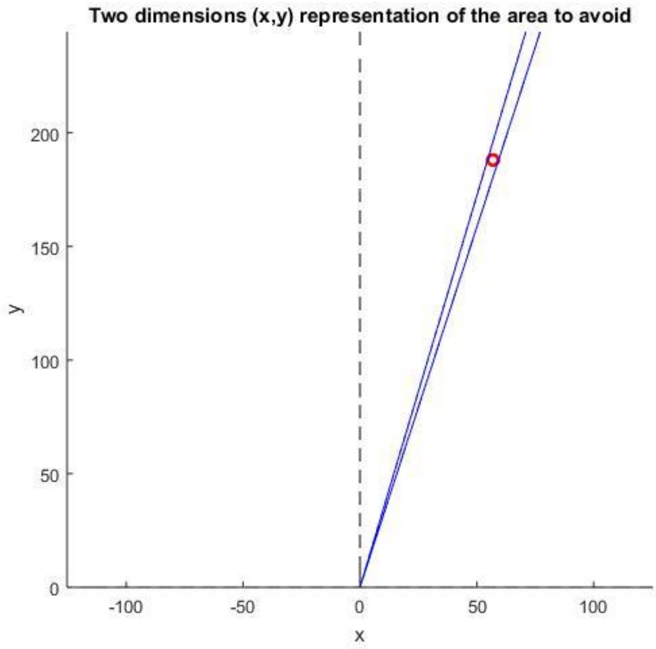


Figure 3.4 - Two dimensions (x,y) representation of the area that the aircraft must avoid in the first situation.

Table 3.8 – The values of $eta_1$ and $eta_2$ from first situation.

| | (degrees) | (radians) |
|---|---|---|
| $eta_1$ | 73.8142 | 1.2883 |
| $eta_2$ | 72.4907 | 1.2652 |

Table 3.9 – The value of the minimum radius from first situation.

| | (meters, m) | (feet, ft) |
|---|---|---|
| Minimum radius | 2.2703 | 7.4485 |

First Situation with the First Set

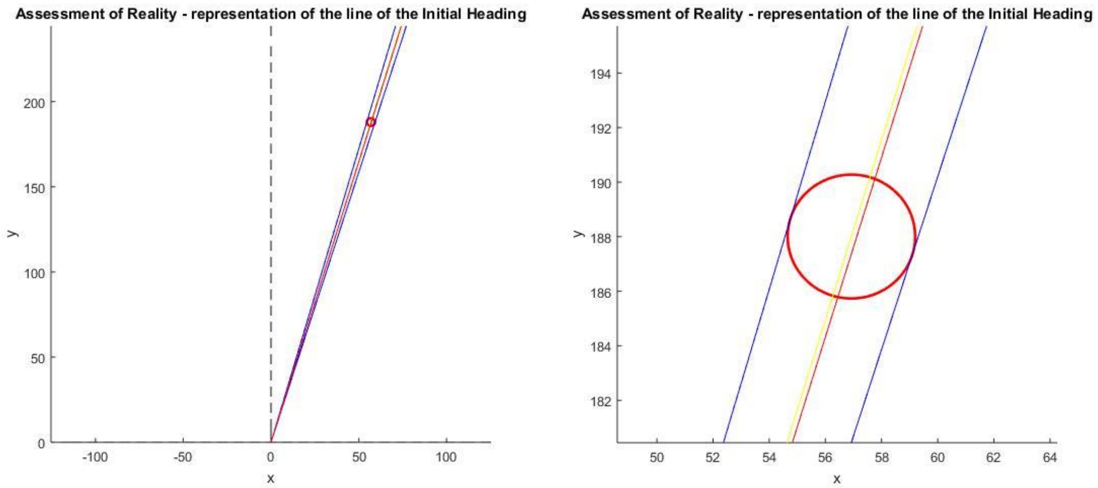


Figure 3.5 - Illustration of 'Assessment of Reality' - representation of the initial heading (first situation - first set).

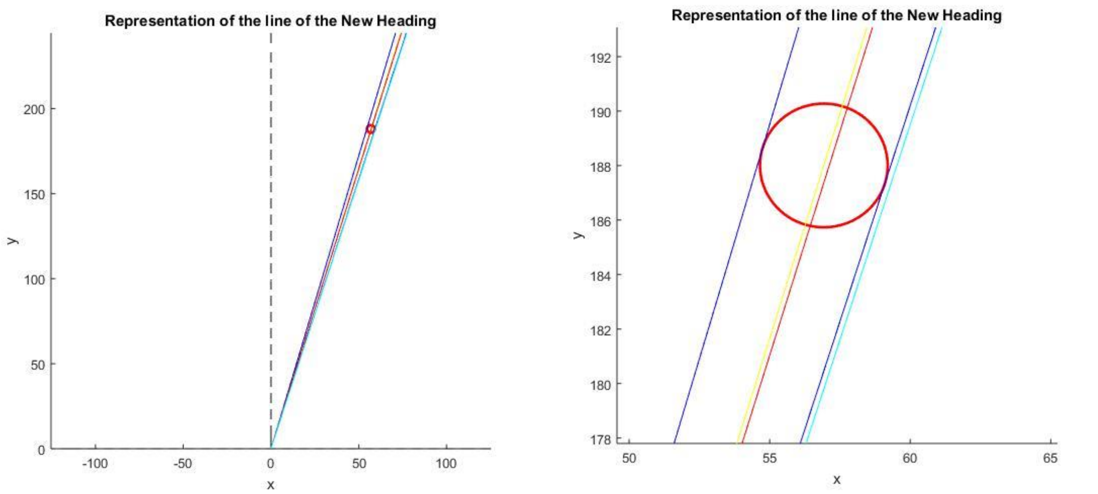


Figure 3.6. - Representation of the new heading (first situation with the first set).

Table 3.10 - Initial and final values of Heading and Altitude (first situation - first set).

| | Initial Value | | Final Value | |
|---|---|---|---|---|
| Heading | (degrees) | (radians) | (degrees) | (radians) |
| | 73.1000 | 1.2758 | 72.4330 | 1.2642 |
| Altitude | (meters, m) | (feet, ft) | (meters, m) | (feet, ft) |
| | 150 | 492.1260 | 166.0450 | 544.7671 |

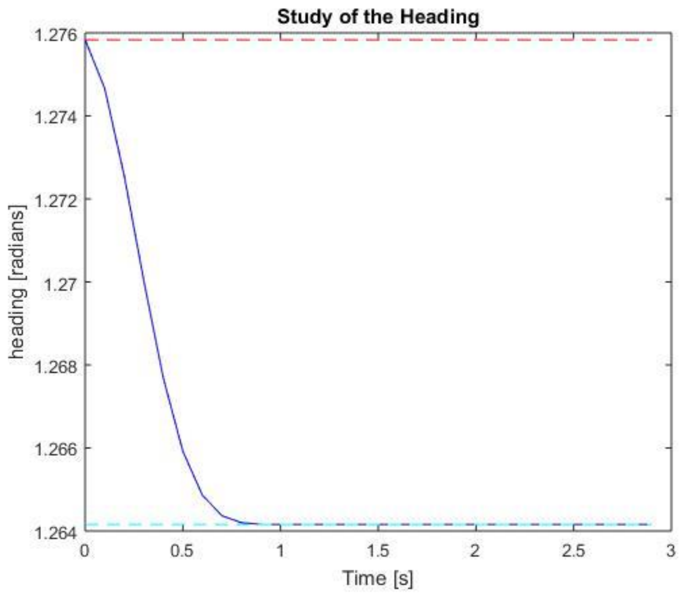


Figure 3.7 - Study of the behaviour of the aircraft's heading over time (first situation - first set).

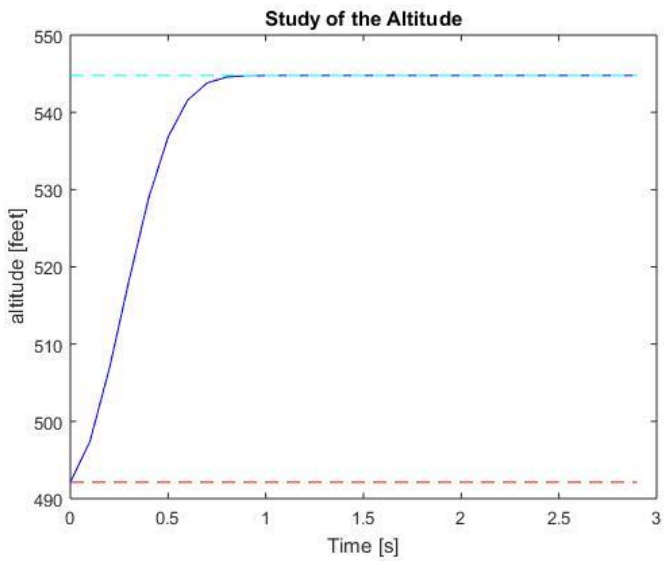


Figure 3.8 - Study of the behaviour of the aircraft's altitude over time (first situation - first set).

First Situation with the Second Set

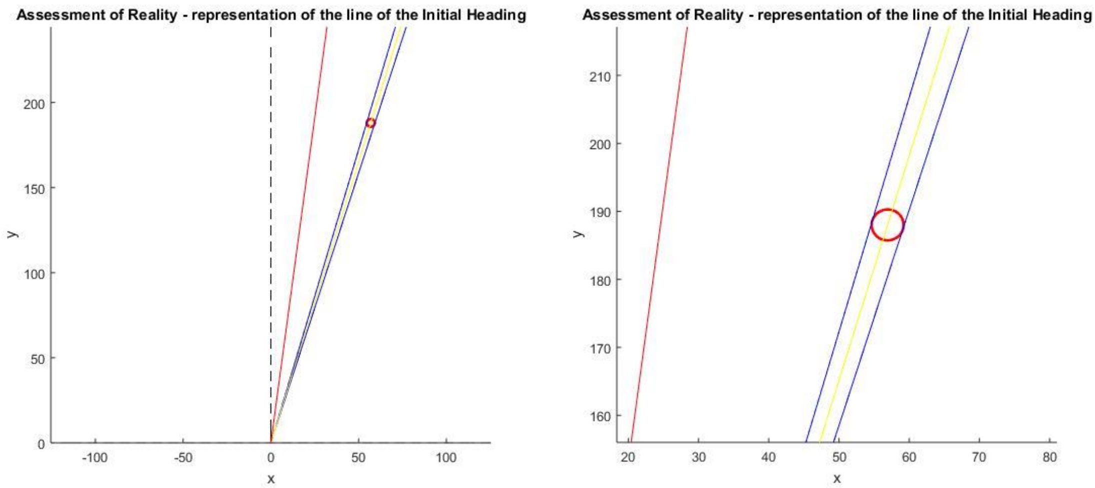


Figure 3.9 - Illustration of the process of ‘Assessment of Reality’ - representation of the line of the initial heading (first situation - second set).

Table 3.11 - Initial and final values of Heading and Altitude (first situation - second set).

| | Initial Value | | Final Value | |
|---|---|---|---|---|
| Heading | (degrees) | (radians) | (degrees) | (radians) |
| | 82.5500 | 1.4408 | 82.5500 | 1.4408 |
| Altitude | (meters, m) | (feet, ft) | (meters, m) | (feet, ft) |
| | 150 | 492.1260 | 150 | 492.1260 |

First Situation with the Third Set

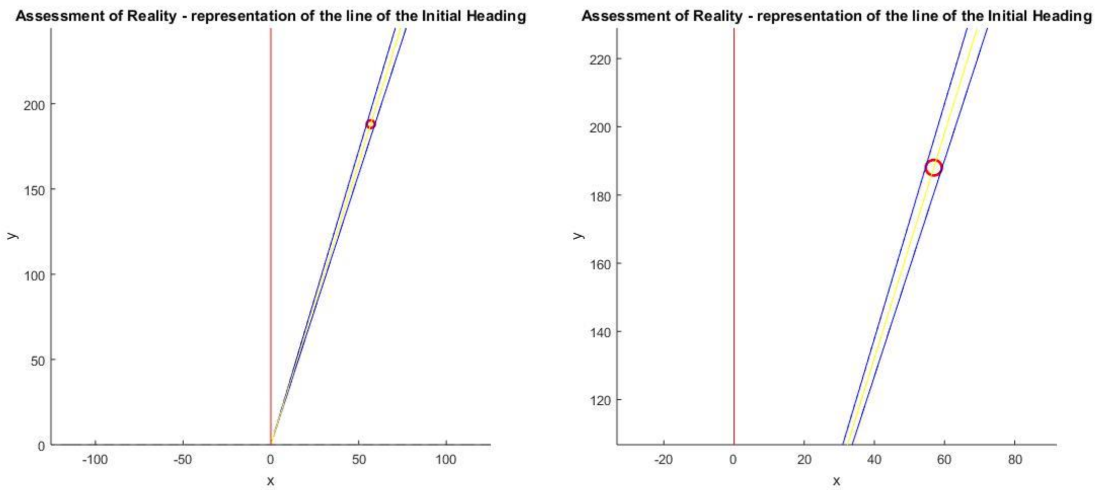


Figure 3.10 - Illustration of the process of ‘Assessment of Reality’ - representation of the line of the initial heading (first situation - third set).

Table 3.12 - Initial and final values of Heading and Altitude (first situation - third set).

| | Initial Value | | Final Value | |
|---|---|---|---|---|
| Heading | (degrees) | (radians) | (degrees) | (radians) |
| | 90 | 1.5708 | 90 | 1.5708 |
| Altitude | (meters, m) | (feet, ft) | (meters, m) | (feet, ft) |
| | 150 | 492.1260 | 150 | 492.1260 |

First Situation with the Fourth Set

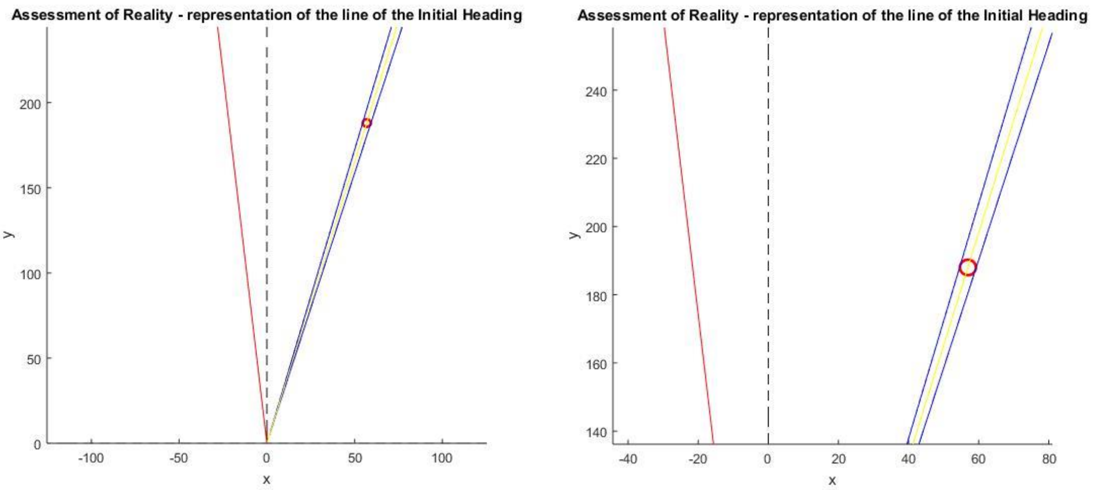


Figure 3.11 - Illustration of the process of 'Assessment of Reality' - representation of the line of the initial heading (first situation - fourth set).

Table 3.13 - Initial and final values of Heading and Altitude (first situation - fourth set).

| | Initial Value | | Final Value | |
|---|---|---|---|---|
| Heading | (degrees) | (radians) | (degrees) | (radians) |
| | 96.5500 | 1.6851 | 96.5500 | 1.6851 |
| Altitude | (meters, m) | (feet, ft) | (meters, m) | (feet, ft) |
| | 150 | 492.1260 | 150 | 492.1260 |

### 3.1.3 Discussion of Results

In terms of situation I, the first results allow for concluding that the danger of collision is a possibility. In fact, the distance between the aircraft and the obstacle (Table 3.7) is 16.0030 meters (52.5034 feet) vertically and 196.4563 meters (644.5417 feet) laterally so, both distances are less than 300 meters (984.252 feet). Figure 3.1 is a two dimensions' representation of the points based on Table 3.6, which allows for visualization of the points in the space, more precisely in the 'xz' plane, and to conclude that the obstacle has a higher altitude than the aircraft. Knowing that there is a possible threat of collision, the next step is to calculate the area that the aircraft must avoid in order to prevent any accidents.

Figure 3.2 is the product of the convex hull method, it represents the convex polygon, which is an approximation to the real format of the obstacle. The following two figures describe the exact area to avoid in two dimensions or, by other words, the conflict zone. Figure 3.3 is a projection in terms of 'xz' plane, in which the area inside the red circle, including its limits, is the representation of the vertical area that the aircraft must escape. While Figure 3.4 is a projection of the conflict zone but in the 'xy' plane, in this case the area to avoid includes the red circle and the area between the two dark blue lines tangent to the circle. In both figures the red circle has the same exact dimensions, because they are two projections of the same sphere.

The exact values of $eta_1$ and $eta_2$ are included in Table 3.8, which will allow a more detailed analysis. Table 3.9 delivers the value of the sphere minimum radius.

Since the possibility of collision exists, the four sets with different values of heading and altitude were tested in this situation. They generated four unique scenarios.

- Situation I with the first set

By observation of Figure 3.5, it is possible to conclude that the red line, which represents the initial heading of 1.2758 radians, is inside the area delimited by the two dark blue lines so, it is coincident with the conflict zone, which means the danger of collision is real. Actually, the value of heading is almost in the middle of the values of $eta_1$ and $eta_2$, respectively, 1.2883 radians and 1.2652 radians. With this information, the process of assessment of reality is done. The following step is to determinate the necessary changes to prevent the imminent collision.

Figure 3.6 is mostly equal to the previous one. However, it includes a new light blue line that represents the new value for the heading. As it is possible to observe this new line is outside the conflict zone, close to the right border of the area to avoid. Comparing the line of the initial with the line of the new heading it is possible to conclude that the value of the aircraft's heading decreased. Table 3.10 shows both values. The new value of the heading is 1.2642 radians, which means it decreased 0.0116 radians.

In terms of altitude, the value increases to 544.7671 feet, when initially it was 492.1260 feet (Table 3.10). This new value of altitude allows a higher margin of safety to the aircraft and its operations.

In Figure 3.7 it is possible to understand the behaviour of the aircraft's heading over time. The value decreases sharply and, when approaching the desired value, slightly softens. After reaching the new value it does not suffer any other perturbation. On the other hand, Figure 3.8 confirms that the parameter altitude has the opposite behaviour, the value increases until it reaches the reference value and then it stays constant.

- Situation I with second set

In this case, the initial aircraft's heading is equal to 1.4408 radians and it is represented by the red line in Figure 3.9. Analysing the figure previously mentioned, it is possible to conclude that the red line is not inside the area delimited by the two dark blue lines, or in other words, the conflict zone. So, the obvious conclusion in this scenario is that the danger of collision is not real. The process of assessment of reality is done and the aircraft can follow its path without any modification in the flight characteristics (Table 3.11).

- Situation I with the third set

Analysing Figure 3.10, it is possible to conclude that the red line, which represents the initial heading of 1.5708 radians, is not coincident with the area limited by the two dark blue lines so, the threat of collision is not real. Knowing that the aircraft is actually safe, the process of assessment of reality is complete, no modifications are required, which implies that the values of heading and altitude remain the same (Table 3.12).

- Situation I with the fourth set

By observation of Figure 3.11, the obvious conclusion is that the red line, which represents the initial heading of 1.6851 radians, is outside the area delimited by the two dark blue lines, which means the danger of collision is not real. In fact, the line of the aircraft's heading is located on the opposite side of the obstacle. So, the process of assessment of reality is done, no necessary changes (Table 3.13), which means the aircraft can follow its path.

## 3.2 Situation II

In this subsection, the initial data, the results and the discussion of results are related to the second situation.

### 3.2.1 Data

Table 3.14 - Initial data for the second simulation.

| Points | Angles | | | | | | | |
|---|---|---|---|---|---|---|---|---|
| | Beta | | Alpha | | Gama | | Delta | |
| | (degrees) | (radians) | (degrees) | (radians) | (degrees) | (radians) | (degrees) | (radians) |
| 1 | -4.6528 | -0.0812 | -4.6589 | -0.0813 | -8.5810 | -0.1498 | -8.0680 | -0.1408 |
| 2 | -4.0397 | -0.0705 | -4.0441 | -0.0706 | -7.4650 | -0.1303 | -6.9610 | -0.1215 |
| 3 | -4.4463 | -0.0776 | -4.4515 | -0.0777 | -7.7380 | -0.1351 | -7.2160 | -0.1259 |
| 4 | -4.7496 | -0.0829 | -4.7553 | -0.0830 | -7.8090 | -0.1363 | -7.2830 | -0.1271 |
| 5 | -4.9669 | -0.0867 | -4.9727 | -0.0868 | -7.7380 | -0.1351 | -7.2160 | -0.1259 |
| 6 | -4.6673 | -0.0815 | -4.6725 | -0.0816 | -7.2970 | -0.1274 | -6.7820 | -0.1184 |
| 7 | -4.6750 | -0.0816 | -4.6796 | -0.0817 | -6.5240 | -0.1139 | -6.0070 | -0.1048 |

### 3.2.2 Results

Table 3.15 - Points coordinates from second situation.

| Points | Coordinates | | |
|---|---|---|---|
| | x | Y | z |
| 1 | -16.0001 | 109.3459 | -8.9999 |
| 2 | -14.1611 | 111.8892 | -7.9695 |
| 3 | -14.1620 | 107.9027 | -8.4675 |
| 4 | -14.1810 | 107.0481 | -8.9775 |
| 5 | -14.1620 | 107.9027 | -9.4636 |
| 6 | -13.5321 | 109.5823 | -9.0194 |
| 7 | -12.0229 | 109.5029 | -9.0130 |

Table 3.16 - Vertical and Lateral distances from second situation.

| Points | Separation | | | |
|---|---|---|---|---|
| | Vertical | | Lateral | |
| | (meters, m) | (feet, ft) | (meters, m) | (feet, ft) |
| 1 | -8.9999 | -29.5273 | 110.5103 | 362.5665 |
| 2 | **-7.9695** | **-26.1467** | 112.7818 | 370.0190 |
| 3 | -8.4675 | -27.7804 | 108.8281 | 357.0475 |
| 4 | -8.9775 | -29.4538 | **107.9833** | **354.2760** |
| 5 | -9.4636 | -31.0486 | 108.8281 | 357.0475 |
| 6 | -9.0194 | -29.5911 | 110.4146 | 362.2527 |
| 7 | -9.0130 | -29.5703 | 110.1609 | 361.4204 |

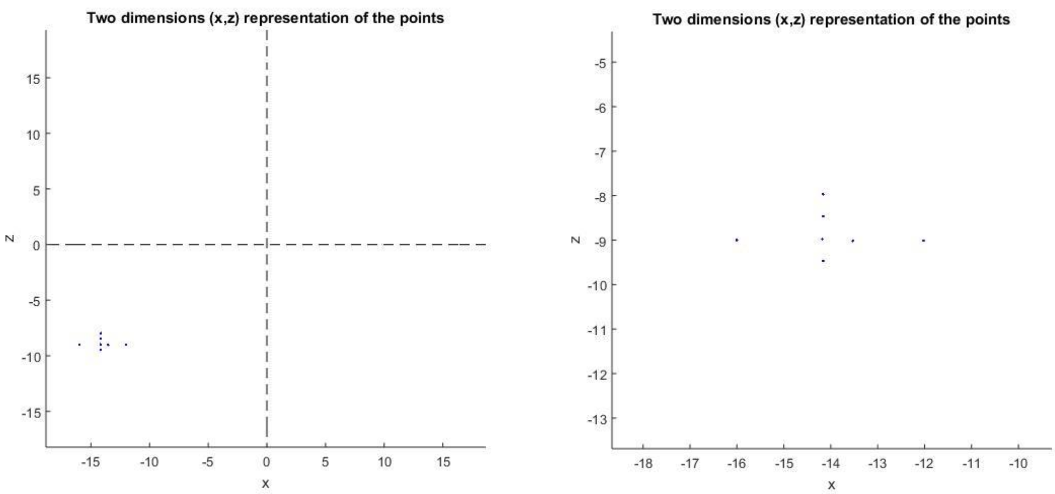


Figure 3.12 - Two dimensions (x,z) representation of the points in the space from second situation.

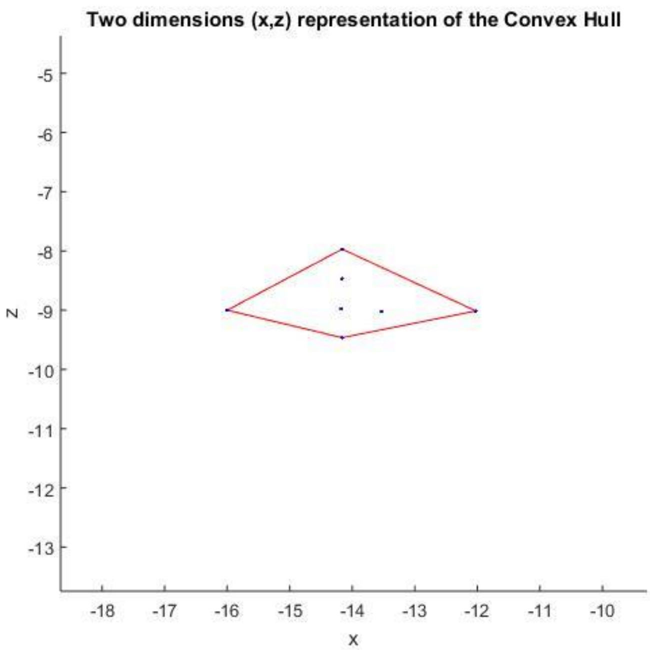


Figure 3.13 - Two dimensions (x,z) representation of the convex hull, more specifically the convex polygon from second situation.

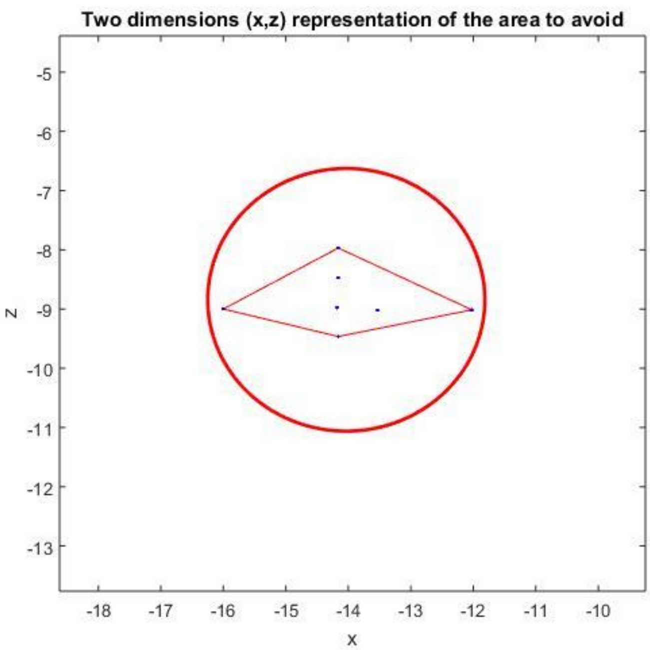


Figure 3.14 - Two dimensions (x,z) representation of the area that the aircraft must avoid in the second situation.

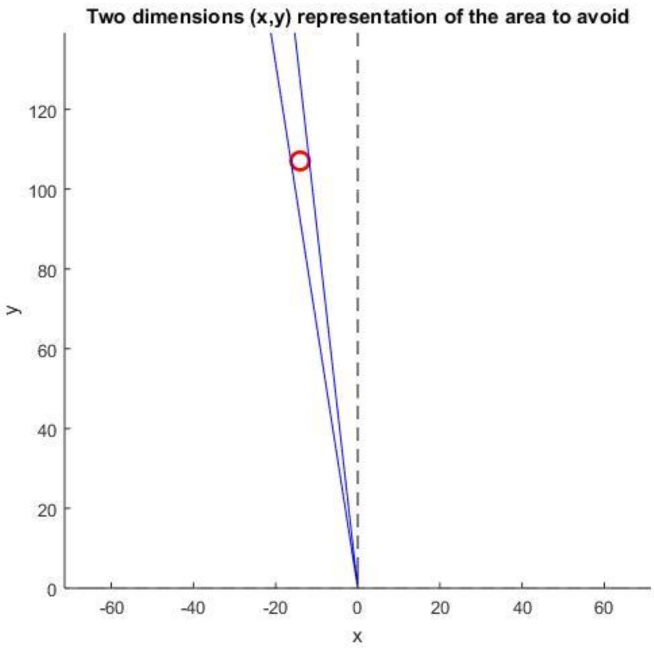


Figure 3.15 - Two dimensions (x,y) representation of the area that the aircraft must avoid in the second situation.

Table 3.17 – The values of $eta_1$ and $eta_2$ from second situation.

| | (degrees) | (radians) |
|---|---|---|
| $eta_1$ | 98.6462 | 1.7217 |
| $eta_2$ | 96.2914 | 1.6806 |

Table 3.18 – The value of the minimum radius from second situation.

| | (meters, m) | (feet, ft) |
|---|---|---|
| Minimum radius | 2.2174 | 7.2749 |

Situation II with the First Set

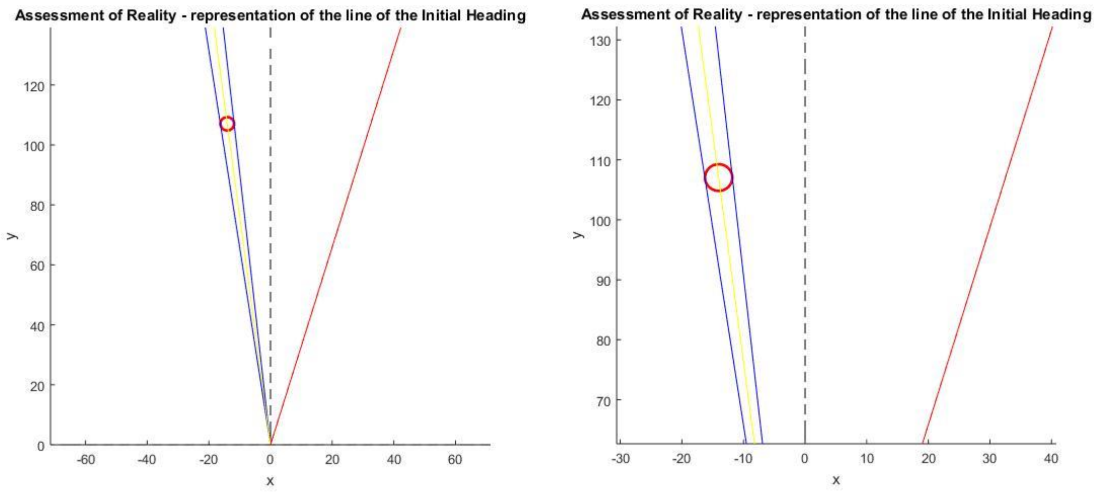


Figure 3.16. - Illustration of the process of ‘Assessment of Reality’ - representation of the line of the initial heading (second situation - first set).

Table 3.19 - Initial and final values of Heading and Altitude (second situation – first set).

| | Initial Value | | Final Value | |
|---|---|---|---|---|
| Heading | (degrees) | (radians) | (degrees) | (radians) |
| | 73.1000 | 1.2758 | 73.1000 | 1.2758 |
| Altitude | (meters, m) | (feet, ft) | (meters, m) | (feet, ft) |
| | 150 | 492.1260 | 150 | 492.1260 |

Situation II with the Second Set

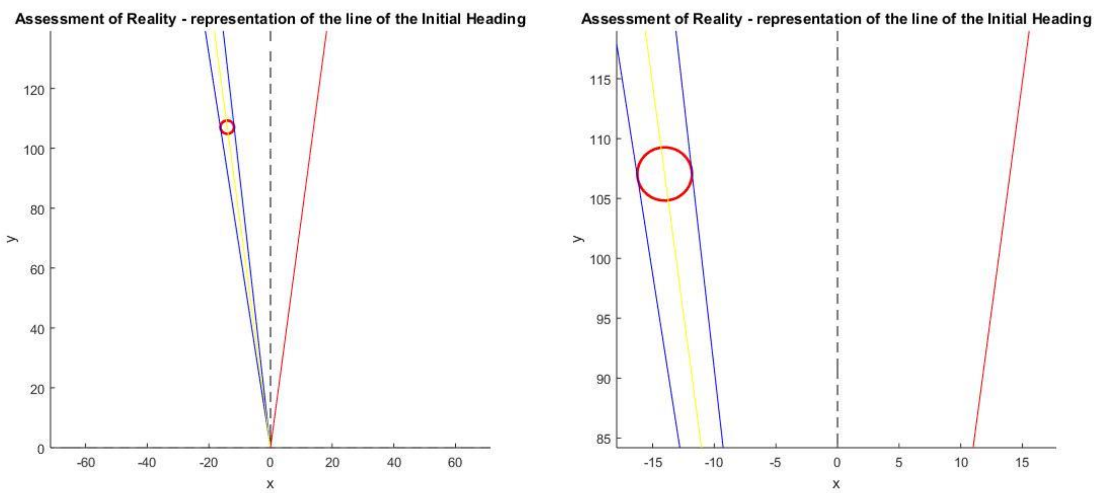


Figure 3.17 - Illustration of the process of ‘Assessment of Reality’ - representation of the line of the initial heading (second situation - second set).

Table 3.20 - Initial and final values of Heading and Altitude (second situation – second set).

| | Initial Value | | Final Value | |
|---|---|---|---|---|
| Heading | (degrees) | (radians) | (degrees) | (radians) |
| | 82.5500 | 1.4408 | 82.5500 | 1.4408 |
| Altitude | (meters, m) | (feet, ft) | (meters, m) | (feet, ft) |
| | 150 | 492.1260 | 150 | 492.1260 |

## Situation II with the Third Set

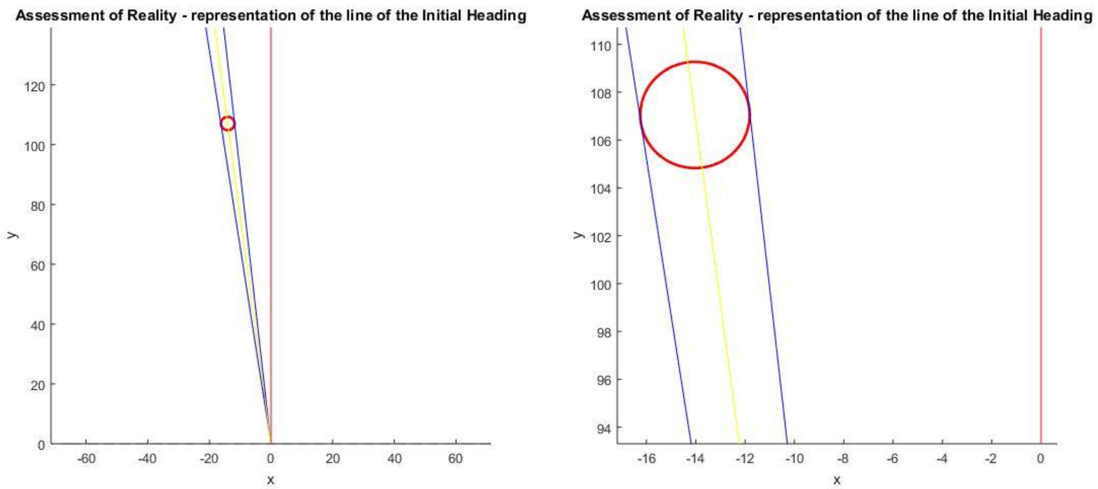


Figure 3.18. - Illustration of the process of 'Assessment of Reality' - representation of the line of the initial heading (second situation - third set).

Table 3.21 - Initial and final values of Heading and Altitude (second situation – third set).

| | Initial Value | | Final Value | |
|---|---|---|---|---|
| Heading | (degrees) | (radians) | (degrees) | (radians) |
| | 90 | 1.5708 | 90 | 1.5708 |
| Altitude | (meters, m) | (feet, ft) | (meters, m) | (feet, ft) |
| | 150 | 492.1260 | 150 | 492.1260 |

Situation II with the Fourth Set

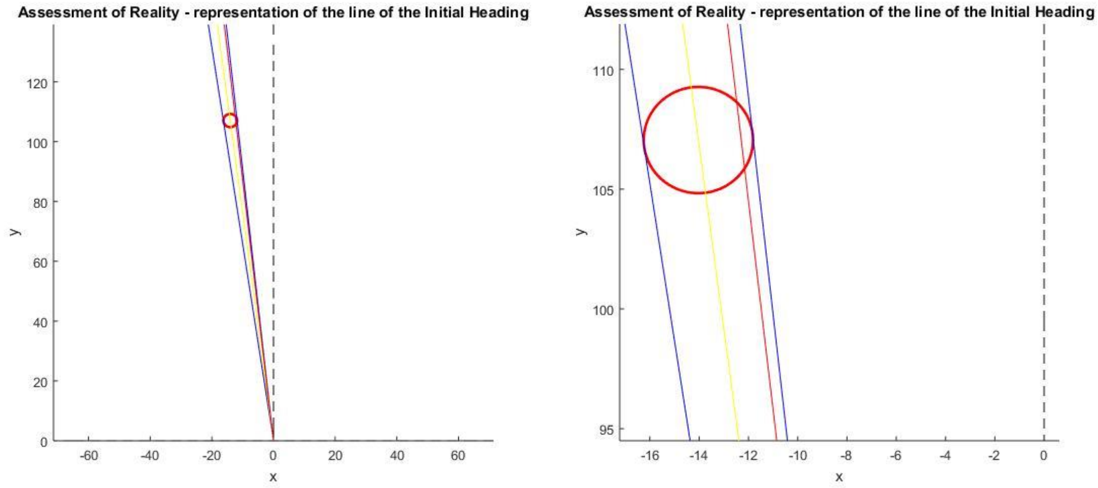


Figure 3.19 - Illustration of 'Assessment of Reality' - representation of the initial heading (second situation - fourth set).

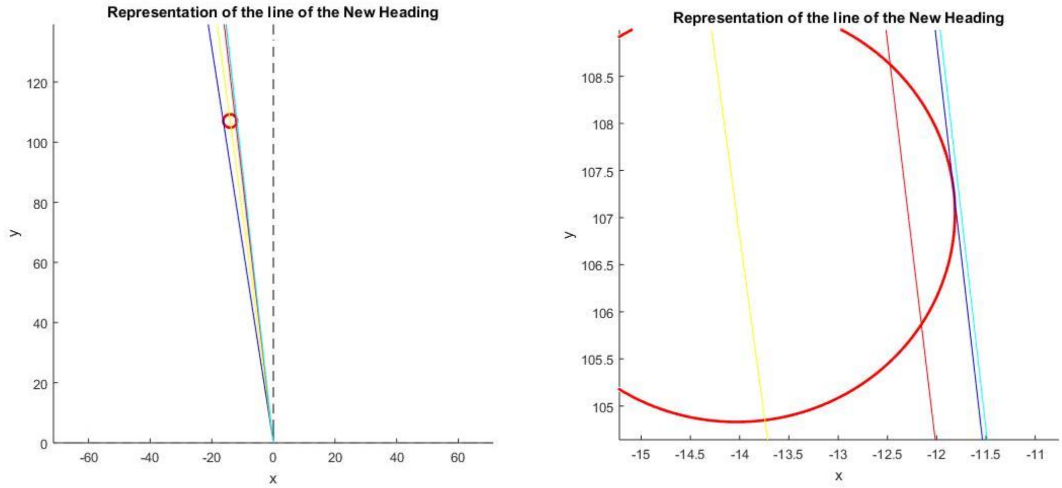


Figure 3.20 - Representation of the new heading (second situation - fourth set).

Table 3.22 - Initial and final values of Heading and Altitude (second situation - fourth set).

| | Initial Value | | Final Value | |
|---|---|---|---|---|
| Heading | (degrees) | (radians) | (degrees) | (radians) |
| | 96.5500 | 1.6851 | 96.2630 | 1.6801 |
| Altitude | (meters, m) | (feet, ft) | (meters, m) | (feet, ft) |
| | 150 | 492.1260 | 157.2900 | 516.0422 |

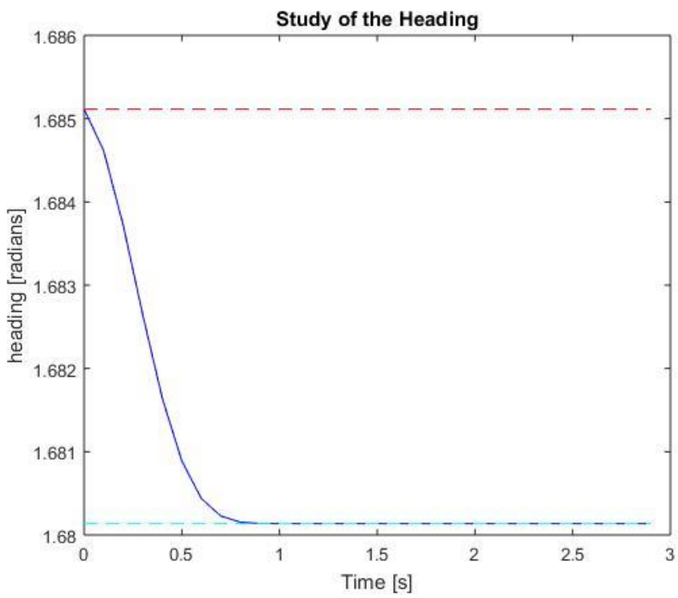


Figure 3.21 - Study of the behaviour of the aircraft’s heading over time (second situation - fourth set).

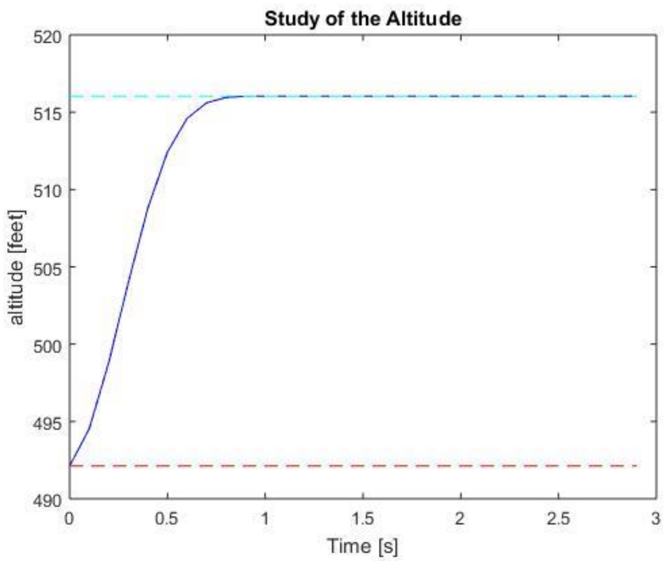


Figure 3.22 - Study of the behaviour of the aircraft’s altitude over time (second situation - fourth set).

### 3.2.3 Discussion of Results

In situation II, the first group of results allows for the conclusion that there is a possible threat of collision. In fact, the minimum distance between the aircraft and the obstacle (Table 3.16) is 7.9695 meters (26.1467 feet) vertically and 107.9833 meters (354.2760 feet) laterally, which are both less than 300 meters (984.252 feet). Figure 3.12 is a two dimensions’ representation of the points based on Table 3.15, which helps to visualise the points in the space, more precisely in the ‘xz’ plane, and to confirm that the obstacle has a lower altitude than the aircraft. Because there is danger of collision, the next step is to calculate the exact area that the aircraft must avoid.

Figure 3.13 is the product of the convex hull method and represents the convex polygon, which is an approximation to the real format of the obstacle. The following two figures describe the exact area to avoid in two dimensions. Figure 3.14 is a projection of the conflict zone in the 'xz' plan. To be more precise, the area inside the red circle, including its limits, is the vertical area that the aircraft must avoid. Figure 3.15 is also a projection of the conflict zone but in the 'xy' plan, in this case the area to avoid includes the red circle and the area between the two dark blue lines tangent to the circle. In both figures the red circle has the same exact dimensions, because they are two projections of the same sphere.

The exact values of $eta_1$ and $eta_2$ are included in Table 3.17, which will allow a more detailed analysis. Table 3.18 delivers the value of the sphere minimum radius.

Since the danger of collision is a possibility, the four sets of initial heading and altitude were tested in this situation. They generate four unique scenarios.

- Situation II with the first set

By observation of Figure 3.16, the obvious conclusion is that the red line, which represents the initial heading of 1.2758 radians, is not coincident with the area limited by the two dark blue lines. Actually, the line of the aircraft's heading is located on the opposite side of the obstacle. So, the threat of collision is not real and, with this conclusion, the process of assessment of reality is done. No necessary changes (Table 3.19), which means the aircraft can continue its path normally.

- Situation II with the second set

Analysing Figure 3.17 carefully it is possible to conclude that the red line, which represents the initial heading of 1.4408 radians, is not between the two dark blue lines so the threat of collision is not real. In fact, the obstacle is located on the opposite side of the red line, just like the previous case. With the confirmation that the threat is not real and the aircraft is safe, the process of assessment of reality is complete and no modifications on the values of heading and altitude were needed (Table 3.20).

- Situation II with the third set

This scenario has 1.5708 radians as initial aircraft's heading and it is represented by the red line in Figure 3.18. By observing the figure previously mentioned, it is possible to confirm that the red line is not inside the area limited by the two dark blue lines, or in other words, the conflict zone. With the conclusion that the threat of collision is not real, the process of assessment of reality is done and the aircraft can continue without any modification regarding the flight characteristics (Table 3.21).

- Situation II with the fourth set

Observing Figure 3.19 it is possible to conclude that the red line, which represents the initial heading of 1.6851 radians, is inside the area limited by the two dark blue lines, which means the danger of collision is real. In fact, the value of heading is very similar to the $eta_2$, 1.6806 radians (Table 3.17).

The following step is to determinate the necessary changes to prevent the imminent collision. Figure 3.20 is mostly equal to Figure 3.19. Yet, it includes a new light blue line, which represents the new value for the heading. Although the light blue line is close to the right border of the area to avoid, it is in the safe zone. Comparing the lines of the headings, it is possible to comprehend that the new value is smaller than the initial one, which is confirmed by Table 3.22. The new heading decreased 0.005 radians, assuming the value of 1.6801 radians. Table 3.22 also includes information about the altitude. A slight increase of the value can be observed. Initially, the value of the altitude was 492.1260 feet, after the necessary changes to prevent the collision, the new value is 516.0422 feet.

In terms of studies, Figure 3.21 allows for the analysis of the behaviour of the aircraft's heading over time. The value decreases sharply and only slows down a little bit when approaching the desired value. After reaching the new value, the behaviour does not suffer any other perturbation. Figure 3.22 illustrates how and how much the value of the altitude changes over time. The altitude rapidly increases and near the reference value it tends to be a litter bit slower.

## 3.3 Situation III

In this subsection, the initial data, the results and the discussion of results are related to the third situation.

### 3.3.1 Data

Table 3.23 - Initial data for the third simulation.

| Points | Angles | | | | | | | |
|---|---|---|---|---|---|---|---|---|
| | Beta | | Alpha | | Gama | | Delta | |
| | (degrees) | (radians) | (degrees) | (radians) | (degrees) | (radians) | (degrees) | (radians) |
| 1 | 1.2248 | 0.0214 | 1.2243 | 0.0214 | 6.9320 | 0.1210 | 7.1530 | 0.1248 |
| 2 | 1.1058 | 0.0193 | 1.1052 | 0.0193 | 7.4410 | 0.1299 | 7.6600 | 0.1337 |
| 3 | 0.8898 | 0.0155 | 0.8893 | 0.0155 | 7.4840 | 0.1306 | 7.7050 | 0.1345 |
| 4 | 1.4154 | 0.0247 | 1.4147 | 0.0247 | 7.4360 | 0.1298 | 7.6520 | 0.1336 |
| 5 | 1.2278 | 0.0214 | 1.2271 | 0.0214 | 7.6240 | 0.1331 | 7.8450 | 0.1369 |
| 6 | 1.1183 | 0.0195 | 1.1178 | 0.0195 | 7.6390 | 0.1333 | 7.8610 | 0.1372 |
| 7 | 1.0046 | 0.0175 | 1.0041 | 0.0175 | 7.6240 | 0.1331 | 7.8450 | 0.1369 |
| 8 | 0.8893 | 0.0155 | 0.8888 | 0.0155 | 7.7050 | 0.1345 | 7.9260 | 0.1383 |
| 9 | 1.2211 | 0.0213 | 1.2204 | 0.0213 | 8.2550 | 0.1441 | 8.4740 | 0.1479 |

### 3.3.2 Results

Table 3.24 - Points coordinates from third situation.

| Points | Coordinates | | |
|---|---|---|---|
| | x | y | z |
| 1 | 31.5469 | 255.3595 | 5.4998 |
| 2 | 34.0798 | 257.1072 | 5.0049 |
| 3 | 33.9636 | 254.7284 | 3.9902 |
| 4 | 34.5241 | 260.6859 | 6.4958 |
| 5 | 34.5745 | 254.5609 | 5.5045 |
| 6 | 34.4861 | 253.3956 | 4.9907 |
| 7 | 34.5745 | 254.5609 | 4.5036 |
| 8 | 34.9276 | 254.4627 | 3.9859 |
| 9 | 37.6541 | 256.0880 | 5.5158 |

Table 3.25 - Vertical and Lateral distances from third situation.

| Points | Separation | | | |
|---|---|---|---|---|
| | Vertical | | Lateral | |
| | (meters, m) | (feet, ft) | (meters, m) | (feet, ft) |
| 1 | 5.4998 | 18.0440 | 257.3008 | 844.1628 |
| 2 | 5.0049 | 16.4202 | 259.3560 | 850.9055 |
| 3 | 3.9902 | 13.0913 | 256.9826 | 843.1189 |
| 4 | 6.4958 | 21.3116 | 262.9621 | 862.7366 |
| 5 | 5.5045 | 18.0594 | 256.8981 | 842.8417 |
| 6 | 4.9907 | 16.3737 | **255.7315** | **839.0142** |
| 7 | 4.5036 | 14.7757 | 256.8981 | 842.8417 |
| 8 | **3.9859** | **13.0770** | 256.8486 | 842.6790 |
| 9 | 5.5158 | 18.0964 | 258.8414 | 849.2173 |

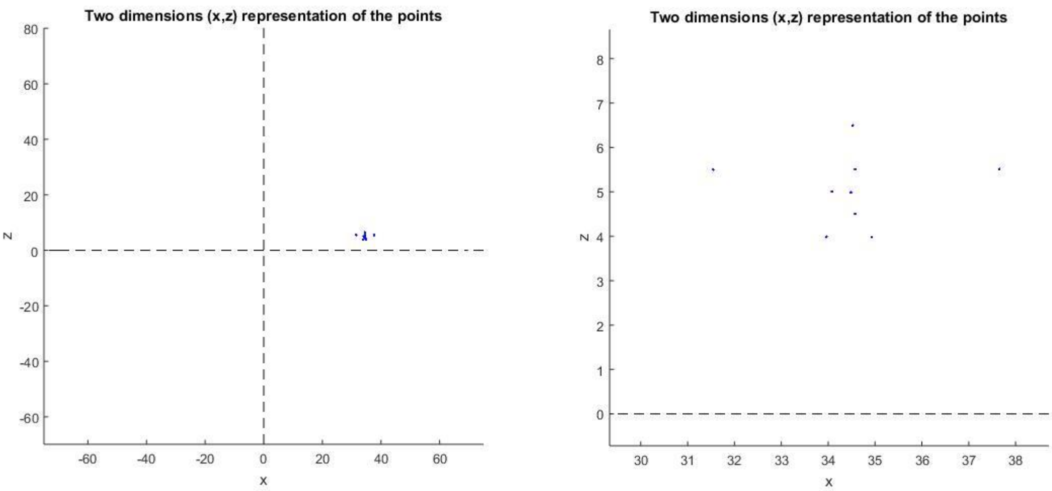


Figure 3.23 - Two dimensions (x,z) representation of the points in the space from third situation.

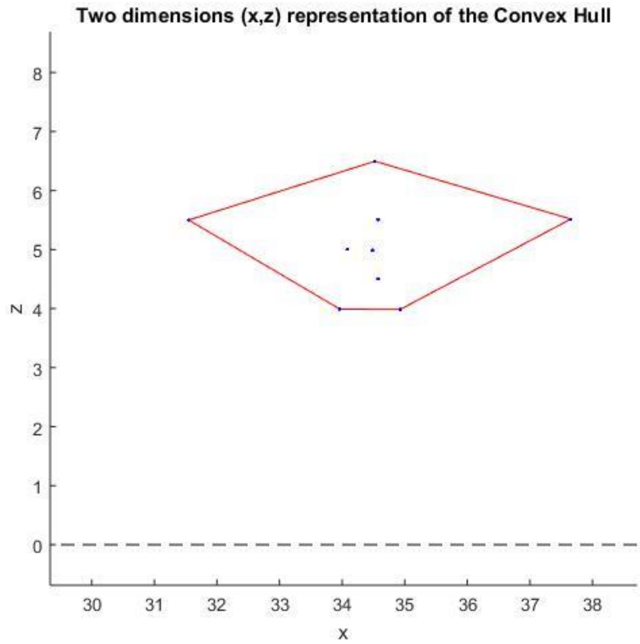


Figure 3.24 - Two dimensions (x,z) representation of the convex hull, more specifically the convex polygon from third situation.

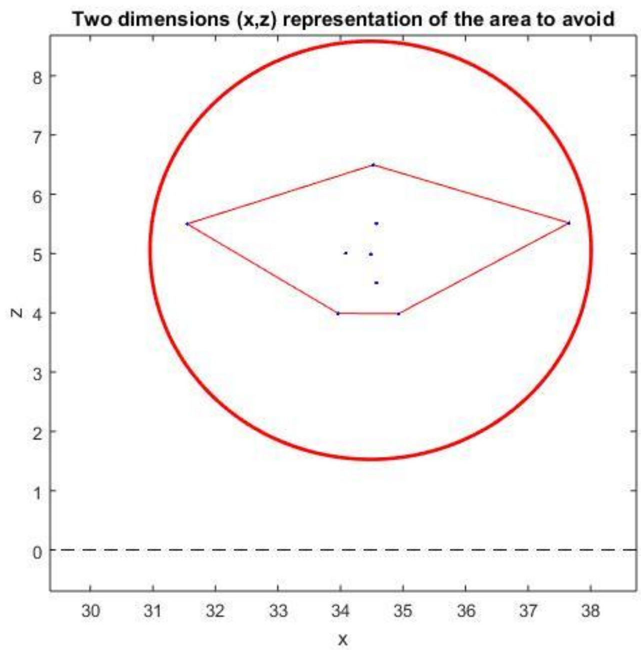


Figure 3.25 - Two dimensions (x,z) representation of the area that the aircraft must avoid in the third situation.

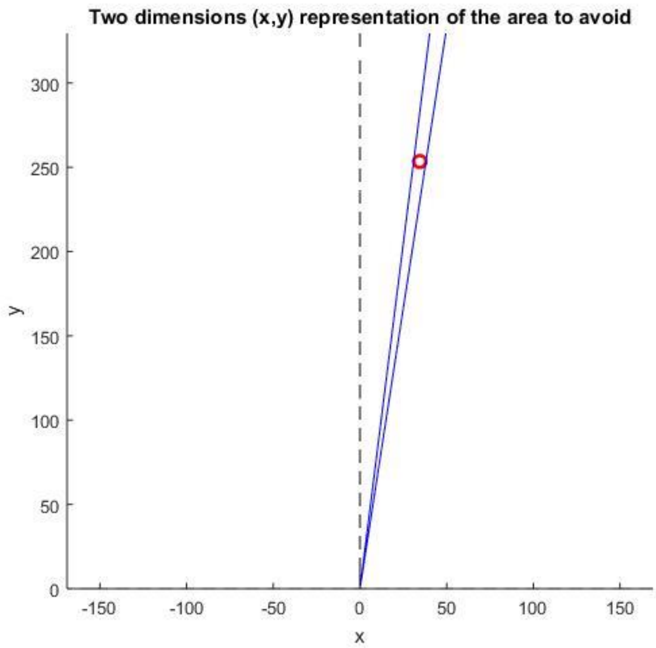


Figure 3.26 - Two dimensions (x,y) representation of the area that the aircraft must avoid in the third situation.

Table 3.26 – The values of $eta_1$ and $eta_2$ from third situation.

| | (degrees) | (radians) |
|---|---|---|
| $eta_1$ | 83.0388 | 1.4493 |
| $eta_2$ | 81.4632 | 1.4218 |

Table 3.27 – The value of the minimum radius from third situation.

| | (meters, m) | (feet, ft) |
|---|---|---|
| Minimum radius | 3.5268 | 11.5709 |

Situation III with the First Set

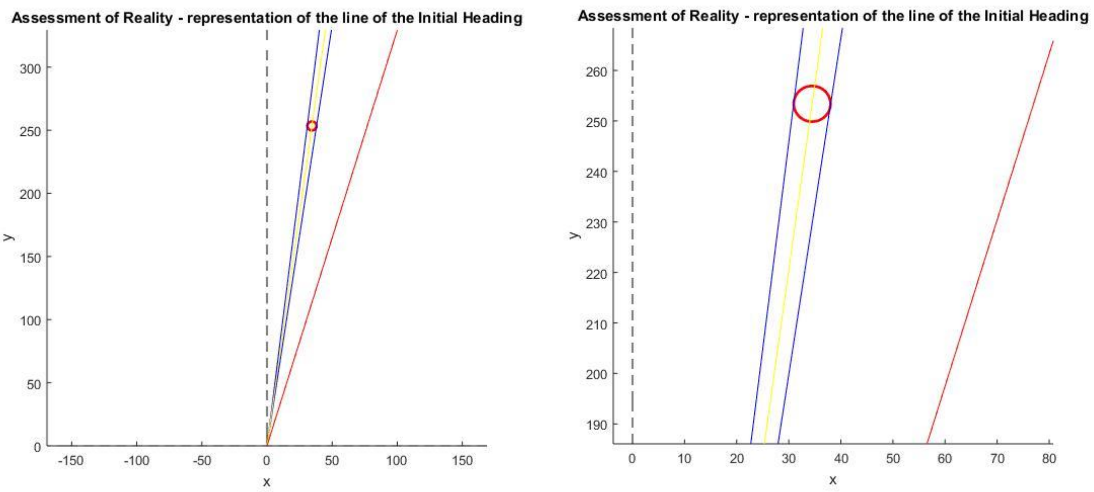


Figure 3.27 - Illustration of the process of 'Assessment of Reality' - representation of the line of the initial heading (third situation - first set).

Table 3.28 - Initial and final values of Heading and Altitude (third situation – first set).

| | Initial Value | | Final Value | |
|---|---|---|---|---|
| Heading | (degrees) | (radians) | (degrees) | (radians) |
| | 73.1000 | 1.2758 | 73.1000 | 1.2758 |
| Altitude | (meters, m) | (feet, ft) | (meters, m) | (feet, ft) |
| | 150 | 492.1260 | 150 | 492.1260 |

Situation III with the Second Set

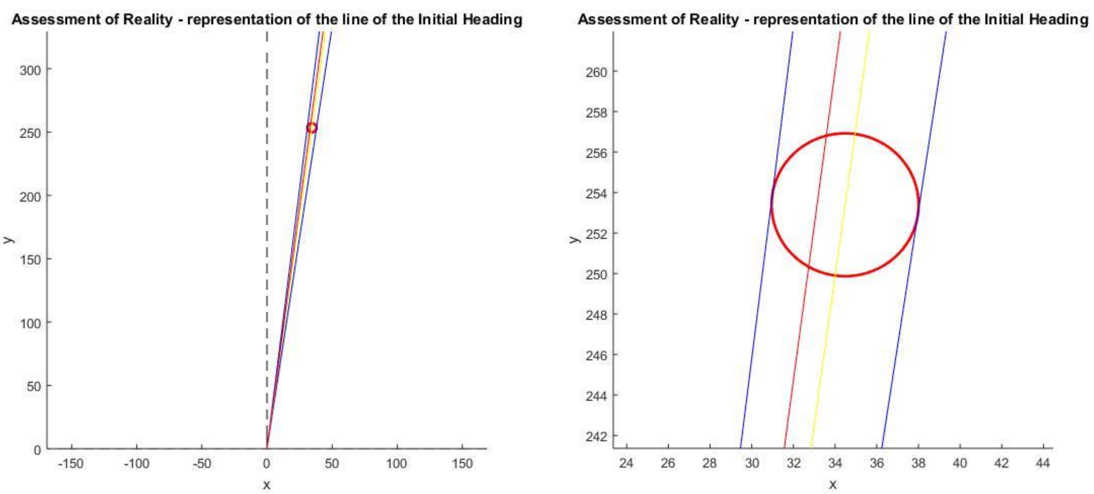


Figure 3.28 - Illustration of 'Assessment of Reality' - representation of the initial heading (third situation - second set).

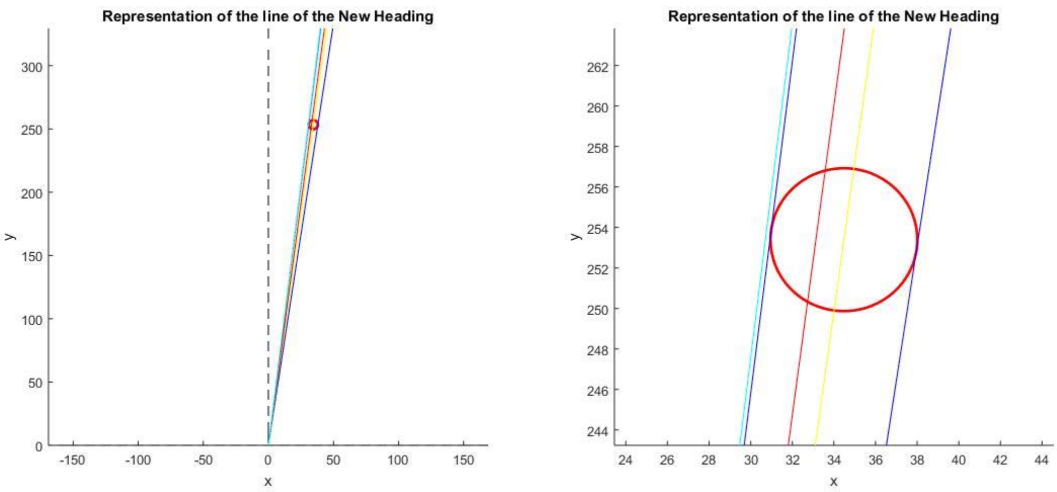


Figure 3.29 - Representation of the new heading (third situation - second set).

Table 3.29 - Initial and final values of Heading and Altitude (third situation – second set).

| | Initial Value | | Final Value | |
|---|---|---|---|---|
| Heading | (degrees) | (radians) | (degrees) | (radians) |
| | 82.5500 | 1.4408 | 83.0900 | 1.4502 |
| Altitude | (meters, m) | (feet, ft) | (meters, m) | (feet, ft) |
| | 150 | 492.1260 | 148.3195 | 486.6125 |

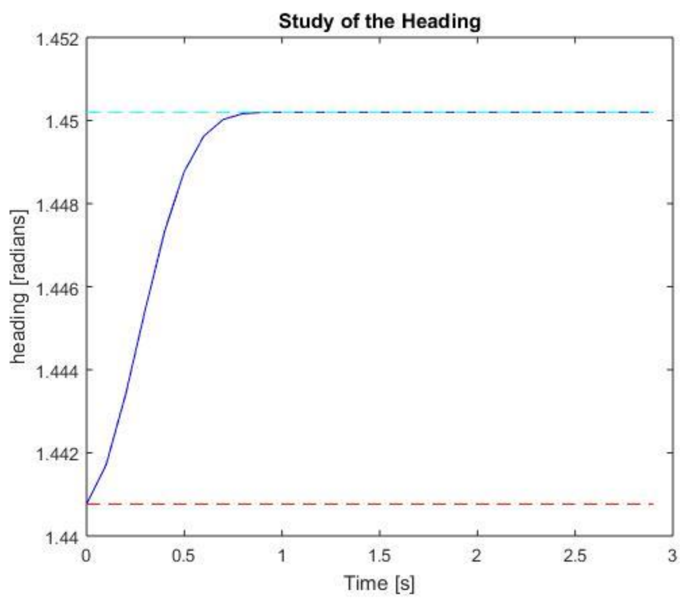


Figure 3.30 - Study of the behaviour of the aircraft’s heading over time (third situation - second set).

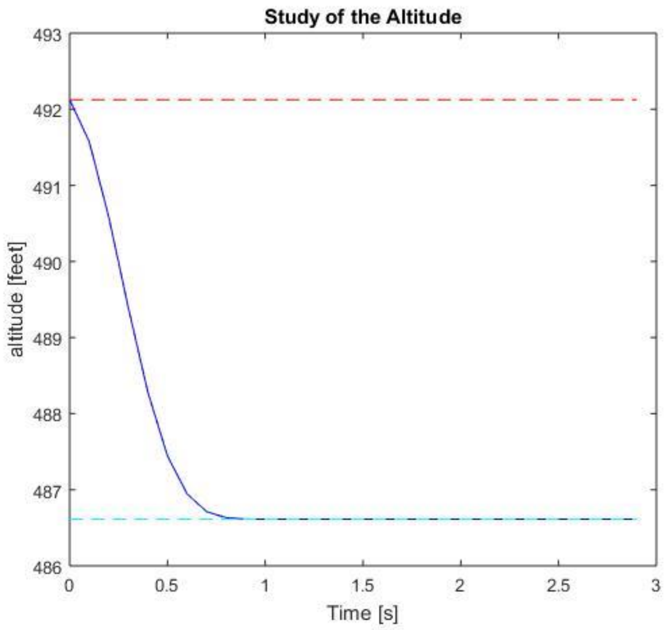


Figure 3.31 - Study of the behaviour of the aircraft's altitude over time (third situation - second set).

Situation III with the Third Set

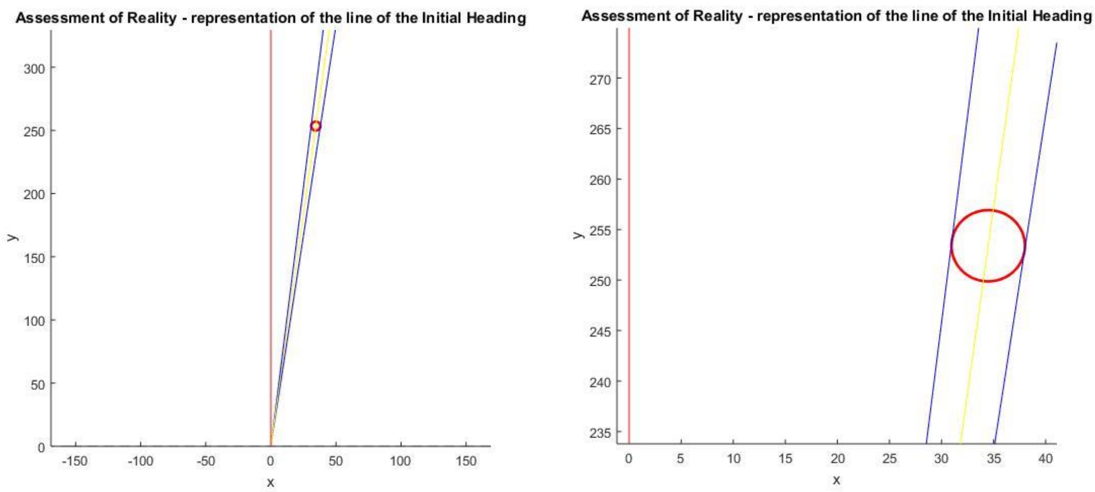


Figure 3.32 - Illustration of the process of 'Assessment of Reality' - representation of the line of the initial heading (third situation - third set).

Table 3.30 - Initial and final values of Heading and Altitude (third situation –third set).

| | Initial Value | | Final Value | |
|---|---|---|---|---|
| Heading | (degrees) | (radians) | (degrees) | (radians) |
| | 90 | 1.5708 | 90 | 1.5708 |
| Altitude | (meters, m) | (feet, ft) | (meters, m) | (feet, ft) |
| | 150 | 492.1260 | 150 | 492.1260 |

<u>Situation III with the Fourth Set</u>

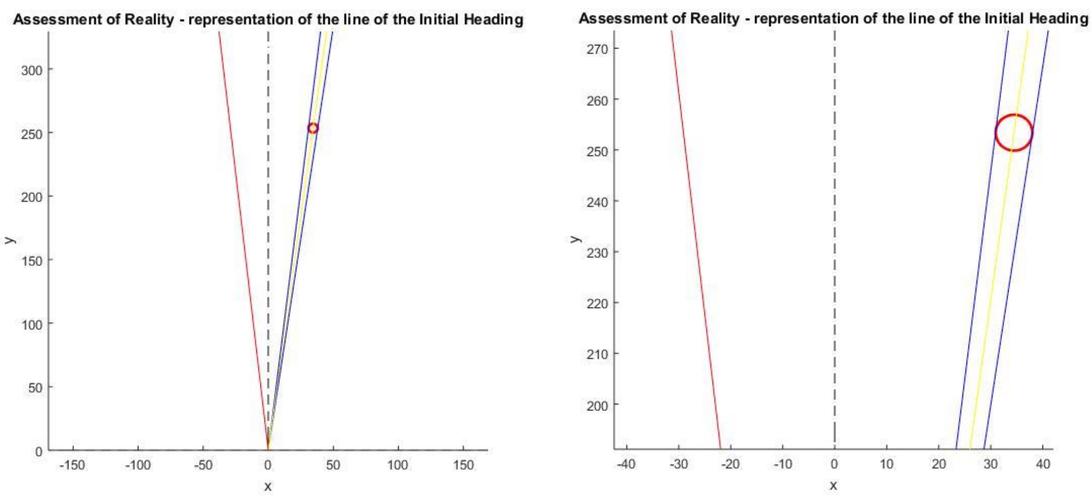


Figure 3.33 - Illustration of the process of 'Assessment of Reality' - representation of the line of the initial heading (third situation - fourth set).

Table 3.31 - Initial and final values of Heading and Altitude (third situation - fourth set).

| | Initial Value | | Final Value | |
|---|---|---|---|---|
| Heading | (degrees) | (radians) | (degrees) | (radians) |
| | 96.5500 | 1.6851 | 96.5500 | 1.6851 |
| Altitude | (meters, m) | (feet, ft) | (meters, m) | (feet, ft) |
| | 150 | 492.1260 | 150 | 492.1260 |

### 3.3.3 Discussion of Results

In terms of the third situation, the first results confirm the possibility of danger of collision. In fact, Table 3.25 shows that the exact minimum distances between the aircraft and the obstacle are 3.9859 meters (13.0770 feet) vertically and 255.7315 meters (839.0142 feet) laterally, which are less than 300 meters (984.252 feet). Figure 3.23 is a two dimensions' representation of the points based on the coordinates established in Table 3.24, which allows for visualisation of the points in the space, more precisely in the 'xz' plane, and to conclude that the obstacle has a slightly higher altitude than the aircraft.

With the possible threat of collision, the next necessary step is to calculate the area that the aircraft must avoid. Figure 3.24 represents the convex polygon, which is not exactly the format of the obstacle but it is an approximation to it. The following two figures, Figure 3.25 and Figure 3.26, describe the exact area to avoid in two dimensions. Figure 3.25 is a projection in terms of 'xz' plan, in which the area inside the red circle, including its limits, is the vertical area to avoid, while Figure 3.26 is a projection of the conflict zone but in the 'xy' plane. In this last figure, the area to avoid includes the red circle and the area between the two dark blue lines tangent to the circle. The red circle is a projection of the same sphere so, in both figures, it has the same exact dimensions.

The exact values of $eta_1$ and $eta_2$ are included in Table 3.26, which will allow a more detailed analysis. Table 3.27 delivers the value of the sphere minimum radius.

Since the possibility of collision exists, the four sets with different values of heading and altitude were tested in this situation. They generate four different scenarios.

- Situation III with the first set

In this case, the aircraft's heading assumes the value of 1.2758 radians and, in Figure 3.27, is the red line outside the area limited by the two dark blue lines. The obvious conclusion is that the danger of collision is not real. So, the process of assessment of reality is done and no changes are necessary (Table 3.28), which means the aircraft can continue its path.

- Situation III with the second set

Observing Figure 3.28 carefully, it is possible to conclude that the red line, which represents the initial heading of 1.4408 radians, is between the two dark blue lines or, in other words, is inside the conflict zone. So, the threat of collision is real. In fact, the line representing the heading is between the values of $eta_1$ and $eta_{c.}$ $Eta_c$ is equal to the average value of $eta_1$ and $eta_2$, respectively, 1.4493 radians and 1.4218 radians. With this information, the process of assessment of reality is done. The following step is to increase the value of heading and if necessary change the aircraft's altitude.

Figure 3.29 is very similar to the previous one. However, it includes a new light blue line that represents the new value for the heading. This new line is outside the conflict zone, close to the left border of the area to avoid. The new heading assumes a higher value than $eta_1$ just as expected. Table 3.29 shows the exact values. The new value of the heading is 1.4502 radians, which means it increase 0.0094 radians. In terms of the aircraft's altitude, it decreases from 492.1260 feet to 486.6125 feet, due to the fact that the real value along with the safety margin of '1.1' happens to be in the conflict zone.

Figure 3.30 is the study of the value of the parameter heading over time. Analysing the chart, it is possible to conclude that initially the value increases abruptly then, when approaching the new value, tends to slow down and eventually becomes constant. Figure 3.31 is a similar study to the previous one but to analyse the behaviour of the aircraft's altitude over time. The altitude initially decreases sharply and, when reaching the new value, slows down. Basically, the altitude assumes a symmetrical behaviour to the heading.

- Situation III with the third set

In this scenario, Figure 3.32 allows for the conclusion that the red line, which represents the initial heading of 1.5708 radians, is not inside the area limited by the two dark blue lines so, the threat of collision is not real and the process of assessment of reality is done. No modifications were required, which implies that the values of heading and altitude remain the same (Table 3.30).

- Situation III with the fourth set

The initial aircraft's heading is equal to 1.6851 radians and, in Figure 3.33, is represented as the red line. Analysing the figure, it is possible to conclude that the red line is not coincident with the conflict zone, which means that the danger of collision is not real. With this information, the process of assessment of reality is done and the aircraft can continue its path without changing any of the flight characteristics (Table 3.31).

## 3.4 Situation IV

In this subsection, the initial data, the results and the discussion of results are related to the fourth situation.

### 3.4.1 Data

Table 3.32 - Initial data for the fourth simulation.

| Points | Angles | | | | | | | |
|---|---|---|---|---|---|---|---|---|
| | Beta | | Alpha | | Gama | | Delta | |
| | (degrees) | (radians) | (degrees) | (radians) | (degrees) | (radians) | (degrees) | (radians) |
| 1 | 28.7334 | 0.5015 | 28.7364 | 0.5015 | -1.6250 | -0.0284 | -1.3543 | -0.0236 |
| 2 | 28.6927 | 0.5008 | 28.6943 | 0.5008 | -0.9503 | -0.0166 | -0.6788 | -0.0118 |
| 3 | 28.4266 | 0.4961 | 28.4282 | 0.4962 | -0.9481 | -0.0165 | -0.6772 | -0.0118 |
| 4 | 28.3299 | 0.4944 | 28.3312 | 0.4945 | -0.7921 | -0.0138 | -0.5281 | -0.0092 |
| 5 | 28.8553 | 0.5036 | 28.8567 | 0.5036 | -0.8165 | -0.0143 | -0.5444 | -0.0095 |
| 6 | 28.8083 | 0.5028 | 28.8097 | 0.5028 | -0.8185 | -0.0143 | -0.5457 | -0.0095 |
| 7 | 28.6461 | 0.5000 | 28.6475 | 0.5000 | -0.8165 | -0.0143 | -0.5444 | -0.0095 |
| 8 | 28.4282 | 0.4962 | 28.4292 | 0.4962 | -0.6772 | -0.0118 | -0.4063 | -0.0071 |
| 9 | 28.7432 | 0.5017 | 28.7429 | 0.5017 | 0.0000 | 0.0000 | 0.2709 | 0.0047 |

### 3.4.2 Results

Table 3.33 - Points coordinates from fourth situation.

| Points | Coordinates | | |
|---|---|---|---|
| | X | Y | z |
| 1 | -5.5008 | 211.5146 | 116.0077 |
| 2 | -3.0001 | 210.9913 | 115.4952 |
| 3 | -2.9997 | 211.4588 | 114.4778 |
| 4 | -2.5005 | 217.0005 | 116.9999 |
| 5 | -2.5008 | 210.5389 | 116.0212 |
| 6 | -2.5004 | 209.9985 | 115.4990 |
| 7 | -2.5008 | 210.5389 | 115.0210 |
| 8 | -2.0000 | 211.4825 | 114.4906 |
| 9 | 0.5000 | 211.4409 | 115.9677 |

Table 3.34 - Vertical and Lateral distances from fourth situation.

| Points | Separation | | | |
|---|---|---|---|---|
| | Vertical | | Lateral | |
| | (meters, m) | (feet, ft) | (meters, m) | (feet, ft) |
| 1 | 116.0077 | 380.6027 | 211.5861 | 694.1801 |
| 2 | 115.4952 | 378.9213 | 211.0126 | 692.2987 |
| 3 | **114.4778** | **375.5834** | 211.4801 | 693.8323 |
| 4 | 116.9999 | 383.8579 | 217.0149 | 711.9910 |
| 5 | 116.0212 | 380.6469 | 210.5538 | 690.7932 |
| 6 | 115.4990 | 378.9336 | **210.0134** | **689.0204** |
| 7 | 115.0210 | 377.3653 | 210.5538 | 690.7932 |
| 8 | 114.4906 | 375.6252 | 211.4919 | 693.8711 |
| 9 | 115.9677 | 380.4713 | 211.4414 | 693.7055 |

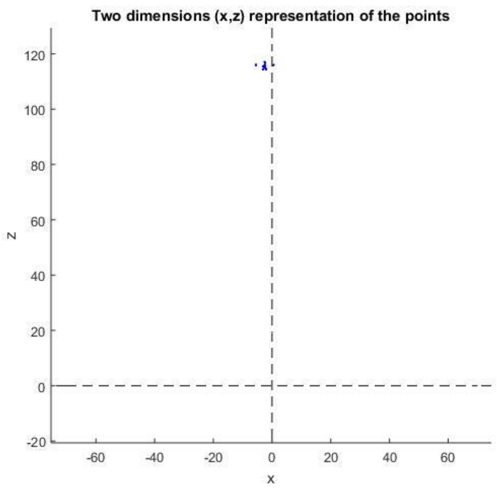


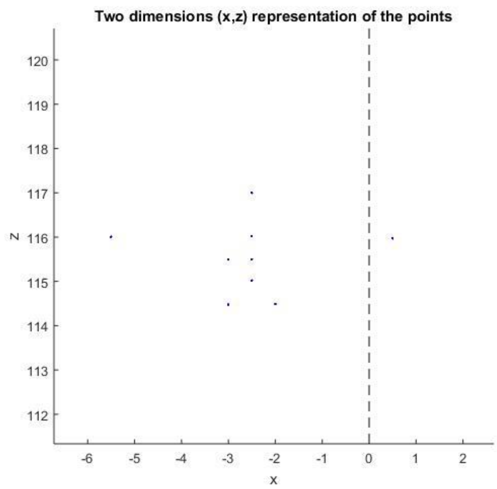


Figure 3.34 - Two dimensions (x,z) representation of the points in the space from fourth situation.

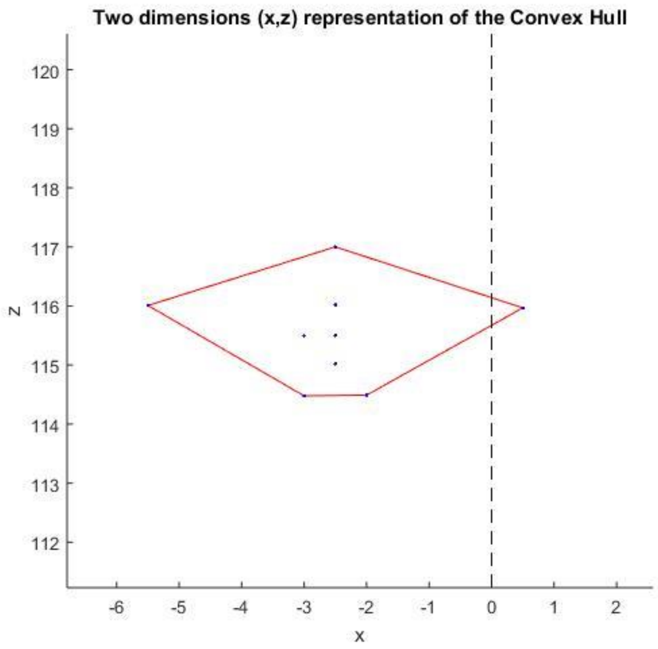


Figure 3.35 - Two dimensions (x,z) representation of the convex hull, more specifically the convex polygon from fourth situation.

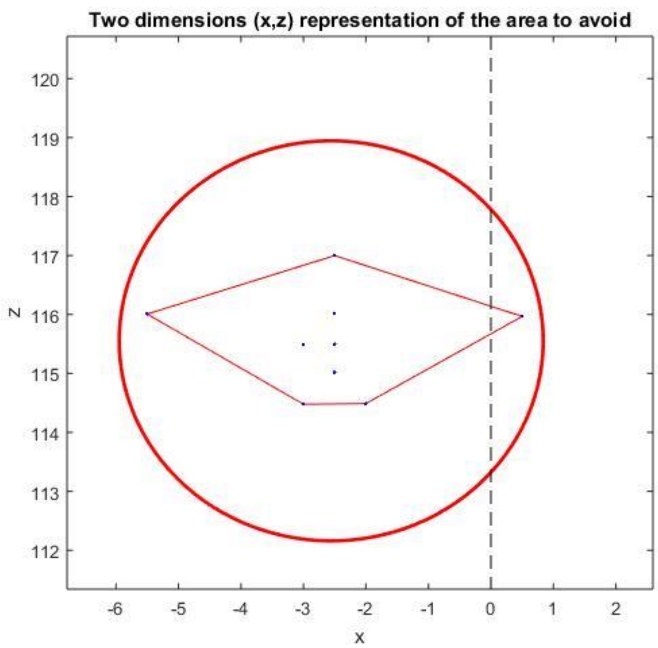


Figure 3.36 - Two dimensions (x,z) representation of the area that the aircraft must avoid in the fourth situation.

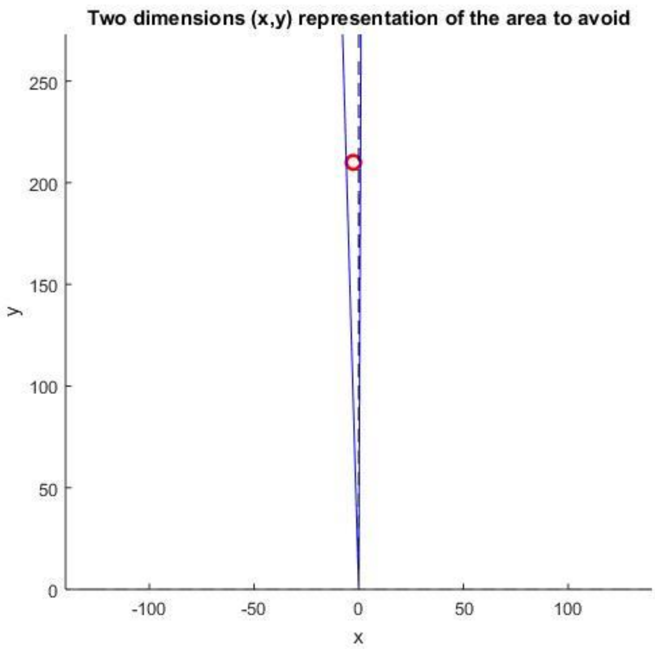


Figure 3.37 - Two dimensions (x,y) representation of the area that the aircraft must avoid in the fourth situation.

Table 3.35 – The values of $eta_1$ and $eta_2$ from fourth situation.

| | (degrees) | (radians) |
|---|---|---|
| $eta_1$ | 91.6218 | 1.5991 |
| $eta_2$ | 89.7711 | 1.5668 |

Table 3.36 – The value of the minimum radius from fourth situation.

| | (meters, m) | (feet, ft) |
|---|---|---|
| Minimum radius | 3.3922 | 11.1293 |

Situation IV with the First Set

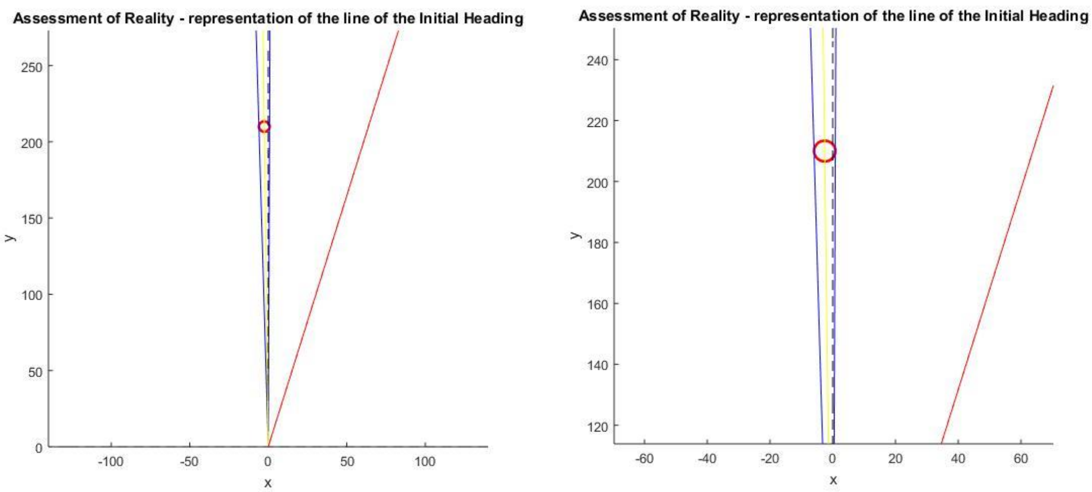


Figure 3.38 - Illustration of the process of ‘Assessment of Reality’ - representation of the line of the initial heading (fourth situation - first set).

Table 3.37 - Initial and final values of Heading and Altitude (fourth situation – first set).

| | Initial Value | | Final Value | |
|---|---|---|---|---|
| Heading | (degrees) | (radians) | (degrees) | (radians) |
| | 73.1000 | 1.2758 | 73.1000 | 1.2758 |
| Altitude | (meters, m) | (feet, ft) | (meters, m) | (feet, ft) |
| | 150 | 492.1260 | 150 | 492.1260 |

Situation IV with the Second Set

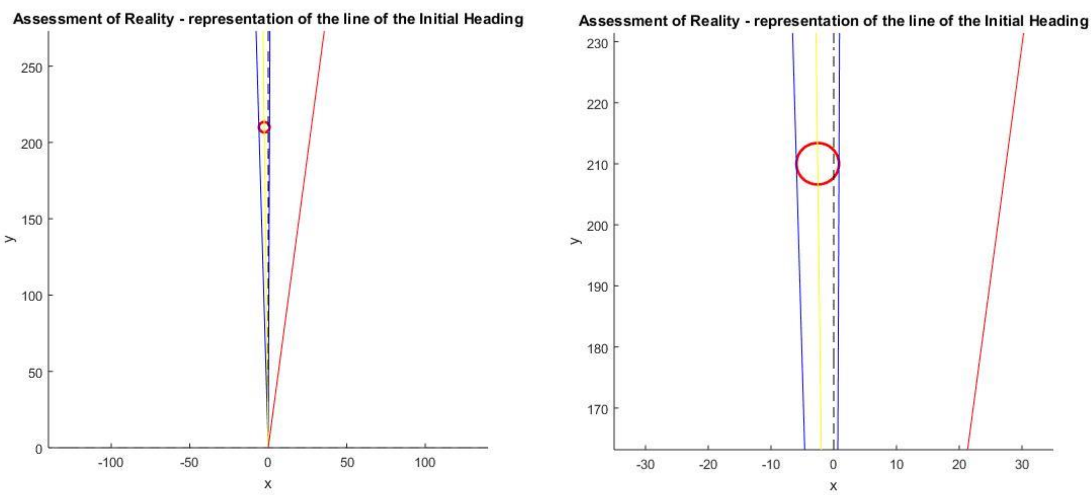


Figure 3.39 - Illustration of the process of ‘Assessment of Reality’ - representation of the line of the initial heading (fourth situation - second set).

Table 3.38 - Initial and final values of Heading and Altitude (fourth situation – second set).

| | Initial Value | | Final Value | |
|---|---|---|---|---|
| Heading | (degrees) | (radians) | (degrees) | (radians) |
| | 82.5500 | 1.4408 | 82.5500 | 1.4408 |
| Altitude | (meters, m) | (feet, ft) | (meters, m) | (feet, ft) |
| | 150 | 492.1260 | 150 | 492.1260 |

Situation IV with the Third Set

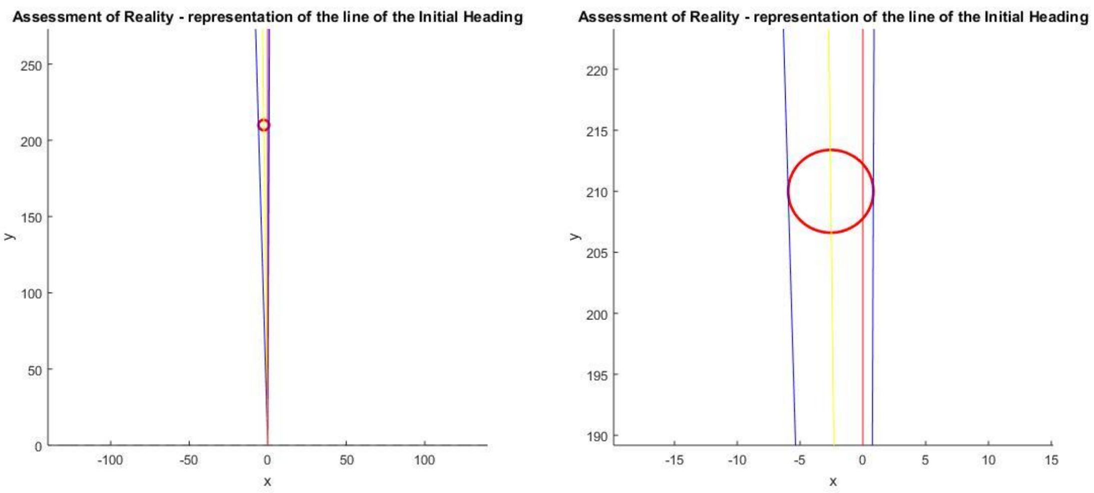


Figure 3.40 - Illustration of 'Assessment of Reality' - representation of the initial heading (fourth situation - third set).

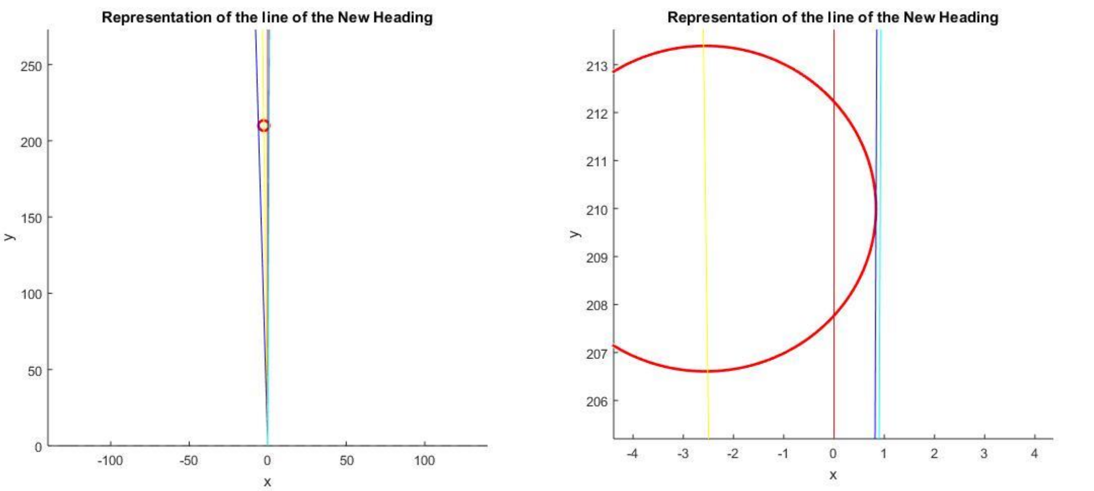


Figure 3.41 - Representation of the new heading (fourth situation - third set).

Table 3.39 - Initial and final values of Heading and Altitude (fourth situation – third set).

| | Initial Value | | Final Value | |
|---|---|---|---|---|
| Heading | (degrees) | (radians) | (degrees) | (radians) |
| | 90 | 1.5708 | 89.7480 | 1.5664 |
| Altitude | (meters, m) | (feet, ft) | (meters, m) | (feet, ft) |
| | 150 | 492.1260 | 150 | 492.1260 |

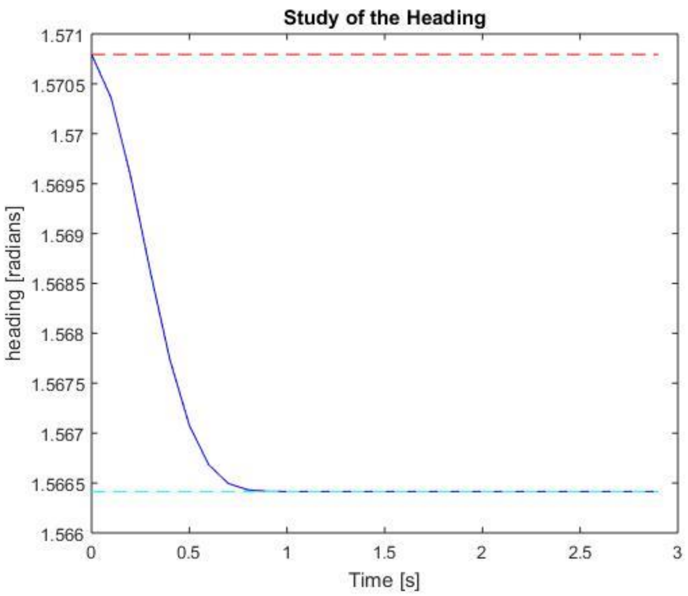


Figure 3.42 - Study of the behaviour of the aircraft’s heading over time (fourth situation - third set).

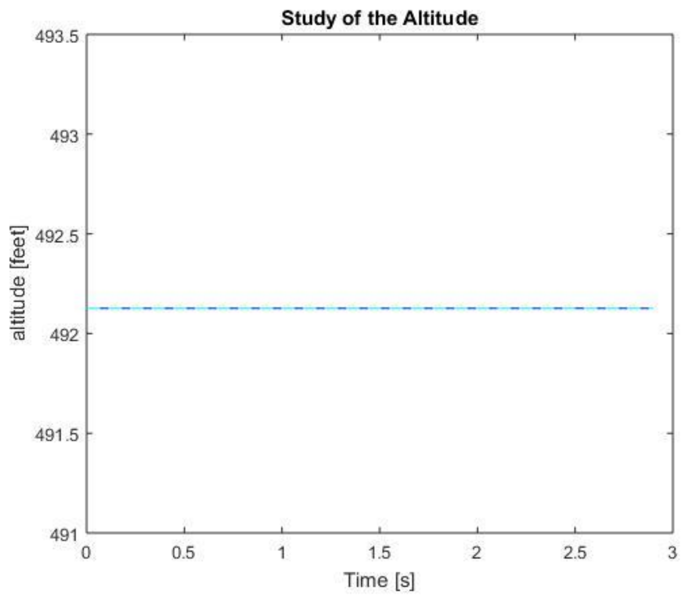


Figure 3.43 - Study of the behaviour of the aircraft’s altitude over time (fourth situation - third set).

Situation IV with the Fourth Set

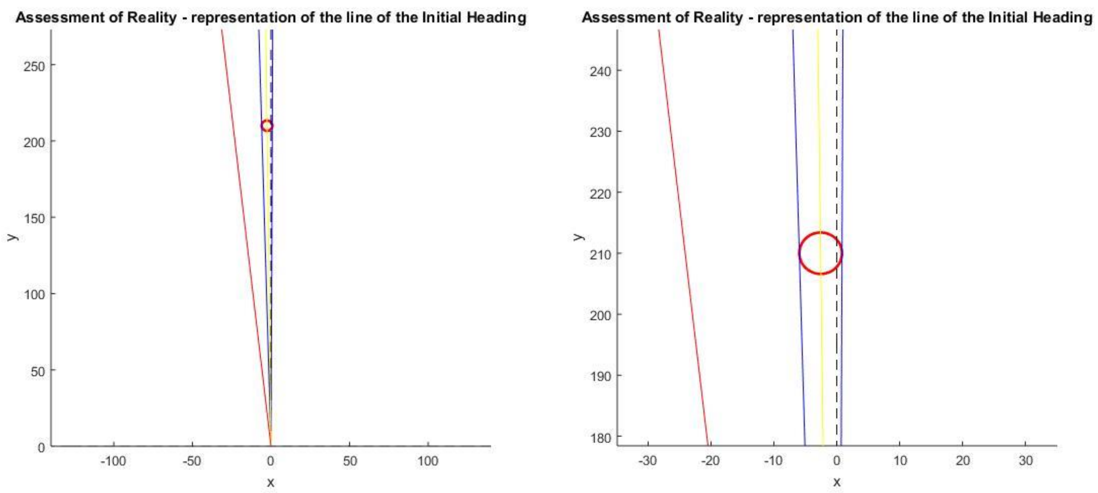


Figure 3.44 - Illustration of the process of ‘Assessment of Reality’ - representation of the line of the initial heading (fourth situation - fourth set).

Table 3.40 - Initial and final values of Heading and Altitude (fourth situation - fourth set).

| | Initial Value | | Final Value | |
|---|---|---|---|---|
| Heading | (degrees) | (radians) | (degrees) | (radians) |
| | 96.5500 | 1.6851 | 96.5500 | 1.6851 |
| Altitude | (meters, m) | (feet, ft) | (meters, m) | (feet, ft) |
| | 150 | 492.1260 | 150 | 492.1260 |

### 3.4.3 Discussion of Results

In situation IV, a possible threat of collision is detected by analysis of the first results. Table 3.34 confirms that the minimum distance between the aircraft and the obstacle is 114.4778 meters (375.5834 feet) vertically and 210.0134 meters (689.0204 feet) laterally, both distances are less than 300 meters (984.252 feet). Table 3.33 has all the points coordinates, which were necessary to calculate the distances (Table 3.34). Figure 3.34 is a two dimensions’ representation of the points in the ‘xz’ plan, which allows to visualise them in the space and to conclude that the obstacle has a much higher altitude than the aircraft.

The next step is to calculate the area that the aircraft must avoid. Figure 3.35 represents the convex polygon, which gives an idea of the real format of the obstacle. In Figure 3.36 and Figure 3.37 it is possible to find two different descriptions of the exact area to avoid. Figure 3.36 is a projection in terms of ‘xz’ plan, in which the area inside the red circle, including its limits, corresponds to the vertical area that the aircraft must avoid. While in Figure 3.37, which is also a projection of the conflict zone but in a ‘xy’ plan, the area to avoid includes the red circle and the area between the two dark blue lines tangent to the circle. In both figures the red circle has the same exact dimensions.

The exact values of $eta_1$ and $eta_2$ are included in Table 3.35, which will allow a more detailed analysis. Table 3.36 delivers the value of the sphere minimum radius.

Since the possibility of collision exists, the four sets with different values of heading and altitude were tested in this situation. They generated four unique scenarios.

- Situation IV with the first set

Observing Figure 3.38, the obvious conclusion is that the red line, which represents the initial heading of 1.2758 radians, is not between the two dark blue lines. So, the danger of collision in this scenario is not real and the process of assessment of reality is done. No necessary changes (Table 3.37), which means the aircraft can follow its path.

- Situation IV with the second set

The initial aircraft's heading, in this scenario, is equal to 1.4408 radians and it is represented by the red line in Figure 3.39. In the figure, the red line is not inside the area limited by the two dark blue lines, which means that the threat of collision is not real. So, the process of assessment of reality is done and the aircraft can continue its path without any modification in the flight characteristics (Table 3.38).

- Situation IV with the third set

Figure 3.40 describes this specific case and allows for concluding that the red line, which represents the initial heading of 1.5708 radians, is inside the area delimited by the two dark blue lines, closer to the left border, which is the line of $eta_2$. In this case, the value of $eta_2$ corresponds to 1.5668 radians. It is obvious that the danger of collision is real. The process of assessment of reality is done and, next, it is necessary to modify the flight characteristics to prevent the imminent collision.

Figure 3.41, despite having many similarities with the previous figure, includes a new light blue line, which represents the new value for the heading. The line of the new heading is in the safe zone but still remains close to the left border of the area to avoid. Table 3.39 has both initial and new values for the heading and altitude. In terms of heading, the value decreased to 1.5664 radians, which was expected since the value of the heading was very close to the value of $eta_2$ and the better option, in this case, is to decrease the heading to a new value lower than $eta_2$. The aircraft's altitude did not suffer any modifications mostly because the vertical distance between the aircraft and the obstacle is substantially high.

In Figure 3.42 it is possible to visualise the behaviour of the aircraft's heading over time. Initially, the value decreases abruptly and, when approaching the new value, slightly softens. When it assumes the new value, it stays constant. Figure 3.43 confirms that the value of altitude does not change over time.

- Situation IV with the fourth set

This scenario does not confirm the threat of collision. By observation of Figure 3.44 it is possible to conclude that the red line, which represents the initial heading of 1.6851 radians, is in the safe zone. The process of assessment of reality is now complete, no modifications are required (Table 3.40) so, the aircraft can continue its path.

## 3.5 Situation V

In this subsection, the initial data, the results and the discussion of results are related to the third situation.

### 3.5.1 Data

Table 3.41 - Initial data for the fifth simulation.

| Points | Angles | | | | | | | |
|---|---|---|---|---|---|---|---|---|
| | Beta | | Alpha | | Gama | | Delta | |
| | (degrees) | (radians) | (degrees) | (radians) | (degrees) | (radians) | (degrees) | (radians) |
| 1 | 35.6536 | 0.6223 | 35.6455 | 0.6221 | 5.7070 | 0.0996 | 5.8770 | 0.1026 |
| 2 | 35.6165 | 0.6216 | 35.6078 | 0.6215 | 6.1410 | 0.1072 | 6.3110 | 0.1101 |
| 3 | 35.4632 | 0.6189 | 35.4545 | 0.6188 | 6.1319 | 0.1070 | 6.3016 | 0.1100 |
| 4 | 35.3031 | 0.6162 | 35.2946 | 0.6160 | 6.1167 | 0.1068 | 6.2837 | 0.1097 |
| 5 | 35.7090 | 0.6232 | 35.7000 | 0.6231 | 6.2353 | 0.1088 | 6.4055 | 0.1118 |
| 6 | 35.6928 | 0.6230 | 35.6839 | 0.6228 | 6.2446 | 0.1090 | 6.4150 | 0.1120 |
| 7 | 35.5959 | 0.6213 | 35.5870 | 0.6211 | 6.2353 | 0.1088 | 6.4055 | 0.1118 |
| 8 | 35.4545 | 0.6188 | 35.4455 | 0.6186 | 6.3016 | 0.1100 | 6.4712 | 0.1129 |
| 9 | 35.6011 | 0.6214 | 35.5915 | 0.6212 | 6.7255 | 0.1174 | 6.8948 | 0.1203 |

### 3.5.2 Results

Table 3.42 - Points coordinates from fifth situation.

| Points | Coordinates | | |
|---|---|---|---|
| | x | Y | z |
| 1 | 33.8394 | 333.6015 | 240.4994 |
| 2 | 36.3364 | 333.0699 | 239.9766 |
| 3 | 36.3474 | 333.6705 | 239.0491 |
| 4 | 36.8383 | 339.0865 | 241.4887 |
| 5 | 36.8351 | 332.5580 | 240.4687 |
| 6 | 36.8457 | 332.1556 | 240.0388 |
| 7 | 36.8351 | 332.5580 | 239.4686 |
| 8 | 37.3450 | 333.6489 | 239.0340 |
| 9 | 39.8480 | 333.6688 | 240.5481 |

Table 3.43 - Vertical and Lateral distances from fifth situation.

| Points | Separation | | | |
|---|---|---|---|---|
| | Vertical | | Lateral | |
| | (meters, m) | (feet, ft) | (meters, m) | (feet, ft) |
| 1 | 240.4994 | 789.0400 | 335.3134 | 1.0e+03 *1.1001 |
| 2 | 239.9766 | 787.3247 | 335.0461 | 1.0e+03 *1.0992 |
| 3 | 239.0491 | 784.2818 | 335.6443 | 1.0e+03 *1.1012 |
| 4 | 241.4887 | 792.2858 | 341.0816 | 1.0e+03 *1.1190 |
| 5 | 240.4687 | 788.9394 | 334.5918 | 1.0e+03 *1.0977 |
| 6 | 240.0388 | 787.5287 | **334.1930** | **1.0e+03 *1.0964** |
| 7 | 239.4686 | 785.6581 | 334.5918 | 1.0e+03 *1.0977 |
| 8 | **239.0340** | **784.2322** | 335.7324 | 1.0e+03 *1.1015 |
| 9 | 240.5481 | 789.1999 | 336.0397 | 1.0e+03 *1.1025 |

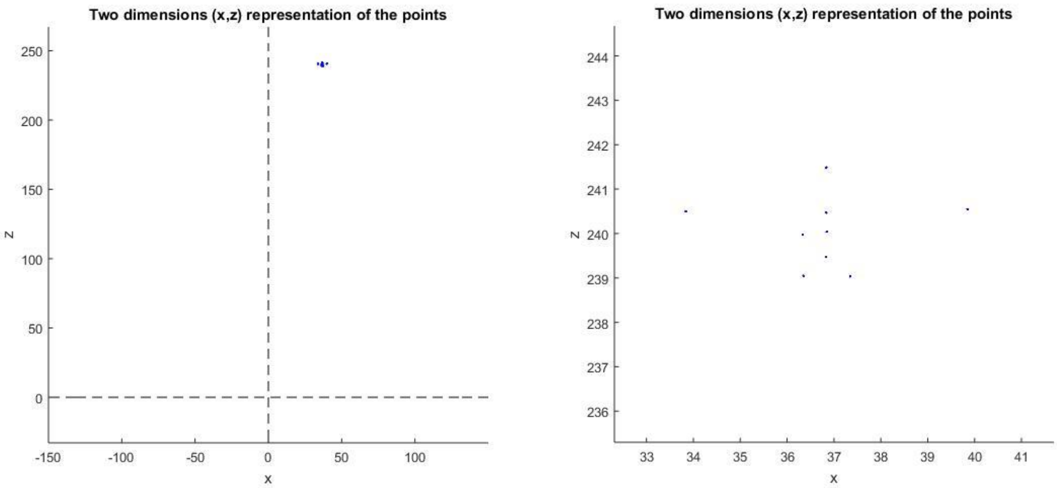


Figure 3.45 - Two dimensions (x,z) representation of the points in the space from fifth situation.

### 3.5.3 Discussion of Results

In the fifth situation, Table 3.43 allows for verifying that the lateral distance is more than 300 meters (984.252 feet). In fact, the minimum distance between the aircraft and the obstacle is 239.0340 meters (784.2322 feet) vertically and 334.1930 meters (1.0e+03 *1.0964 feet) laterally. So, the possibility of an imminent collision does not apply to this case.

Figure 3.45 is a two dimensions' representation of the points that allows for visualisation of the points in the space, more precisely in the 'xz' plan.

Since the possibility of collision does not exist, the four sets with different values of heading and altitude were not tested in this situation.

## 3.6 Situation VI

In this subsection, the initial data, the results and the discussion of results are related to the sixth situation.

### 3.6.1 Data

Table 3.44 - Initial data for the sixth simulation.

| Points | Angles | | | | | | | |
|---|---|---|---|---|---|---|---|---|
| | Beta | | Alpha | | Gama | | Delta | |
| | (degrees) | (radians) | (degrees) | (radians) | (degrees) | (radians) | (degrees) | (radians) |
| 1 | 3.1220 | 0.0545 | 3.1221 | 0.0545 | -0.5209 | -0.0091 | 0.0000 | 0.0000 |
| 2 | 3.1221 | 0.0545 | 3.1218 | 0.0545 | 0.2604 | 0.0045 | 0.7813 | 0.0136 |
| 3 | 3.5446 | 0.0619 | 3.5442 | 0.0619 | 0.5070 | 0.0088 | 1.0140 | 0.0177 |
| 4 | 3.4125 | 0.0596 | 3.4121 | 0.0596 | 0.5256 | 0.0092 | 1.0512 | 0.0183 |
| 5 | 3.1651 | 0.0552 | 3.1647 | 0.0552 | 0.5281 | 0.0092 | 1.0560 | 0.0184 |
| 6 | 2.8885 | 0.0504 | 2.8881 | 0.0504 | 0.5256 | 0.0092 | 1.0512 | 0.0183 |
| 7 | 3.1218 | 0.0545 | 3.1213 | 0.0545 | 0.7813 | 0.0136 | 1.3020 | 0.0227 |
| 8 | 3.1210 | 0.0545 | 3.1201 | 0.0545 | 1.5622 | 0.0273 | 2.0826 | 0.0363 |

### 3.6.2 Results

Table 3.45 - Points coordinates from sixth situation.

| Points | Coordinates | | |
|---|---|---|---|
| | x | Y | z |
| 1 | -0.5000 | 109.9748 | 5.9986 |
| 2 | 1.0000 | 109.9841 | 5.9991 |
| 3 | 1.5000 | 112.9889 | 6.9992 |
| 4 | 1.5000 | 108.9889 | 6.4993 |
| 5 | 1.5004 | 108.5139 | 6.0008 |
| 6 | 1.5000 | 108.9889 | 5.4994 |
| 7 | 2.0002 | 109.9990 | 5.9999 |
| 8 | 3.4998 | 109.9875 | 5.9994 |

Table 3.46 - Vertical and Lateral distances from sixth situation.

| Points | Separation | | | |
|---|---|---|---|---|
| | Vertical | | Lateral | |
| | (meters, m) | (feet, ft) | (meters, m) | (feet, ft) |
| 1 | 5.9986 | 19.6805 | 109.9760 | 360.8135 |
| 2 | 5.9991 | 19.6822 | 109.9886 | 360.8550 |
| 3 | 6.9992 | 22.9634 | 112.9988 | 370.7311 |
| 4 | 6.4993 | 21.3230 | 108.9992 | 357.6091 |
| 5 | 6.0008 | 19.6877 | **108.5242** | **356.0507** |
| 6 | **5.4994** | **18.0428** | 108.9992 | 357.6091 |
| 7 | 5.9999 | 19.6846 | 110.0172 | 360.9489 |
| 8 | 5.9994 | 19.6830 | 110.0431 | 361.0339 |

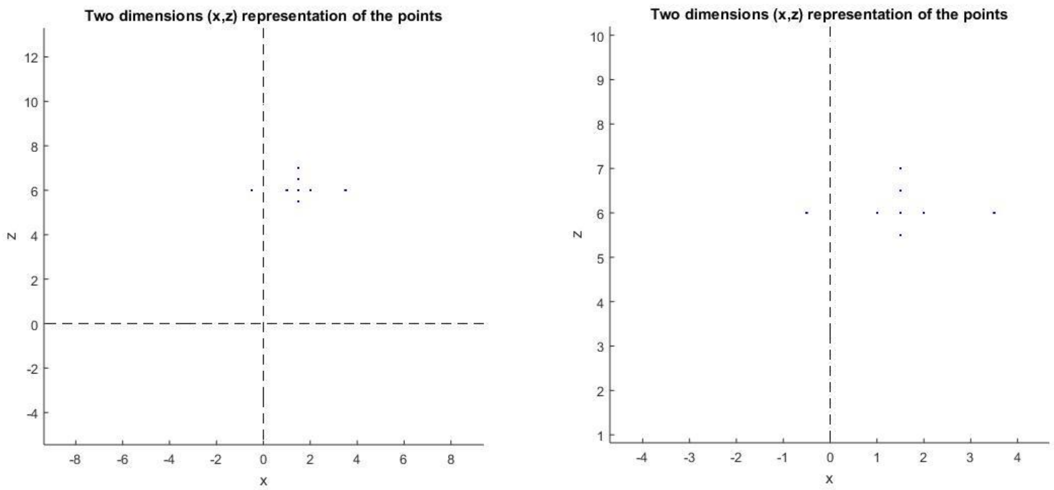


Figure 3.46 - Two dimensions (x,z) representation of the points in the space from sixth situation.

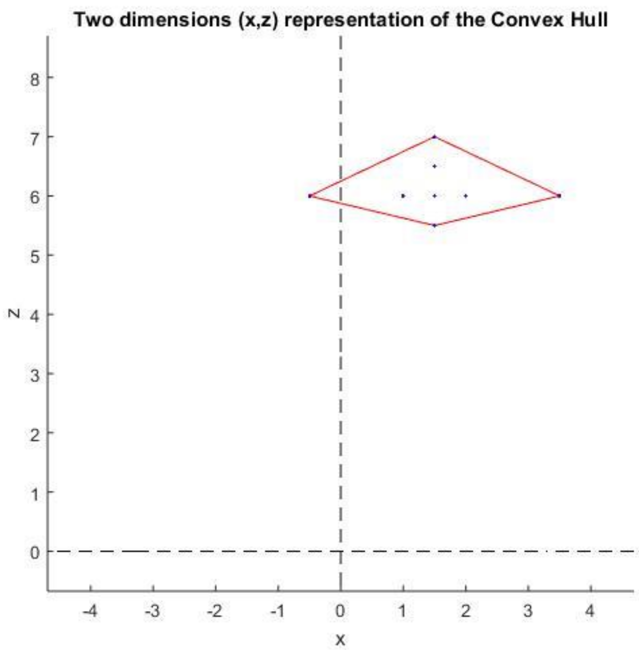


Figure 3.47 - Two dimensions (x,z) representation of the convex hull, more specifically the convex polygon from sixth situation.

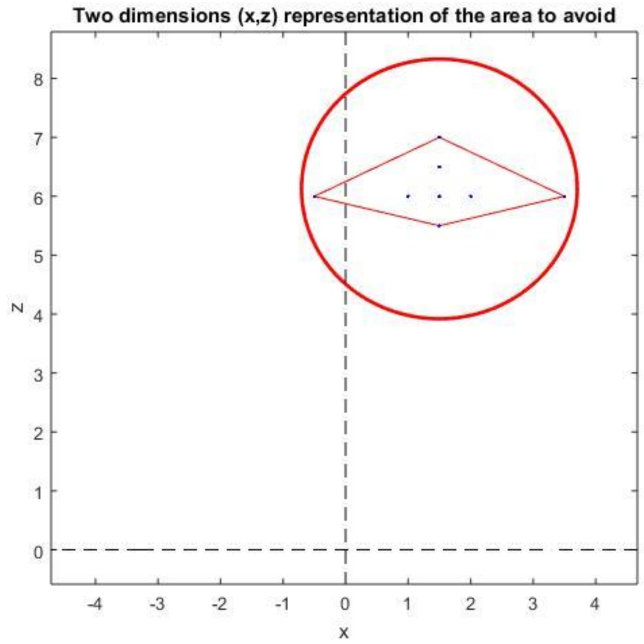


Figure 3.48 - Two dimensions (x,z) representation of the area that the aircraft must avoid in the sixth situation.

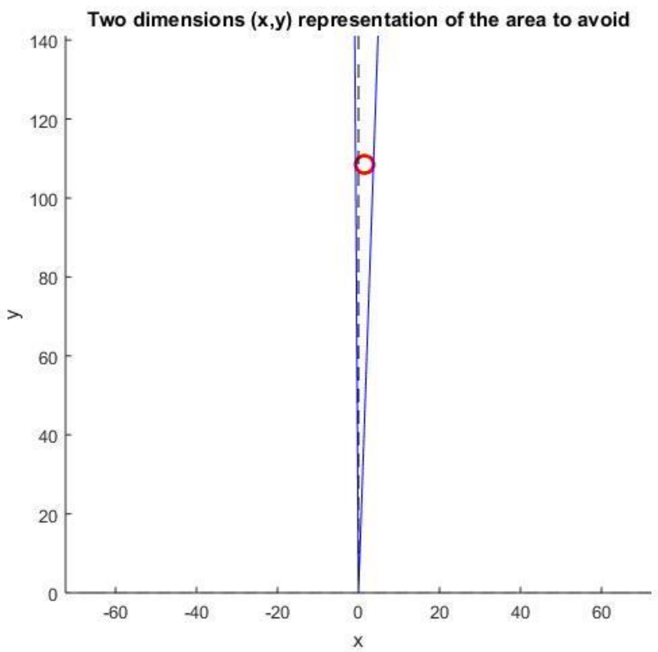


Figure 3.49 - Two dimensions (x,y) representation of the area that the aircraft must avoid in the sixth situation.

Table 3.47 – The values of $eta_1$ and $eta_2$ from sixth situation.

| | (degrees) | (radians) |
|---|---|---|
| $eta_1$ | 90.3727 | 1.5773 |
| $eta_2$ | 88.0465 | 1.5367 |

Table 3.48 – The value of the minimum radius from sixth situation.

| | (meters, m) | (feet, ft) |
|---|---|---|
| Minimum radius | 2.2044 | 7.2323 |

<u>Situation VI with the First Set</u>

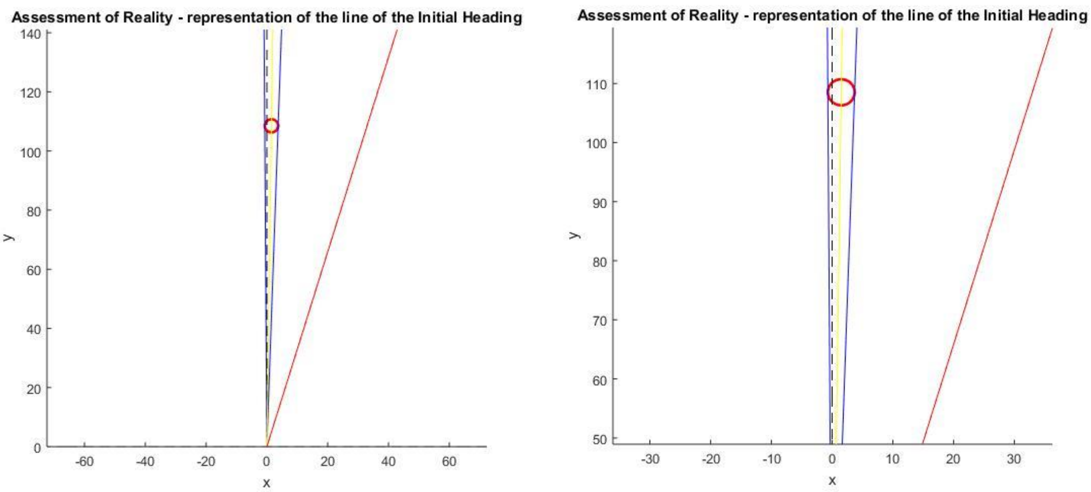


Figure 3.50 - Illustration of the process of 'Assessment of Reality' - representation of the line of the initial heading (sixth situation - first set).

Table 3.49 - Initial and final values of Heading and Altitude (sixth situation – first set).

| | Initial Value | | Final Value | |
|---|---|---|---|---|
| Heading | (degrees) | (radians) | (degrees) | (radians) |
| | 73.1000 | 1.2758 | 73.1000 | 1.2758 |
| Altitude | (meters, m) | (feet, ft) | (meters, m) | (feet, ft) |
| | 150 | 492.1260 | 150 | 492.1260 |

Situation VI with the Second Set

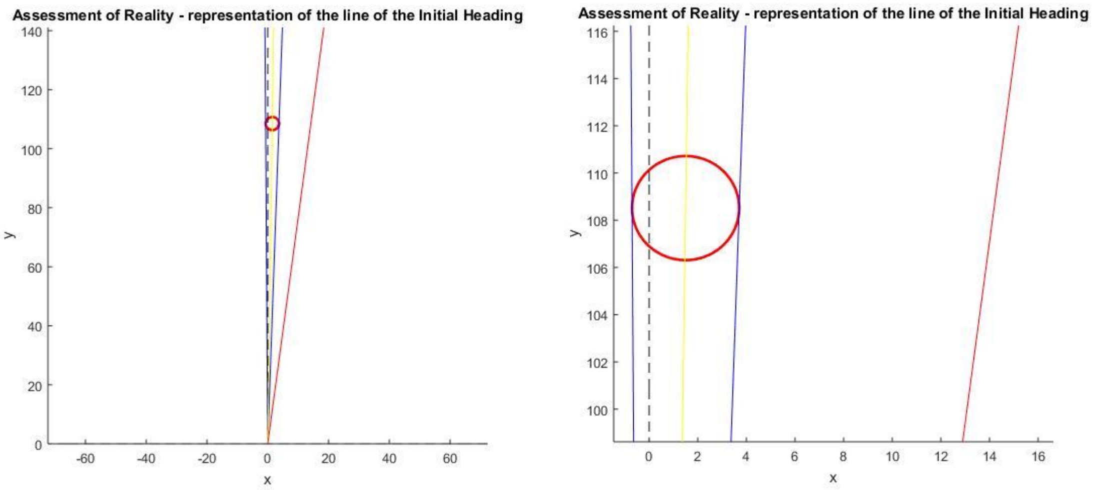


Figure 3.51 - Illustration of the process of 'Assessment of Reality' - representation of the line of the initial heading (sixth situation - second set).

Table 3.50 - Initial and final values of Heading and Altitude (sixth situation – second set).

| | Initial Value | | Final Value | |
|---|---|---|---|---|
| Heading | (degrees) | (radians) | (degrees) | (radians) |
| | 82.550 | 1.4408 | 82.550 | 1.4408 |
| Altitude | (meters, m) | (feet, ft) | (meters, m) | (feet, ft) |
| | 150 | 492.1260 | 150 | 492.1260 |

Situation VI with the Third Set

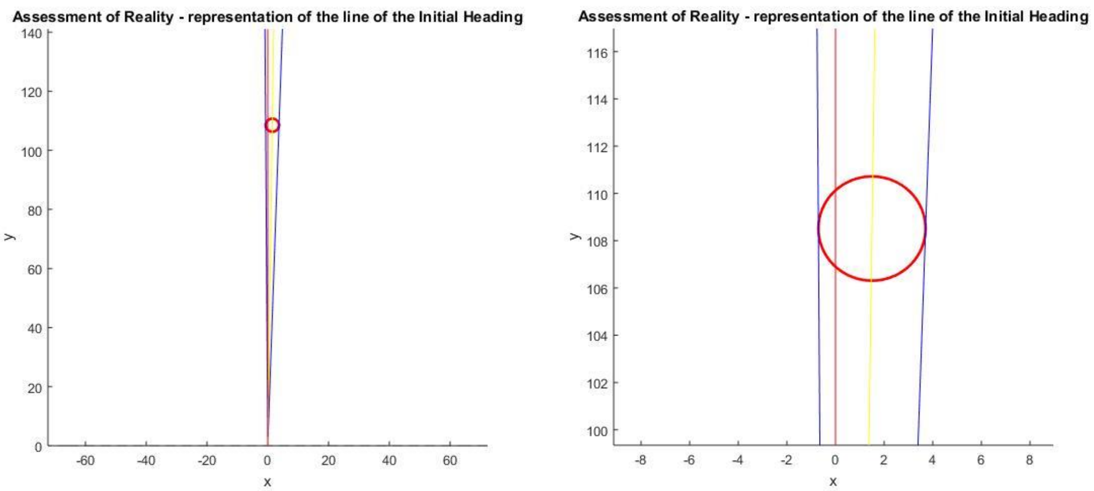


Figure 3.52 - Illustration of 'Assessment of Reality' - representation of the initial heading (sixth situation - third set).

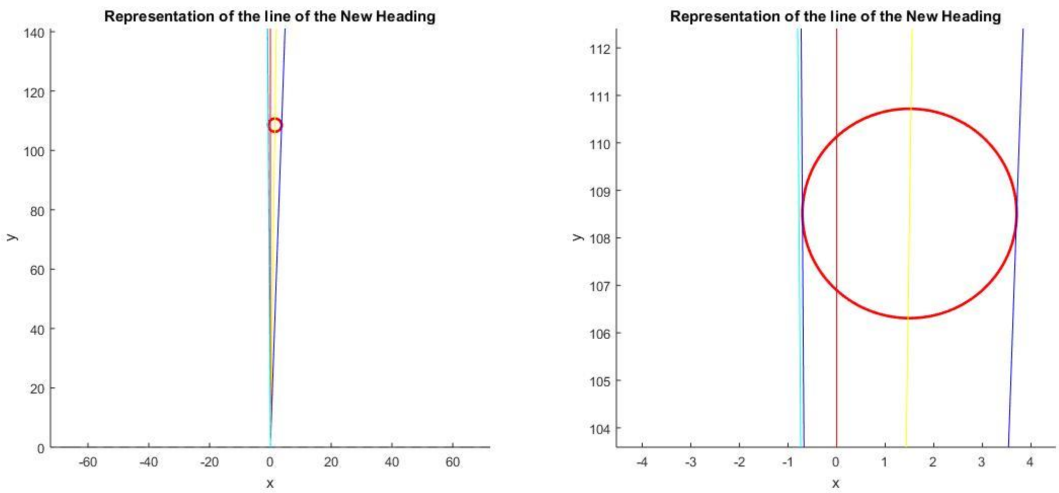


Figure 3.53 - Representation of the new heading (sixth situation - third set).

Table 3.51 - Initial and final values of Heading and Altitude (sixth situation –third set).

| | Initial Value | | Final Value | |
|---|---|---|---|---|
| Heading | (degrees) | (radians) | (degrees) | (radians) |
| | 90 | 1.5708 | 90.407 | 1.5779 |
| Altitude | (meters, m) | (feet, ft) | (meters, m) | (feet, ft) |
| | 150 | 492.1260 | 145.6879 | 477.9787 |

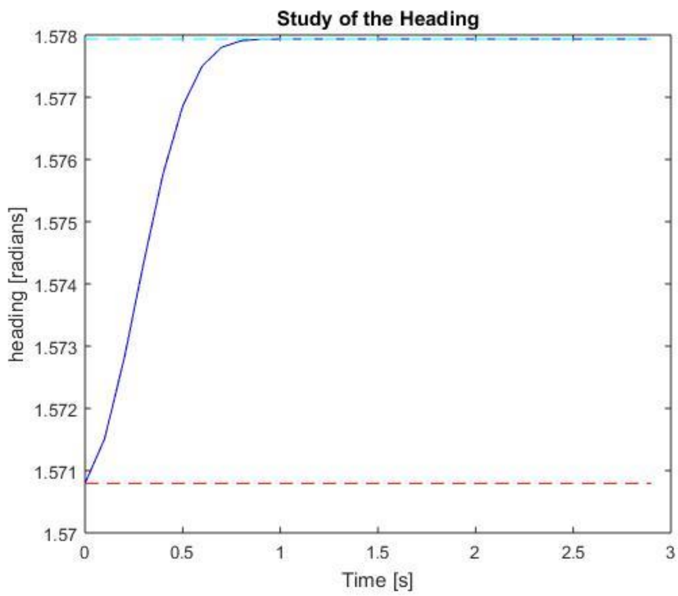


Figure 3.54 - Study of the behaviour of the aircraft’s heading over time (sixth situation - third set).

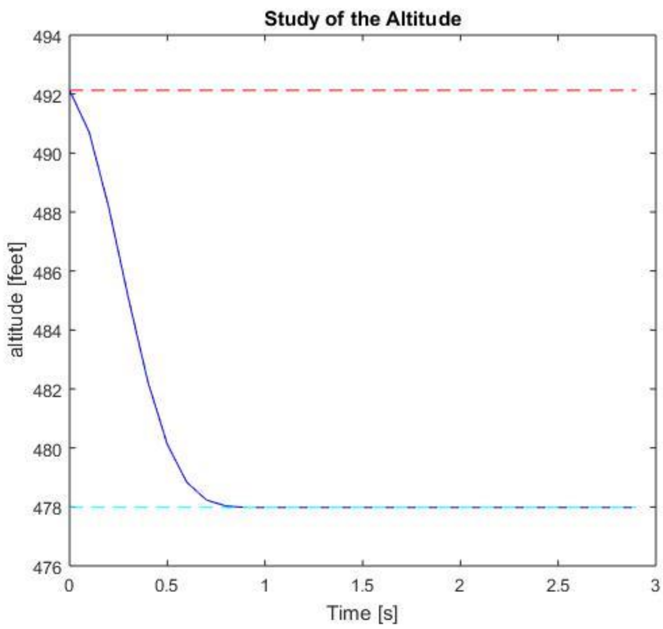


Figure 3.55 - Study of the behaviour of the aircraft’s altitude over time (sixth situation - third set).

Situation VI with the Fourth Set

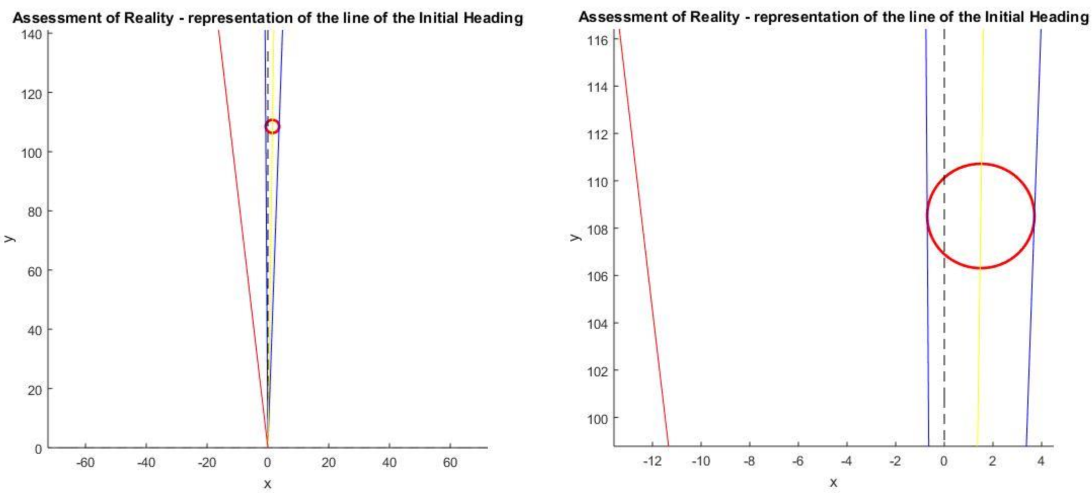


Figure 3.56 - Illustration of the process of ‘Assessment of Reality’ - representation of the line of the initial heading (sixth situation - fourth set).

Table 3.52 - Initial and final values of Heading and Altitude (sixth situation - fourth set).

| | Initial Value | | Final Value | |
|---|---|---|---|---|
| Heading | (degrees) | (radians) | (degrees) | (radians) |
| | 96.550 | 1.6851 | 96.550 | 1.6851 |
| Altitude | (meters, m) | (feet, ft) | (meters, m) | (feet, ft) |
| | 150 | 492.1260 | 150 | 492.1260 |

### 3.6.3 Discussion of Results

In situation VI, the minimum distance between the aircraft and the obstacle is 5.4994 meters (18.0428 feet) vertically and 108.5242 meters (356.0507 feet) laterally (Table 3.46) so, both distances are less than 300 meters (984.252 feet), which implies that the danger of collision is a possibility. Figure 3.46 is a two dimensions' representation of the points in the 'xz' plan and helps to visualise the points in the space. In this case, the obstacle has a higher altitude than the aircraft.

Knowing that there is a possible threat of collision, it is fundamental to calculate the area that the aircraft must avoid. In Figure 3.47, thanks to the convex hull method, it is possible to observe an approximation to the real format of the obstacle, the convex polygon. The following two figures, Figure 3.48 and Figure 3.49, describe the conflict zone. Figure 3.48 is a projection in terms of 'xz' plan, in which the area inside the red circle, including its limits, is the vertical area that the aircraft must avoid. While in Figure 3.49, which is a projection of the conflict zone in the 'xy' plan, the area to avoid includes the red circle and the area between the two dark blue lines tangent to the circle. The red circle has the same exact dimensions in both projections.

The exact values of $eta_1$ and $eta_2$ are included in Table 3.47, which will allow a more detailed analysis. Table 3.48 delivers the value of the sphere minimum radius.

Since the possibility of collision exists, the four sets with different values of heading and altitude were tested in this situation. They generated four unique scenarios.

- Situation VI with the first set

Figure 3.50 allows for concluding that the red line, which represents the initial heading of 1.2758 radians, is on the left side of the obstacle, outside the area delimited by the two dark blue lines. So, the danger of collision is not real, which means the process of assessment of reality is done. No changes of heading and altitude were needed (Table 3.49) and the aircraft can continue its path.

- Situation VI with the second set

In this scenario, the initial aircraft's heading is 1.4408 radians and it is represented by the red line in Figure 3.51. Observing the figure, it is obvious that the red line is in the safe area, more specifically on the left side of the area to avoid. In fact, this situation is similar to the previous scenario. The threat of collision does not exist. With this conclusion, the process of assessment of reality is done and the aircraft can continue its path without any modification in the flight characteristics (Table 3.50).

- Situation VI with the third set

By observation of Figure 3.52, it is possible to conclude that the red line, which represents the initial heading of 1.5708 radians, is inside the area delimited by the two dark blue lines. Each dark blue line is a limit of the conflict zone, more precisely, the right limit corresponds to $eta_2$ (1.5367 radians) and the left limit to $eta_1$ (1.5773 radians). In this case, the value of the heading is closer to $eta_1$. So, the danger of collision is confirmed. Next, it is necessary to change the aircraft's heading and probably its altitude to prevent an imminent collision.

Figure 3.53, although it looks exactly the same as the previous one, includes a new light blue line that represents the new value for the heading. This new line is in the safe zone, close to the left border of the area to avoid. Comparing the lines of the initial and new heading it is possible to conclude that the aircraft's heading increased. Table 3.51, which shows both values, confirms it. The new value of the heading is 1.5779 radians, which means it increased 0.0071 radians. In terms of the aircraft's altitude, the value suffered a decrease of 4.3121 meters (14.1473 feet), which was expected for two reasons: first, the aircraft had a lower altitude than the obstacle and, second, the vertical distance between the aircraft and the obstacle was not too significant so, when the safety margin was applied, the aircraft's altitude entered the vertical area to be avoided.

Figure 3.54 is the study of the aircraft's heading over time. Observing, it is possible to see an abrupt rise of the value and, only when approaching the desired value, it tends to slow down. After reaching the new value, the behaviour does not suffer any further disturbance. Figure 3.55 is a similar study but to analyse the behaviour of the aircraft's altitude over time. The altitude initially decreases abruptly and, when reaching the new value, slows down. This scenario is similar to situation III with the second set.

- Situation VI with the fourth set

In Figure 3.56, it is possible to observe that the red line, which represents the initial heading of 1.6851 radians, is not coincident with the conflict zone so, the possible threat of collision is, in fact, non-existing. With the process of assessment of reality done and no modifications required (Table 3.52), the aircraft can continue normally.

# Chapter 4

# Conclusions

The continuing growth of air traffic increases the necessity of creating new methods and systems capable of preventing any accidents. In this work the focus was on developing a new collision avoidance method ideal to small air vehicles, just like RPAS's. RPAS is a recent technology, which is not only available to professional activities but also to the public in general. Different models with the most varied characteristics, from the size and weight to the range, are on the market. Although, the regulatory institutions are working on new regulations and campaigns to elucidate the owners of this technology and control the air space, the number of incidents between conventional aircrafts and RPAS's are increasing. This problematic is exactly the main reason for the development of this project.

Most of the RPAS's don't have any kind of anti-collision systems included. Equipping them with one may significantly decrease the number of incidents and prevent a major catastrophe.

The collision avoidance method developed in this work allows for keeping the privacy and autonomy of the vehicle, mainly because the detection of any obstacle is carried out by an independent optical system. So, a practical application of it would be suitable for both civilian and military RPAS's.

The optical system consists of two equal and strategically positioned infrared cameras. Due to the fact that actual tests were not done, the process of selecting the cameras is not included in this work. However, it was fundamental to establish their main characteristics. The position of both cameras, which is very important to the process of calculating the distances between the aircraft and the obstacle, is also defined in the beginning and kept constant for all simulations.

Every step of the development of the collision avoidance method is described in detail and includes all the equations and logical reasoning used in the computational algorithm. Any mistake, even a minimum one, could influence the results. So, it was important to review every step more than once and with maximum attention. To test the algorithm many simulations were performed. First, with the purpose of comparing the results with the theoretically expected, which permitted finding and correcting any inconsistencies. Secondly, it tested the efficiency of the algorithm in different scenarios. The first group of tests are not included in this work because they were only the means to the main objective, which is a final algorithm, a collision avoidance method that works.

Six different situations were created to test the algorithm. In only one case did the method immediately conclude that there was no danger of collision. In fact, the lateral distance was higher than three hundred meters so, the conclusion was correct. In the other five situations, the method detected a possible threat of collision, which is consistent with the results, all five situations had minimum distances with lower value than three hundred meters. In the cases with possible danger of collision, four different scenarios were tested. All results are included in this work as well as a discussion of them. All the results, whether they are figures or tables, are consistent since the conclusions taken from a figure are confirmed by the values in the respective table. In addition to being consistent, they do not show any errors. With results like these, it is possible to affirm that this specific collision avoidance method works correctly regardless of the situation.

The computational algorithm proved to be effective and a complete functional collision avoidance method. When an obstacle is detected, the algorithm assesses if the danger of collision is a possibility, in an affirmative case, it determinates the area to avoid and initiates the process of assessment of reality, in case the threat is real, it calculates all the necessary changes to prevent an imminent collision.

The main objective was accomplished, a new collision detection and avoidance method completely developed from scratch. Many difficulties and challenges had to be overcome. The final product meets the initial expectations.

Future work on this method will always be with the intention of improving the general algorithm and possible extension of its capacities. What is now a detection and avoidance method can be developed to a detection and prevention system, which means an anti-collision system.

To achieve a complete anti-collision system, it will be necessary to continue to develop the method to a point where the new values previously calculated are transmitted to the aircraft. The process will be to connect the method described in this work to a guidance system, which will indicate to the autopilot the exact modifications to be made. For last, the autopilot will be responsible of implementing the modifications in the aircraft.

In terms of the flight velocity, it will be essential to analyse how this specific parameter will influence the results. High speeds may not allow enough time to implement the changes in the heading and altitude. So, depending on the velocity this method may or may not be efficient. This problematic should be analysed to improve the present algorithm and solve possible existing limitations.

# References

[1] Ortiz, Andres E.; Neogi, Natasha N., Object Detection and Avoidance Using Optical Techniques in Uninhabited Aerial Vehicles, AIAA Guidance, Navigation and Control Conference and Exhibit 20-23 August 2007, Hilton Head, South Carolina, Paper number AIAA 2007-6610.

[2] Griffiths S., Saunders J., Curtis A., Barber B., McLain T., Beard R. 2007. Obstacle and Terrain Avoidance for Miniature Aerial Vehicles. In: Valavanis K.P. (eds) Advances in Unmanned Aerial Vehicles. Intelligent Systems, Control and Automation: Science and Engineering, Vol. 33, pp 213-244.

[3] Zufferey, J. C.; Floreano, D., Toward 30-gram Autonomous Indoor Aircraft: Vision-based Obstacle Avoidance and Altitude Control, Proceedings of the 2005 IEEE, International Conference on Robotics and Automation, Barcelona, Spain, April 2005, pp. 2594– 2599.

[4] Barrows, G.L.; Neely, C., Mixed-Mode VLSI Optic Flow Sensors for In-Flight Control of a Micro Air Vehicle, Presented at the SPIE 45th Annual Meeting in San Diego, CA, July 31 – August 4, 2000.

[5] International Civil Aviation Organization, 2002, Manual on Implementation of a 300 m (1 000 ft) Vertical Separation Minimum Between FL 290 and FL 410 Inclusive, Manual.

[6] Kuchar, J.; Drumm, A. 2007, The Traffic Alert and Collision Avoidance System, Lincoln Laboratory Journal, Vol. 16 No. 2, pp. 277- 296.

[7] Bousson, K. 2008, Model predictive control approach to global air collision avoidance, Aircraft Engineering and Aerospace Technology: An International Journal, Vol. 80 No. 6, pp. 605-612.

[8] Ibrahim, Y. 2013, Development of a Flight Collision Avoidance System for a Free Flight Environment: An Ecological Interface Design Approach, International Journal of Multidisciplinary and Current Research, Nov/Dec, pp. 120-133.

[9] Srikanthakumar, S.; Liu, C.; Chen, W-H. 2012, Optimization-Based Safety Analysis of Obstacle Avoidance Systems for Unmanned Aerial Vehicles, Journal of Intelligent and Robotic Systems, Vol. 65, pp. 219-231.

[10] Temizer, S.; Kochenderfer, M. J.; Kaelbling, L. P.; Lozano-Pérez, T.; Kuchar, J.K., Collision Avoidance for Unmanned Aircraft using Markov Decision Processes, AIAA Guidance, Navigation and Control Conference 2-5 August 2010, Toronto, Ontario Canada, Paper number AIAA 2010-8040.

[11] Zeitlin, A.; Lacher, A.; Kuchar, J.; Drumm, A. 2006, Collision Avoidance for Unmanned Aircraft: Proving the Safety Case, Lincoln Laboratory, Technical Report number 42PM ATC-329.

[12] Berg, M.; Cheong, O.; van Kreveld, M.; Overmars, M. 1997, Computational Geometry: Algorithms and Applications, Springer-Verlag.

[13] Jarvis, R.A. 1973, On the Identification of the Convex Hull of a Finite Set of Points in the Plane, Information Processing Letters, Vol. 2, pp 18-21.

[14] Graham, R.L. 1972, An Efficient Algorithm for Determining the Convex Hull of a Finite Planar Set, Information Processing Letters, Vol. 1, pp 132-133.

[15] Chan, T.M. 1996, Optimal Output-sensitive Convex Hull Algorithms in 2 and 3 Dimensions, Discrete Computational Geometry, Vol. 16, pp 361-368.

[16] Hale, J.K.; Verduyn Lunel, S.M. 1993, Introduction to Functional Differential Equations, Springer-Verlag New York Inc..

# Appendix

## A – Submitted to AVIATION Journal.

### CONE BASED COLLISION DETECTION METHOD USING OPTICAL SYSTEMS

**Ana SILVA[1], Kouamana BOUSSON[2]**

*[1]Aerospace Sciences Department, Faculty of Engineering, University of Beira Interior, Address: Aerospace Sciences Department, Calçada Fonte do Lameiro, 6201-001 Covilhã, Portugal.*
*[2]Department of Aerospace Sciences, Faculty, University, Address: Aerospace Sciences Department, Calçada Fonte do Lameiro, 6201-001 Covilhã, Portugal.*
*E-mails: ana.silva.azoriana7@gmail.com; (Ana Silva) bousson@ubi.pt (Kouamana Bousson)*

**Abstract.** The main interest in this paper is the determination of the area that an aircraft must avoid in order to prevent a possible collision threat which is detected based on optical systems. Collision prevention is a fundamental part of aircraft operations during its flight mission. The main objective of the present paper is to deal with the collision detection characteristics and the description of a safe zone as the area outside a conflict cone. Initially two cameras are strategically placed in the aircraft to provide two images and to enable the calculations of velocities and distances between the aircraft and any object on its way. The analysis of these velocities and distances provides a way to detect possible collision threats. The concepts of Convex Hull and Cone are used to describe the specific area to be avoided. Two simulations were done and all the results showed consistency and effectiveness, which proved that the proposed method can be used efficiently as a part of a collision avoidance system.

**Keywords:** Collision detection, Optical camera, Convex Hull, Conflict Cone, Air Traffic, Computational Algorithm.

#### Introduction

On a world that all countries are increasingly connected, the concept of borderless is growing and spreading. Many aspects of the technological development are related with the appearance of this concept and one of the sectors with great impact on this matter is the aeronautical and aerospace sector. This sector allows to travel small or larger distances in a short time and comfortable way and even to dislocate many types of merchandise from all over the world. The growing demand for air transport, independently of the reason, results on an increasing air traffic.

The perspectives for the future decades is for a continuing growth of the air traffic. More aircrafts operating at the same time requires a bigger control and higher level of precision and efficiency. An aircraft is a complex machine and if there are risks while operating an aircraft on an airspace with reasonable air traffic, in a condense air traffic those risks are much higher. However, one of many strands of this sector development is 'Safety and Security'. Those two words are often connected but they are two different concepts with distinct meaning in aviation. Safety is associated to the defence and care against any accident or mistake/defect during all the most important phases of an aircraft (design, construction, maintenance and operation). In other hand, security is all the existing procedures to avoid any type of malevolent actions, like terrorism, aiming as a target the airplane and who may be inside, crew and passengers. This strand goal is to minimise all risks associated with air transport. One specific risk is collision, between two or more aircrafts or between an aircraft and an object or animal.

Collision is an important risk and a delicate subject, which deserves the correct approach to find the most efficient solution. There are several research activities in collision avoidance, each one with their own approach but all with the same main goal: finding the most efficient and innovative solution to this specific problem. One anti-collision system created, tested, improved and marketed is TCAS (Traffic Collision Avoidance System), which is currently installed in innumerable aircrafts. It is an anti-collision system based on monitoring the airspace around the aircraft looking for others aircrafts equipped with a transponder, and then informs the pilots of the possible existing thread. This system only provides local separation. However, for areas with high density of air traffic this approach is considered by several people not the most efficient.

So, in opposition to the local separation there are the concept of global collision avoidance which consider the global traffic in a specific area and not only pairs of aircrafts. Some research activities focus their attention on this last concept and combine the collision avoidance problem with the future possibility of free-flight (Bousson 2008). Free-flight represents an increase in the autonomy of the aircraft, which means that each aircraft has the capacity to choose its own trajectory but at the same time must ensure its own safety. This idea is possible to be implemented in the future if we think about the increasing air traffic, mentioned before, and all the complications involved, such as the high workload to Air Traffic Controllers. However, this concept involves an increase in the pilot's responsibility and it is essential to support them with innovative systems and new interface designs (Ibrahim 2013).

The current problem is not only about the growing air traffic of conventional aircrafts but also the introduction of RPAS (Remotely Piloted Aircraft System) in the airspace, causing an even more complex situation in terms of air traffic. Different RPASs, with different autonomies, ranges and technologies, have become available on the market. Yet, unlike the traditional aircrafts, most RPASs are not equipped with anti-collision systems like TCAS. So, the operation of RAPS, along with the other aircrafts, demands a higher level of control and management of the airspace. This matter begins to be addressed in several countries and by international associations, which means, that the appropriated regulation is being established and creative campaigns begin to be disclosed. However, there still a lot of work ahead in order to developed and improved this area. Because it is necessary a competent and efficient work to maintain the air control and prevent any accidents. For example, the introduction of anti-collision systems on RAPS is one possibility that deserves to be carefully study.

Regardless of whether the flight collision avoidance system is for an RPAS or a traditional aircraft it is necessary to pay attention to all the details involving the process and it is fundamental to assure that the new system meets not only the mission requirements but also the existing regulations regarding safety issues, for that the designing method should be consistent and efficient (Zeitlin, Lacher, Kuchar and Drumm 2006).

Relatively to this work, the goal is to elaborate a detection method that assess whether there is danger of collision or not and then, in affirmative case, provides the detailed area in two dimensions that the aircraft must avoid to prevent an imminent collision. The process can be resume by creating a computer software capable of combining information with existing optical methods. This specific system values the autonomy and privacy of the aircraft for which it is intend, which makes it appropriated to all kinds of RPASs, more specifically, to military RPASs.

**Problem Statement**

On the principle that our aircraft, or our RPAS, is already equipped with two strategically positioned infrared cameras, which, in case they detect any points from an object, will provide us two images (one each camera), we can determinate if there is in fact danger of collision. This is the first goal to be accomplish but for that it is necessary to calculate the distance vector between our aircraft and each point to know the minimum distance between our aircraft and the object. If both lateral and vertical distance are less than three hundred meters the possibility of collision with the object is real. Then, the second problem to be solved is that of finding the specific area to avoid. Because if the area to avoid is known it is possible to change the aircraft trajectory preventing that way an imminent collision (or a possible future collision) and keeping the aircraft safe and allowing it to continue its mission.

**Proposed Method**

To solve the first problem, it is essential to calculate the distance vectors and all the point coordinates to conclude if the danger is real.

Relative to the second problem, it is necessary to select a method capable of determining based on the point coordinates an approximation to the real format of the object to avoid. The choice was a simple geometrical method named as Convex Hull Method (Berg, Cheong, van Kreveld, Overmars 1997).

**Conflict Assessment**

Based on the cameras images is possible to verify, for each singular case, if there is danger of collision.

First, it is necessary to determinate the distance vector between our aircraft and each point through the angles provided by the cameras (left camera - alpha and delta, right camera - beta and gamma). For each point the distance vector:

$$\vec{D}_i(xd,yd,zd) \tag{1}$$

where '$\vec{D_i}$' is the distance vector, 'i' is the indexing number to identify the point under study, 'xd' is the vector component in 'x', 'yd' is the vector component in 'y' and 'zd' is the vector component in 'z'. These three components can also be interpreted as the points coordinates (x, y and z), when the axis is on our aircraft.

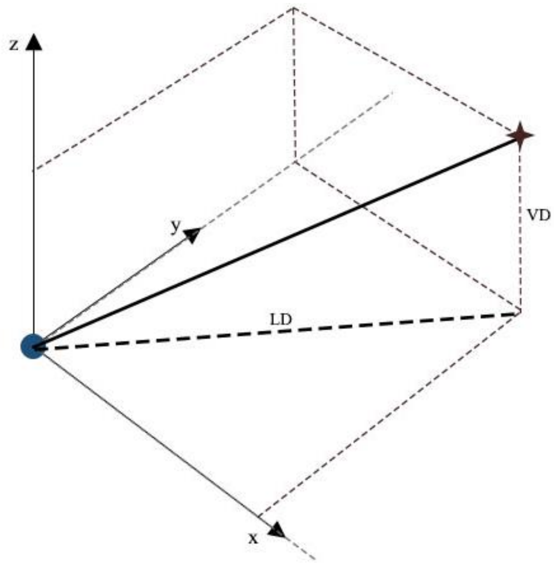


Fig. 1. A three-dimension (x,y,z) representation of one example. The blue circle represents the aircraft and the star is a representation of an object.

In terms of computational algorithm:

For each point 'j':

Component 'y':

- if the value of gamma is smaller than zero and delta is greater than zero (situation one, figure 3), we have:

$$DR_y = \frac{\tan((\frac{3.14159}{2})-|delta(j)|) * d}{\tan((\frac{3.14159}{2})-|gamma(j)|) + \tan((\frac{3.14159}{2})-|delta(j)|)} \quad (2)$$

$$DL_y = d - DR_y \quad (3)$$

$$y = \tan\left(\left(\frac{3.14159}{2}\right) - |gamma(j)|\right) * DR_y \quad (4)$$

- if the value of gamma is equal to zero and delta is greater than zero (situation two, figure 4), we have:

$$DR_y = 0 \quad (5)$$

$$DL_y = d \quad (6)$$

$$y = \tan\left(\left(\frac{3.14159}{2}\right) - |delta(j)|\right) * DL_y \quad (7)$$

- if the value of gamma is smaller than zero and delta is equal to zero (situation three, figure 5), we have:

$$DR_y = d \quad (8)$$

$$DL_y = 0 \tag{9}$$

$$y = \tan\left(\left(\frac{3.14159}{2}\right) - |gamma(j)|\right) * DR_y \tag{10}$$

- if the value of gamma and delta is greater than zero (situation four, figure 6), we have:

$$DR_y = \frac{\tan((\frac{3.14159}{2}) - |delta(j)|) * d}{\tan((\frac{3.14159}{2}) - |gamma(j)|) - \tan((\frac{3.14159}{2}) - |delta(j)|)} \tag{11}$$

$$DL_y = d + DR_y \tag{12}$$

$$y = \tan\left(\left(\frac{3.14159}{2}\right) - |gamma(j)|\right) * DR_y \tag{13}$$

- if the value of gamma and delta is smaller than zero (situation five, figure 7), we have:

$$DR_y = \frac{-\tan((\frac{3.14159}{2}) - |delta(j)|) * d}{\tan((\frac{3.14159}{2}) - |gamma(j)|) - \tan((\frac{3.14159}{2}) - |delta(j)|)} \tag{14}$$

$$DL_y = DR_y - d \tag{15}$$

$$y = \tan\left(\left(\frac{3.14159}{2}\right) - |gamma(j)|\right) * DR_y \tag{16}$$

Where '$DR_y$' is the distance in terms of axis 'x' between the object and the right camera (figure 2), 'delta' and 'gamma' are angles, 'd' is the distance between the cameras, '$DL_y$' is the distance in terms of axis 'x' between the object and the left camera (figure 2).

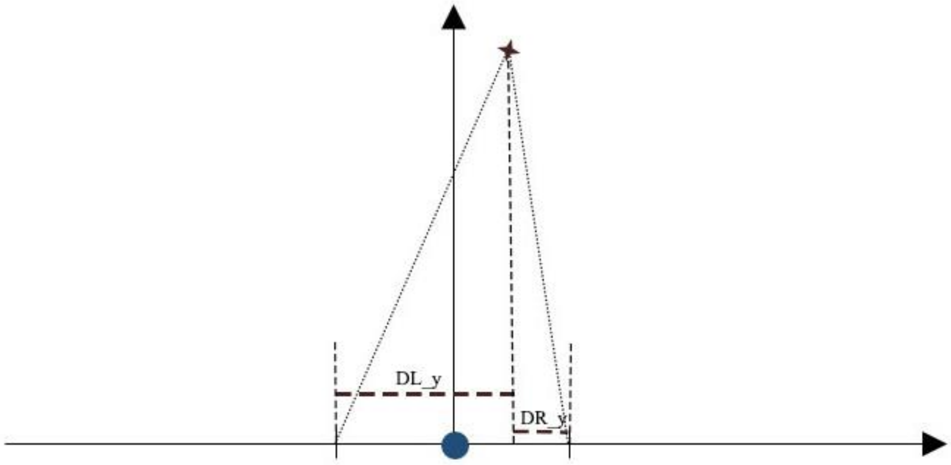


Fig. 2. A two-dimension (x,y) representation of a projection on the ‘xy’ plane of an example. The blue circle represents the aircraft and the star is a representation of an object.

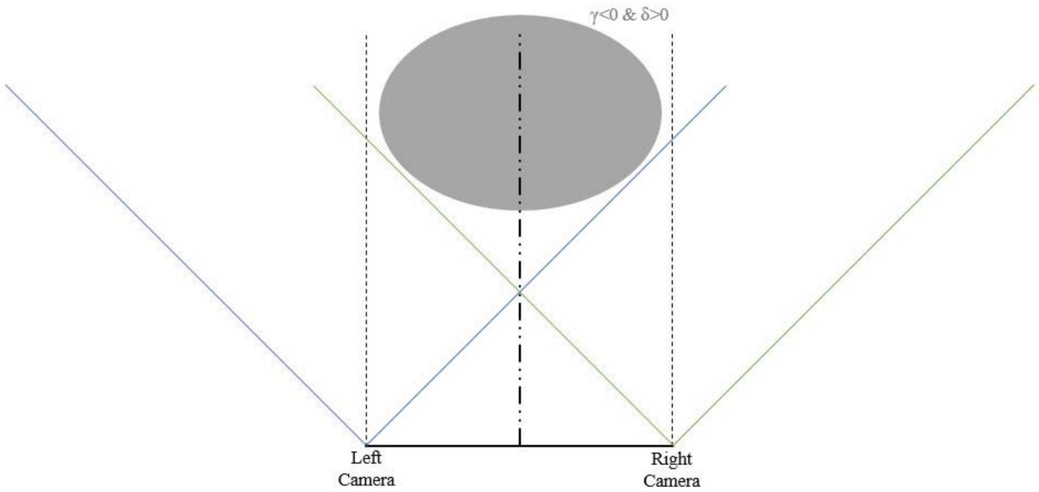


Fig. 3. Scheme representing the first situation: the point detected is in the grey zone; which implies that the value of gamma is smaller than zero and delta is greater than zero.

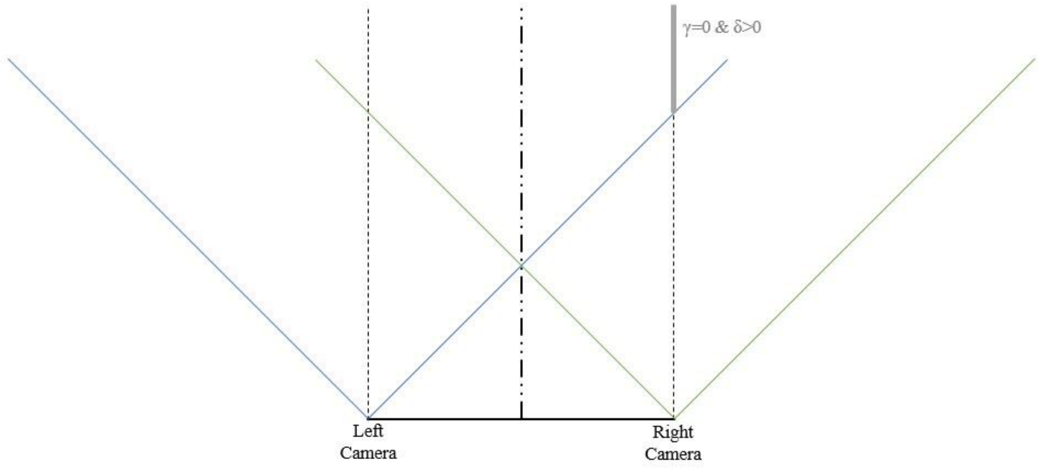


Fig. 4. Scheme representing the second situation: the point detected is in the grey line; which implies that the value of gamma is equal to zero and delta is greater than zero.

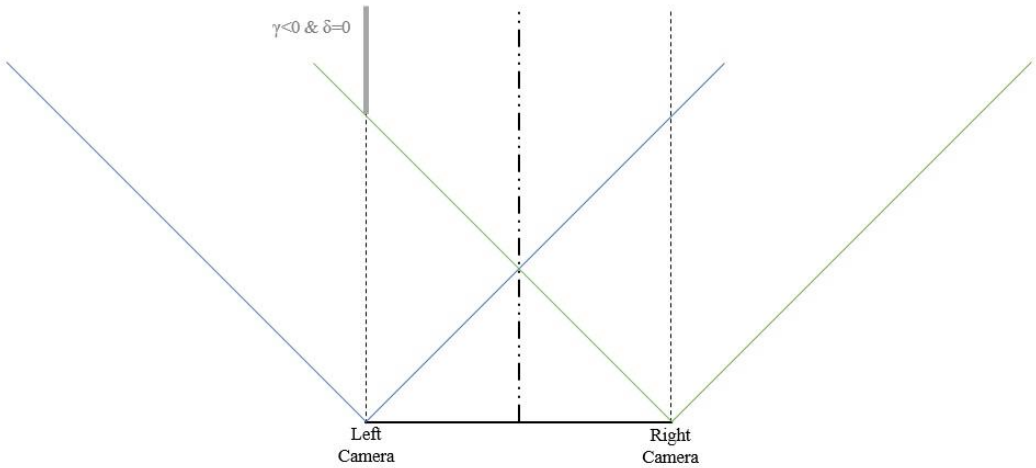


Fig. 5. Scheme representing the third situation: the point detected is in the grey line; which implies that the value of gamma is smaller than zero and delta is equal to zero.

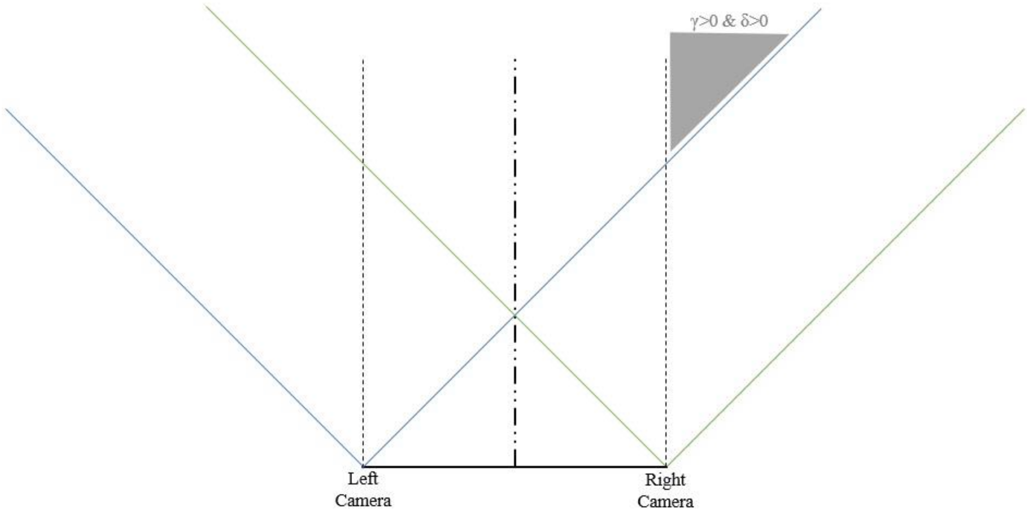


Fig. 6. Scheme representing the fourth situation: the point detected is in the grey zone; which implies that the values of gamma and delta are greater than zero.

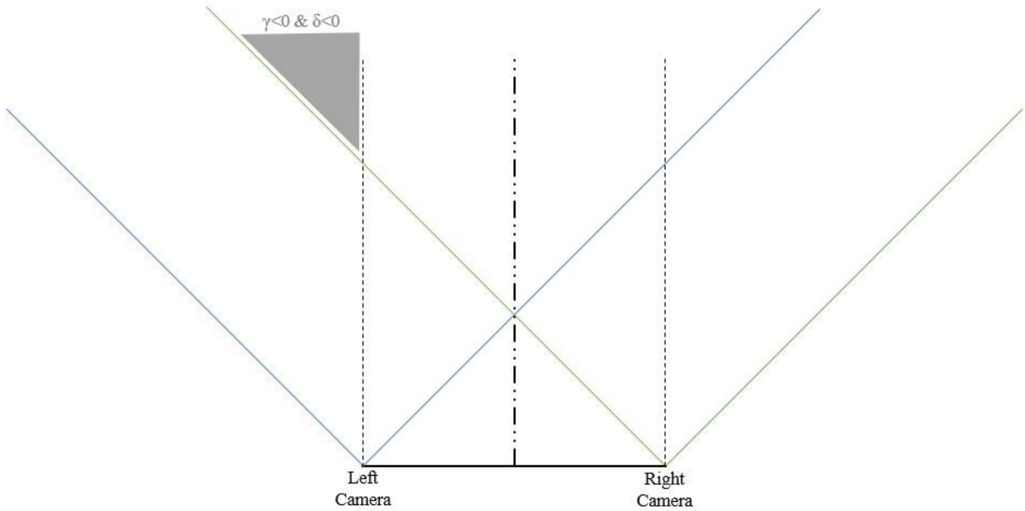


Fig. 7. Scheme representing the fifth situation: the point detected is in the grey zone; which implies that the values of gamma and delta are smaller than zero.

Component 'z':

- if the value of '$DR_y$' is greater than zero:

$$\text{hypotenuse} = \sqrt{(DR_y^2 + y^2)} \tag{17}$$

$$z = \tan(\text{beta}(j)) * \text{hypotenuse} \tag{18}$$

- if the value of '$DR_y$' is equal to zero:

$$\text{hypotenuse} = \sqrt{(DL_y^2 + y^2)} \tag{19}$$

$$z = \tan(\text{alpha}(j)) * \text{hypotenuse} \tag{20}$$

Where 'hypotenuse' is the vector distance between our aircraft and the object when projecting in the 'xy' plane, '$DR_y$' is the distance in terms of axis 'x' between the point and the right camera (figure 2), 'y' is the component calculated before, 'beta' is an angle provided by the right camera, 'z' is the component to be found, '$DL_y$' is the distance in terms of axis 'x' between the point and the left camera (figure 2) and 'alpha' is also an angle but provided by the left camera.

Component 'x':

- if: $DR_y > DL_y$

$$x = -(DR_y - \left(\frac{d}{2}\right)) \tag{19}$$

- else if: $DR_y < DL_y$

$$x = DL_y - \left(\frac{d}{2}\right) \tag{20}$$

- else:

$$x = 0 \tag{21}$$

Where 'x' is the component to be determinate, '$DR_y$' is the distance in terms of axis 'x' between the object and the right camera (figure 2), 'd' is the distance between the cameras and '$DL_y$' is the distance in terms of axis 'x' between the object and the left camera (figure 2).

The vertical distance between our aircraft and each point correspond to the component 'z'. However, in terms of the lateral distance it is necessary to calculate based on the 'x' and 'y' coordinates. Vertical and lateral distance for each point 'j':

$$VD(j) = z(j) \tag{22}$$

$$LD(j) = \sqrt{(x(j)^2 + y(j)^2)} \tag{23}$$

Where 'VD(j)' is the vertical distance between our aircraft and the point 'j', 'j' is the indexing number to identify the point, 'z(j)' is the component 'z' of the point 'j', 'LD(j)' is the lateral distance between our aircraft and the point 'j', 'x(j)' and 'y(j)' are respectively the 'x' component and 'y' component of the point 'j'.

After calculating all the distances, it is necessary to compare the results with the minimum value of three hundred meters. If both vertical distance and lateral distance are greater than three hundred meters (VD>300m and LD>300m) or even equal (VD=300m and LD=300m) the danger of collision does not exist and nothing is changed. If both distances are less than three hundred meters (VD<300m and LD<300m) the danger of collision exists and it is necessary to solve the next problem, finding the specific area to avoid. To solve this next problem it will be applied the concept of convex hull and different algorithms will be explored.

As we can notice this is a three-dimension situation. However, for the following steps it will be adapted to a two-dimension case by assuming that all the points have the same 'y' coordinate, which means that we will project the points to a 'xz' plan.

**Convex Hull**

Convex Hull method is a geometrical method which the main goal is to incorporate a group of points in just one convex polygon.

A more elaborated explanation of this method is: given a specific group of points in two or more dimensions the correspondent convex hull is a convex polygon with the smallest area/volume possible and it must include all the points of the group. Not all the points need to be or must be vertices of the polygon but those points must be inside the polygon.

The convex polygon does not necessarily represent the real format of the figure/object in study. It is just an approximation to the actual format that allow us to calculate the area we must avoid.

**Convex Hull Algorithms in 2D flights**

There are many developed algorithms related with this geometrical method. Some of them have similar approaches and some are no longer used due to terms of efficiency. Three efficient algorithms were chosen to be part of this case study.

Jarvis March (or known as gift wrapping):

To simplify we will assume that all points are in a general position and not in a special position. A special position could be for example three collinear points. Although we are making this assumption, it is important to notice that we could actually include those special positions in the algorithm, it will only turn the algorithm more complex.

The complete implementation of Jarvis' algorithm must include degenerative cases of Convex Hull with one or two vertices and take into consideration arithmetic precision problems.

To apply correctly this algorithm, it's necessary to follow the next steps:

- First, we start with 'i=0' and one point $p_0$ that we know that belong to the convex hull, it is the leftmost point of the group.
- Then, we select the point $p_{i+1}$ making sure that all other points are on the right side of the line $p_i p_{i+1}$. This last point is chosen by polar angle comparison of all points relatively to $p_i$.
- This process is repeated consecutively, just like a cycle in computational programming.

Every time the process is repeated the parameter 'i' suffers an increase: 'i=i+1', which means that our initial point became the last point we found every time we repeat.

Graham scan:

The Graham scan algorithm is a tool to determinate the vertices of convex hull of a specific group of points.

To correctly understand this algorithm, it will be explain by steps:

- The first step is finding the point with smallest 'y' coordinate, if there is more than one point we must chose the point with smallest 'x' coordinate too. The chosen point should be named as point P.
- The second step is number in ascending order the rest of the points according to the angle that each point with point P relatively to axis 'x' make. To successfully complete this step there is no need to calculate the angles, it is possible to use certain functions in an interval of $[0,\pi]$.
- Considering the previously steps before it is now necessary to evaluate for each point if the dislocation to the next two points is a left or right turn. If it is a right turn the line from the second point to the last one (third point) does not belong to the convex hull. Nevertheless, we can conclude that the second point is on the inside.
- Then for the last point we must repeat this procedure. So on until a left turn happens. In that moment, the algorithm keep the line from the second point to the last point and starts again with the last point. However, all the points already known as being inside the convex hull must not be taken into consideration when the process repeats after a left turn.

The correct application of all steps will result in obtaining the convex hull of the initial set of points.

This method does not require the calculation of the angles just simple arithmetic. To better understand, given three points (2D) it is necessary to calculate the 'z' coordinate of the vector product:

$$(x_2 - x_3)(y_3 - y_1) - (y_2 - y_1)(x_3 - x_1) \tag{24}$$

then: if the product is equal to zero the points are collinear; if the result is positive it is a left turn; if the result is negative it is a right turn.

Chan's algorithm:

In computational geometry Chan's algorithm allow us to determinate the convex hull of a set of points in two dimensions (2D). This algorithm is mostly the combination of two other algorithms and allow to optimize the time.

Considering a plane case, two possible algorithms are, for example, the Graham Scan and the Jarvis's March (two algorithms already exposed).

To better understand this algorithm will be presented next a more detail explanation. But before it is necessary to stablish that will be considered a set of n points, named P, and assumed as a planer case.

In a first phase, it is necessary to assume the value of parameter 'h' as known and considering that: m=h. Although these initial considerations are not realistic they are required. Then:

- The set P must be divided in smaller subsets named 'Q'. The maximum number of subsets is:

$$\frac{n}{m}+1 \quad (25)$$

- Through the Graham Scan algorithm, or other algorithm with exactly O(nlogn), is possible to compute the convex hulls of each subset.

The second phase is more complex and includes the application of the Jarvis' algorithm.

- In this phase the convex hulls of the subsets 'Q' are known and with them it is possible to determinate f(pi,Q) in O(logm) time by using binary search. So in O((n/m)logm) time we have determinate f(pi,Q) for all the subsets O(n/m) of Q.
- Then it is possible to define f(pi,P) through the same technique used in the Jarvis' algorithm but considering only the points included on f(pi,Q).

Knowing that Jarvis March repeats this procedure O(h) times we can conclude that this second phase takes O(nlogm) time.

Executing correctly this two phases the result is the convex hull of a set of n points in O(nlogh) time, assuming parameter 'h' as known.

Relatively to the parameter 'm', initially we must consider 'm' as a constant of lower value and then increase it until 'm' is bigger than 'h'.

It is possible to apply any of the previously presented algorithms to our case study because all off them function correctly in two-dimensions situations.

**Implementation Algorithm – Convex Hull**

Since the computational tool chosen to this work was Matlab the determination of the convex hull for each case will be through one specific Matlab function named 'convhull', which allows not only to find the specific points that are vertices but also to graphically demonstrate the convex hull.

In terms of computational algorithm:

```
Convex hull - assuming equal y to all points (2D)
k=convhull(x,z)
plot(x(k),z(k),'r-',x,z,'b.')
```

**Area to Avoid**

The determination of the convex hull is just the first step to accomplish the second objective, finding the specific area to avoid, there are two more necessary steps.

**3.5.1. Establish a circumference, with smaller radius possible, that contains the convex hull previously determinate.**

On the process to determinate the convex hull the points are separated by two categories: inside the convex hull and vertices. Knowing the points belonging to the category 'vertices' is possible to calculate a central point of the convex hull by the average of those points coordinates. If this same procedure is applied to all the points, instead of only the 'vertices', the result is the midpoint, which will be the circumference centre.

The best method to correctly define the minimum radius possible is to calculate the distance between the centre and each point, then the biggest distance calculated is the minimum radius. However, in terms of security and safety issues a safety margin must be added to the minimum radius calculated before.

In terms of computational algorithm:

Central point/Midpoint:

$$c_x = \frac{\sum x(j)}{n_j} \quad (26)$$

$$c_z = \frac{\sum z(j)}{n_j} \quad (27)$$

Where '$c_X$' is the 'x' coordinate of the central point, 'x(j)' is the 'x' coordinate of the point 'j', 'j' is the indexing number to identify the point, '$n_j$' is the total number of points, '$c_Z$' is the 'z' coordinate of the central point and 'z(j)' is the 'z' coordinate of the point 'j'.

Distance between the central point and each point:

$$dis(j) = \sqrt{(x(j) - c_x)^2 + (z(j) - c_z)^2} \tag{28}$$

Where 'dis(j)' is the distance between the central point and the point 'j', 'j' is the indexing number to identify the point, 'x(j)' is the 'x' coordinate of the point 'j', '$c_X$' is the 'x' coordinate of the central point, 'z(j)' is the 'z' coordinate of the point 'j' and '$c_Z$' is the 'z' coordinate of the central point.

Minimum radius:

$$r = 1.5 \times dis_{max} \tag{30}$$

Where 'r' is the radius of the circumference and '$dis_{max}$' is the maximum distance previously calculated.

This circumference is in terms of three-dimensions reality a sphere, so it can be projected in any plan and it will always have the same radius and centre coordinates.

**3.5.2. The final area to avoid.**

In a three-dimensions case, the result must be a cone and it is necessary just two things, a base and a height, to define it. The cone base is the circumference define in the previous point. To determinate the cone height we need to know the vector distance between our aircraft and the circumference centre, if we have the centre coordinates we have the height.

In terms of two-dimensions the representation must be on the 'xy' plane and it will be the junction of the circumference and two lines, which must be tangent to the circumference and pass on the origin. To determinate the equations of the lines it is essential to first find the only two points belonging both to one line and to the circumference. Equations to find the two necessary points:

$$r = \sqrt{\left(p_x - c_x\right)^2 + \left(p_y - c_y\right)^2} \tag{31}$$

$$h_p = \sqrt{p_x^2 + p_y^2} \tag{32}$$

where 'r' is the circumference radius, '$p_x$' is the 'x' coordinate of the tangent point, '$c_x$' is the 'x' coordinate of the central point, '$p_y$' is the 'y' coordinate of the tangent point, '$c_y$' is the 'y' coordinate of the central point and '$h_p$' is the distance vector between the aircraft and the new point. The result of this equations is two set of 'x' and 'y' coordinates corresponding to two different points.

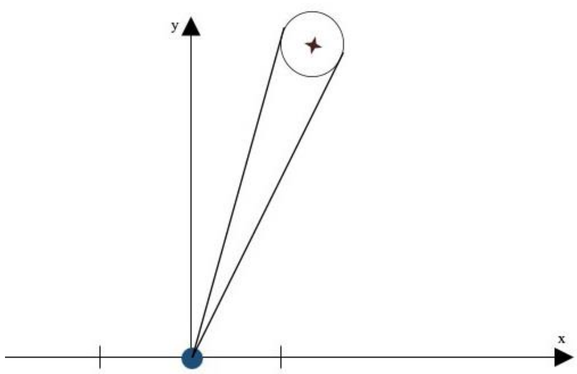


Fig. 8. An example of a two-dimension (x,y) representation of the specific area to avoid. The blue circle represents the aircraft and the star is a representation of an object.

**Analysis of reality**

This papers focus is on the specific area to avoid to prevent an imminent collision due to the distance between the aircraft and a not identified object. However, after finding the specific area that the aircraft must avoid it is necessary to compare it with the aircraft's heading to understand if it is definitely needed to make any change in the aircraft's path in order to escape the area already calculated. Beyond the aircraft's heading it is possible to also change the aircraft's altitude or velocity, all are flight's characteristics and they can assume different values during the flight.

To better understand it, it is possible to visualise in Figure 4 (shown below) one example with three possibilities for the aircraft's heading. The blue circle is representing the aircraft and the star is the object. In the possibilities (a) and (c) it is obvious that the aircraft's heading is not coincident with the area to avoid, so it is not necessary to make any change. However, in the possibility (b) the situation is the opposite, the aircraft's heading is right in the specific area to avoid and with this information it is possible to conclude that a collision will happen, so it will be essential to work efficiently in the aircraft trajectory.

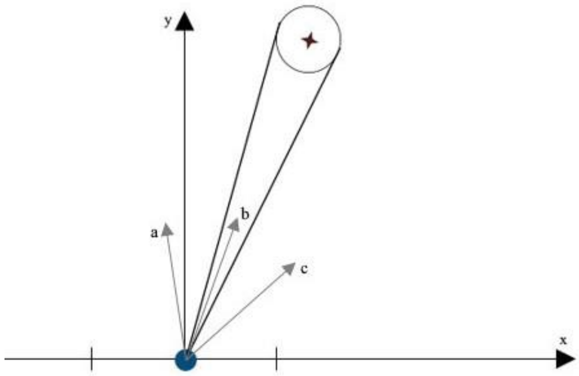


Fig.9. An example of a two-dimension (x,y) representation of the specific area to avoid with three possibilities to an aircraft's heading (a, b, c). The blue circle represents the aircraft and the star is a representation of an object.

**Simulation**

In order to verify the efficiency of this method, a computational program was developed for these specific work and it was created two different conflict situations. In both cases the number of points was greater than five to obtain the most accurate results. To simplify this first phase of simulations it was considered as existing danger of collision if the nearest point was less than three meters from our aircraft, both laterally and vertically, and not the usual three hundred meters.

**Data**

The initial information is the angles provided by the cameras and their position in the aircraft (distance between them). In both cases the distance between cameras is equal to two meters. The angles are received in degrees and then changed to radians. The data from the first situation and second situation is respectively presented in the Table 1 and Table 2.

Table 1. Data from situation I

| Points | Angles | | | | | | | |
|---|---|---|---|---|---|---|---|---|
| | Beta (degrees) | Beta (radians) | Alpha (degrees) | Alpha (radians) | Gama (degrees) | Gama (radians) | Delta (degrees) | Delta (radians) |
| 1 | 7,50 | 0,1309 | 7,10 | 0,1239 | -14,00 | -0,2443 | 23,00 | 0,4014 |
| 2 | 4,00 | 0,0698 | 3,80 | 0,0663 | -15,00 | -0,2618 | 24,50 | 0,4276 |
| 3 | 8,00 | 0,1396 | 7,30 | 0,1274 | -9,50 | -0,1658 | 26,00 | 0,4538 |
| 4 | 5,50 | 0,0960 | 4,90 | 0,0855 | -10,50 | -0,1833 | 29,00 | 0,5061 |
| 5 | 2,00 | 0,0349 | 1,80 | 0,0314 | -11,00 | -0,1920 | 30,00 | 0,5236 |
| 6 | 7,50 | 0,1309 | 6,50 | 0,1134 | -6,00 | -0,1047 | 31,00 | 0,5411 |
| 7 | 4,00 | 0,0698 | 3,40 | 0,0593 | -6,50 | -0,1134 | 32,00 | 0,5585 |

Table 2. Data from situation II

| Points | Angles | | | | | | | |
|---|---|---|---|---|---|---|---|---|
| | Beta (degrees) | Beta (radians) | Alpha (degrees) | Alpha (radians) | Gama (degrees) | Gama (radians) | Delta (degrees) | Delta (radians) |
| 1 | 0,90 | 0,0157 | 0,90 | 0,0157 | -3,50 | -0,0559 | 0,00 | 0,0000 |
| 2 | 1,00 | 0,0175 | 1,00 | 0,0175 | 1,50 | 0,0262 | 5,40 | 0,0873 |
| 3 | 1,50 | 0,0262 | 1,49 | 0,0262 | 1,55 | 0,0218 | 5,50 | 0,0916 |
| 4 | 2,50 | 0,0436 | 2,49 | 0,0435 | 3,00 | 0,0524 | 6,00 | 0,1047 |
| 5 | 0,00 | 0,0000 | 0,00 | 0,0000 | 3,90 | 0,0611 | 7,95 | 0,1309 |
| 6 | 1,95 | 0,0340 | 1,94 | 0,0339 | 3,95 | 0,0567 | 8 | 0,1353 |
| 7 | 1,00 | 0,0175 | 0,99 | 0,0173 | 4 | 0,0515 | 8,1 | 0,1405 |
| 8 | 1,00 | 0,0175 | 0,99 | 0,0173 | 5,5 | 0,0829 | 8,95 | 0,1571 |
| 9 | 1,50 | 0,0262 | 1,49 | 0,0262 | 5,55 | 0,0873 | 9,05 | 0,1614 |
| 10 | 0,90 | 0,0157 | 0,89 | 0,0155 | 11,00 | 0,1920 | 14,90 | 0,2601 |

**Simulation Results**

Both situations are equally processed but with their own results. Relatively to the analysis of the results, it must be equally critical but it should take into consideration the specificities of each case.

### 4.2.1. Situation I - Results

Table 3. Coordinates from situation I

| Points | Coordinates | | |
|---|---|---|---|
| | x | y | z |
| 1 | 0,1300 | 1,4841 | 0,2014 |
| 2 | 0,1297 | 1,3818 | 0,1000 |
| 3 | 0,2445 | 1,5265 | 0,2175 |
| 4 | 0,2494 | 1,3520 | 0,1324 |
| 5 | 0,2481 | 1,2958 | 0,0461 |
| 6 | 0,3511 | 1,4165 | 0,1875 |
| 7 | 0,3458 | 1,3535 | 0,0953 |

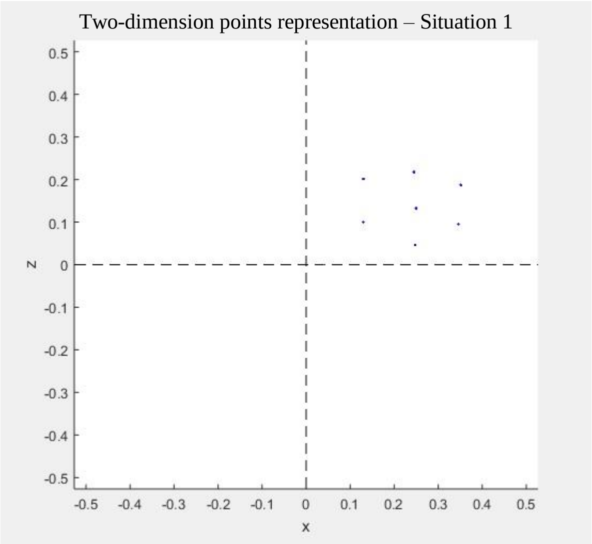


Fig. 10. A two-dimension (x,z) points representation.

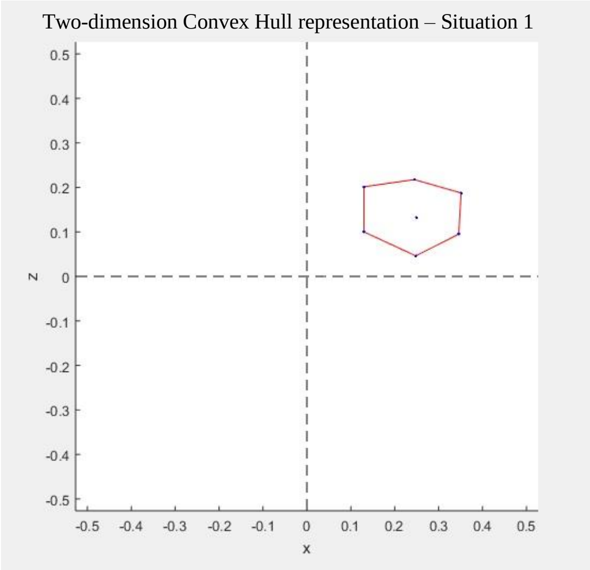


Fig. 11. A two-dimension (x,z) Convex Hull representation.

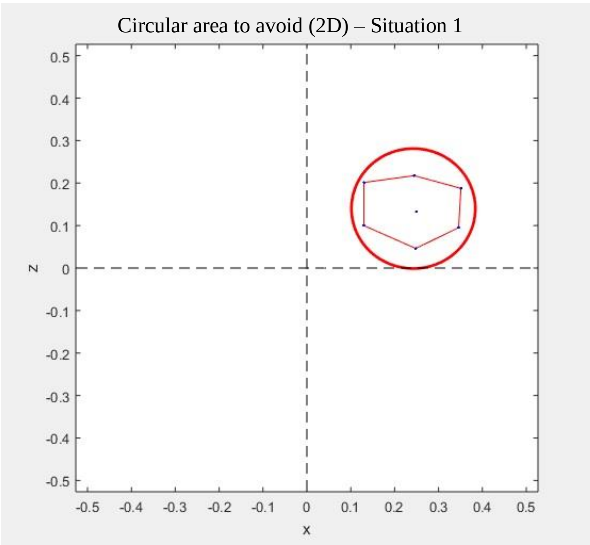


Fig. 12. A two-dimension (x,z) circular area to avoid representation.

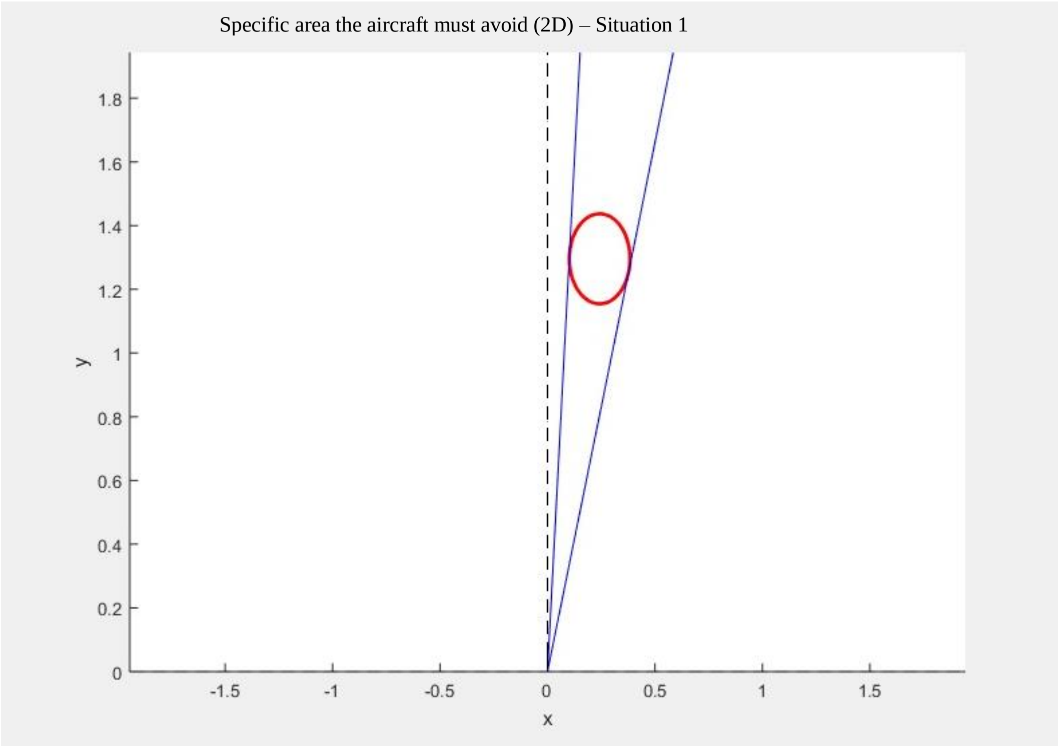


Fig. 13. The specific area the aircraft must avoid to prevent collision in two dimensions (x,y).

#### 4.2.2. Situation II - Results

Table 4. Coordinates from situation II

| Points | Coordinates | | |
|---|---|---|---|
| | x | y | z |
| 1 | -0,5000 | 16,3495 | 0,2573 |
| 2 | 0,8832 | 14,6323 | 0,2555 |
| 3 | 0,8909 | 14,4446 | 0,3784 |
| 4 | 1,4945 | 18,9766 | 1,0291 |
| 5 | 1,4538 | 13,9904 | 0,0000 |
| 6 | 1,4659 | 13,9878 | 0,4774 |
| 7 | 1,4659 | 13,8133 | 0,2417 |
| 8 | 2,0733 | 16,3396 | 0,2865 |
| 9 | 2,0645 | 16,1007 | 0,4236 |
| 10 | 3,2111 | 13,9472 | 0,2232 |

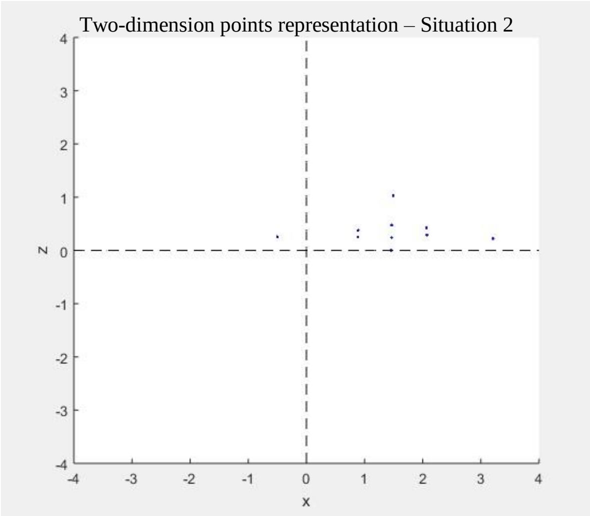


Fig. 14. A two-dimension (x,z) points representation.

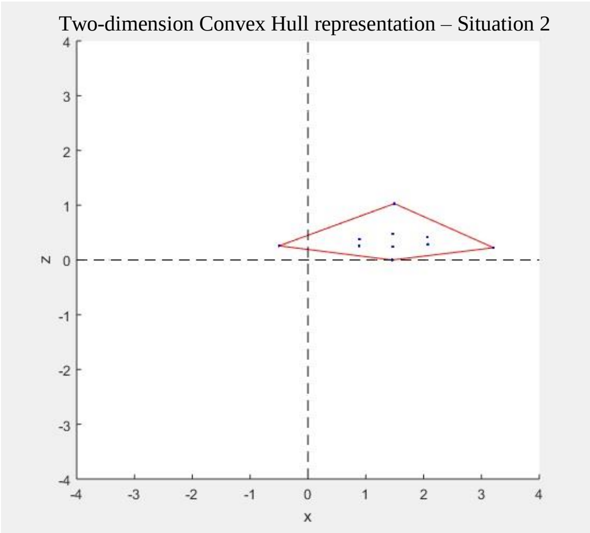


Fig. 15. A two-dimension (x,z) Convex Hull representation.

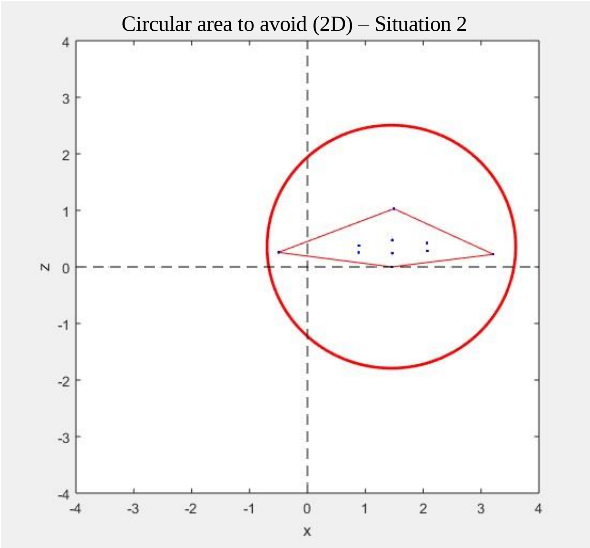


Fig. 16. A two-dimension (x,z) circular area to avoid representation.

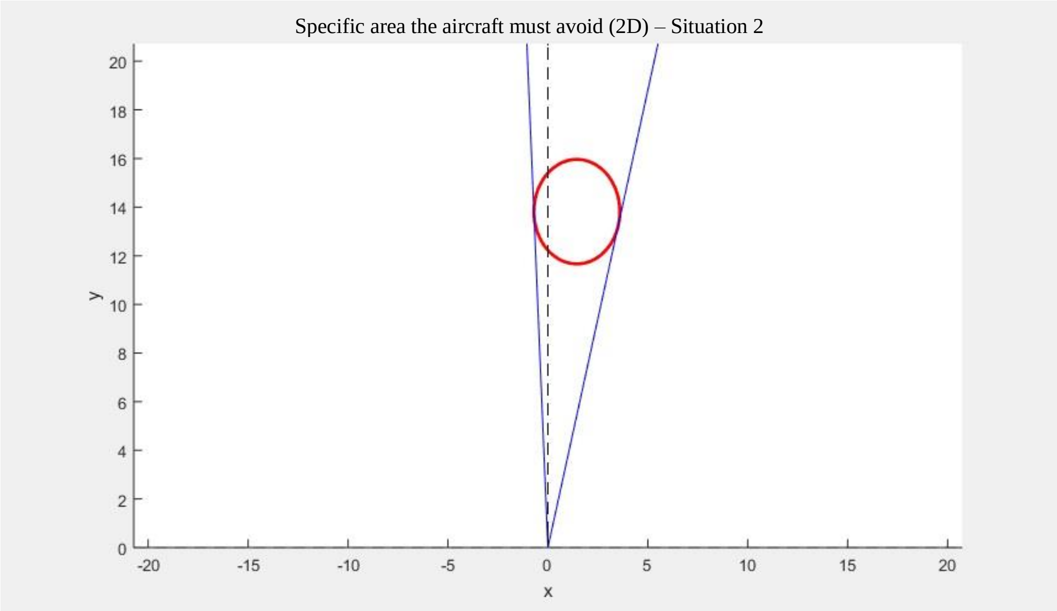


Fig. 17. The specific area the aircraft must avoid to prevent collision in two dimensions (x,y).

**4.2.3. Discussion of results**

The first result, Table 3 for the situation one and Table 4 for the situation two, is a table with all the points coordinates, through this information the computational program can calculate the distances and so determinate the closest point to our aircraft. In the first situation, the closest point is number five, which is approximately 1,32 meters sideways and only 0,05 meters vertically from our aircraft. The obvious conclusion in this case is the existence of imminent danger of collision. Regarding the second situation, the closest point is number seven, which is approximately 13,89 meters sideways and 0 meters vertically from our aircraft. The same conclusion as that of the previous situation can be taken.

Although Table 3 and Table 4 mention a three-dimensions situation, which in fact it is, the graphic results will be in two-dimensions. The first three charts are two-dimensions representations in an 'xz' plane. Only the last one displays a view in an 'xy' plane.

Figure 5 and Figure 9 are two different graphics generated according to the information present in the Table 3 and Table 4 respectively, more specifically the points' coordinates 'x' and 'z' from each situation. In these two charts, it is possible to visualise the points projected on the 'xz' plane.

The next step is analysing the convex hull of each set of points, which are in the Figure 6 (situation one) and Figure 10 (situation two). By observation of the convex hull it is possible to have an approximate idea of the real object format and the position relative to our aircraft. In the first case seems like a cube and it is above and slightly to the right. On other hand, the object from the second case appears to be wider and with a kind of a flat diamond shape. About the position of the object, it is similar to the first situation.

The goal of Figure 7 and Figure 11 is to show the circular area which includes the object plus a safety margin. That circular area is, in the 'xz' plane, the area to avoid. So, the fact that the convex hull is again represented, it is merely illustrative. As we can observe the convex hull in both cases is inside the circle, as it should be, and no point touches the line, thanks to the safety margin added to the circle radius.

The last two charts, Figure 8 and Figure 12, are the final results to achieve the solution to the second problem: finding the specific area to avoid. Both charts include a two-dimension representation, in the 'xy' plane, of the area that the aircraft must avoid to prevent collision. Figure 8 presents the area to avoid in the first situation and Figure 12 the same but in relation to the second case. In each graphic, Figure 8 and Figure 12, the circle has the same radius as the Figure 7 and Figure 11 respectively.

The reason that the circle in the 'xz' plane and the circle in the 'xy' plane has not only the same radius value but also the same x-coordinate of the center is because they are two projections on different planes of the same sphere.

**Conclusions**

This paper develops a collision detection method capable of dealing with different situations in which the data is provided by optical methods. In each case, it firsts evaluates if there is danger of collision, and then, if the response is affirmative, the system immediately calculates the specific area to avoid. This system works with a simple and efficient method, which is the base to the computational algorithm. Two simulations were carried out successfully, even if the first one showed a situation more unrealistic. In both situations, the risk of collision was quickly detected and the results for each case showed effectively the specific area to avoid. The two situations were not the most realistic but, the good results prove that this method of description of the safe zone outside the cone works correctly so, it can be properly applied to an anti-collision system.

A future work following the presented method shall deal with the development of the 'Analysis of reality' and the integration of this detection method in an anti-collision system with the functionality to automatically change the aircraft trajectory in order to avoid collision. This system will be simulated and adapted to the three-dimension reality.

**Contribution**

The main result from this work is the described algorithm based on convex hull and cone concepts, which has the capacity to determine not only if there is a collision threat but also the area that the aircraft must avoid to prevent an imminent collision.

**References**

Bousson, K., 2008, Model predictive control approach to global air collision avoidance, Aircraft Engineering and Aerospace Technology: An International Journal, Vol. 80 No. 6, pp. 605-612.

Ibrahim, Y., 2013, Development of a Flight Collision Avoidance System for a Free Flight Environment: An Ecological Interface Design Approach, International Journal of Multidisciplinary and Current Research, Nov/Dec, pp. 120-133.

Zeitlin, A., Lacher, A., Kuchar, J., Drumm, A., 2006, Collision Avoidance for Unmanned Aircraft: Proving the Safety Case, paper.

International Civil Aviation Organization, 2002, Manual on Implementation of a 300 m (1 000 ft) Vertical Separation Minimum Between FL 290 and FL 410 Inclusive, Manual.

Berg, M.; Cheong, O.; van Kreveld, M.; Overmars, M. 1997, Computational Geometry: Algorithms and Applications, Springer-Verlag.

Jarvis, R.A., 1973, On the Identification of the Convex Hull of a Finite Set of Points in the Plane, North-Holland Publishing Company, pp 18-21.

Graham, R.L., 1972, An Efficient Algorithm for Determining the Convex Hull of a Finite Planar Set, North-Holland Publishing Company, pp 132-133.

Chan, T.M., 1996, Optimal Output-sensitive Convex Hull Algorithms in 2 and 3 Dimensions, Discrete Computational Geometry, Vol. 16, pp 361-368.